A Thesis for the Degree of Doctor of Philosophy in Pharmacy

ROLE of NICOTINAMIDE N-METHYLTRANSFERASE and BONE MORPHOGENETIC PROTEIN 4 in EGFR-TKI-RESISTANCE of NON-SMALL CELL LUNG CANCER CELLS

August 2018

Duc-Hiep Bach

Natural Products Science Major, College of Pharmacy
Doctoral Course in the Graduate School
Seoul National University

ROLE of NICOTINAMIDE N-METHYLTRANSFERASE and BONE MORPHOGENETIC PROTEIN 4 in EGFR-TKI-RESISTANCE of NON-SMALL CELL LUNG CANCER CELLS

Under the Direction of Prof. Sang Kook Lee
Submitted to the Faculty of Graduate School,
Seoul National University in Korea

By
Duc-Hiep Bach
Pharmacy in Natural Products Science Major
Doctor Course in the Graduate School
Seoul National University

Approved as a qualified thesis of Duc-Hiep Bach
For the degree of Doctor of Philosophy in Pharmacy
By the committee members
August 2018

CHAIRMAN ---------- Minsoo Noh ---------- (인)

VICE-CHAIRMAN ---------- Yeong Shik Kim ---------- (인)

MEMBER ---------- Dong-Chan Oh ---------- (인)

MEMBER ---------- Young-Won Chin ---------- (인)

MEMBER ---------- Sang Kook Lee ---------- (인)

Abstract

ROLE of NICOTINAMIDE N-METHYLTRANSFERASE and BONE MORPHOGENETIC PROTEIN 4 in EGFR-TKI-RESISTANCE of NON-SMALL CELL LUNG CANCER CELLS

Duc-Hiep Bach
Natural Products Science Major
College of Pharmacy
The Graduate School
Seoul National University

Lung cancer is considered as the leading cause of cancer-associated deaths worldwide and epidermal growth factor receptor tyrosine kinase inhibitors (EGFR-TKIs) are used clinically as target therapies for lung cancer patients. However, the occurrence of acquired EGFR-TKI-mediated resistance such as gefitinib, remains a major problem in non-small cell lung cancer (NSCLC) treatment and limits their efficacy. Subsequently, various studies are ongoing to investigate the mechanisms of drug resistance and explore the novel therapeutics strategies for NSCLC treatment. The present study suggests the mechanisms of acquired gefitinib resistance using PC9-Gef cells, HCC827-Gef cells, H1993-Gef cells and H292-Gef cells that gained resistance through continuous exposure to gefitinib. Moreover, employing a natural product daphnane diterpenoid yuanhuadine (YD), an antitumor agent, a novel strategy was confirmed to overcome this resistance via modulation the targeted genes.

Accumulating evidence also suggests that microRNAs (miRNAs), a new class of small, nonprotein-encoding RNAs, play a significant role in epigenetically modulating various phenotypic changes in cancer cells. Indeed, miRNAs may affect genetic programs through post-transcriptional silencing of target genes, either by inhibiting the translation of target mRNAs or by promoting their degradation. These actions may lead to the regulation of numerous aspects of cancer biology, including drug resistance.

Recently, overexpression of Nicotinamide *N*-methyltransferase (NNMT), a cancer-associated metabolic enzyme, is correlated with various human tumors. However, their precise roles in regulating the development of drug-resistant tumorigenesis are still poorly understood. Herein, establishing EGFR-TKI-resistant NSCLC models indicates that there is a negative correlation between the expression levels of NNMT and miR-449a in tumor cells. Additionally, knockdown of NNMT suppressed p-Akt and tumorigenesis, while re-expression of miR-449a induced phosphatase and tensin homolog, and inhibited tumor growth. Furthermore, YD, significantly upregulated miR-449a levels while critically suppressing NNMT expression.

Bone morphogenetic proteins (BMPs) are a family of signaling molecules that belong to the transforming growth factor-β superfamily and the activation of the BMP-BMP receptor pathway conferred resistance to EGFR-TKIs in lung cancer patients harboring EGFR mutations. Recent studies have also suggested the possibility that small-molecule BMP4 antagonists were able to effectively inhibit the growth of lung cancer cells and chemotherapy-resistant cancer cells. In the present study, in comparison with the gene expression pattern of parental NSCLC cells, acquired gefitinib-resistant cell lines displayed that BMP4 gene was up-regulated in the gefitinib-resistant cell lines. Therefore, the role of BMP4 in EGFR-TKI resistance in NSCLC cells and the dynamic interactions of BMP4 with the tumor microenvironment such as miRNA or fatty acids were also elucidated.

Based on these findings, up-regulation of NNMT and BMP4 or down-regulation of miR-449a expression can be regarded as novel cancer biomarkers of acquired gefitinib resistance and therapeutic targets overcome this resistance. Moreover, YD, which induces the expression of miRNAs while suppresses NNMT and BMP4 expression may be considered as a potential lead compound for the gefitinib-resistant NSCLC.

Keywords: non-small cell lung cancer, gefitinib, NNMT, BMP4, miRNAs, yuanhuadine, metabolism, drug resistance.

Student number: 2014 – 22148

Table of contents

List of Figures

List of Tables

Abbreviations

1-MNA	1-methylnicotinamide
ACSL4	Acyl-CoA synthetase long-chain family member 4
ACVR1	Activin A receptor type 1
ALK	Anaplastic lymphoma kinase
BMPs	Bone morphogenetic proteins
CRC	Colorectal cancer
EGFR-TKIs	Epidermal growth factor receptor – tyrosine kinase inhibitors
Erl	Erlotinib
GBM	Glioblastoma multiforme
Gef	Gefitinib
GFP	Green fluorescent protein
IHC	Immunohistochemistry
miRNA	microRNA
NNMT	Nicotinamide N-methyltransferase
NSCLC	Non-small cell lung cancer
RISC	RNA-induced silencing complex
SAM	S-adenosyl methionine
siRNA	small interfering RNA
TGF-β	Transforming growth factor-β
TIMPs	Tissue inhibitors of metalloproteinases
YD	Yuanhuadine

[Chapter 1]

General introduction

1. 1 Background

1.1.1 Drug resistance in non-small cell lung cancer

Chemotherapy, one of the principal approaches for lung cancer patients, plays a crucial role in controlling tumor progression. Clinically, tumors reveal a satisfactory response following the first exposure to the chemotherapeutic drugs in treatment. However, most tumors sooner or later become resistant to even chemically unrelated anticancer agents after repeated treatment. This may contribute to an increase in the drug dosage and fail to improve the clinical prognosis or outcome. Subsequently, drug resistance is considered a major impediment in medical oncology. Although the different chemotherapy and endocrine regiments as well as targeted drugs have been commonly investigated, chemotherapy resistance is still major obstacle to successful treatment. It is well known that there are two main types of resistance in cancer, which include the following: (1) inherent resistance, where insensitivity already exists before treatment, and (2) acquired resistance, which subsequently appears following the initial positive response (Bach et al., 2017a). Subsequently, drug resistance is related to a wide variety of solid tumors, especially with lung cancer, the most common cause of cancer-related mortality. Small-cell lung cancer cells can acquire resistance with continued administration of the drug whereas non-small cell lung cancer (NSCLC) that constitutes about 85% of all lung cancers are often intrinsically resistant to certain anticancer drugs (Shanker et al., 2010).

Targeted therapies have significantly improved the survival and quality of life for a subgroup of patients with advanced NSCLC in 2005. However, the first acquired resistance was found in NSCLC patients treated with epidermal growth factor receptor – tyrosine kinase inhibitors (EGFR-TKIs), who initially showed an excellent response to treatment (Pao et al., 2005). Subsequently, various molecular mechanisms that relate to drug resistance have been explored, including those that are both non-mutational (presumably epigenetic) and mutational (genetic). Somatic mutations in the EGFR gene such as T790M mutation, deletion in exon 19 or wild-type EGFR amplification (Nakata and Gotoh, 2012) are highly associated with favorable response to the EGFR-TKI, gefitinib (Sharma et al., 2007), a pioneer targeted drug that has been used as the first-line treatment for patients with EGFR mutations (Mok et al., 2009).

1.1.2 The role of exosomal miRNAs in drug-resistance of cancer cells

Cell to cell interaction is crucial for all multicellular organisms. There are robust biological interaction networks comprising protein-protein, gene-gene, gene-microRNA (miRNA) and parallel signaling as well as intracellular and distant cell communications for aggressive and therapy resistant cancers (Kitano, 2003; Kitano, 2004). miRNAs are a new class of small, nonprotein-encoding RNAs, which have been discovered in diverse organisms and are thought to regulate other genes' expression (Lagos-Quintana et al., 2001). It is well known that miRNAs are involved in various biological processes, including stress resistance, cell differentiation and cell death (Ambros, 2003). They can also act as either oncogenes or tumor suppressors to regulate tumor progression and many contribute to tumor metastasis (Lu et al., 2005; Ma et al., 2007). Recent studies have demonstrated that miRNAs are secreted from various cells, including cancer cells, into body fluids such as blood, urine, breast milk and saliva (Hu et al., 2012; Ogawa et al., 2008; Taylor and Gercel-Taylor, 2008) (Figure 1).

Previous studies also revealed that drug-resistant tumor cells are an abundant source of exosomes that may serve as paracrine modulators via the horizontal transfer of genetic cargo (Corcoran et al., 2012; O'Brien et al., 2013; Safaei et al., 2005). Because of this role, exosomes may have a defined set of miRNAs that transfer a resistance phenotype to sensitive cancer cells by altering cell growth and inducing anti-apoptosis programs. For example, through competing with endogenous RNA for exosomal miR-34 and miR-449, lncARSR is suggested as a mediator of sunitinib resistance in renal cell carcinoma. In epithelial ovarian cancer, Sun *et al*. suggested that miR-9 can mediate the down-regulation of BRCA1 and impede DNA damage repair. Therefore, miR-9 may improve chemotherapeutic efficacy by increasing the sensitivity of cancer cells to DNA damage and may play a positive function in the treatment of ovarian cancer (Sun et al., 2013). Taken together, these studies have revealed the significance of exosomal miRNAs in drug resistance and intercellular communication (Simons and Raposo, 2009).

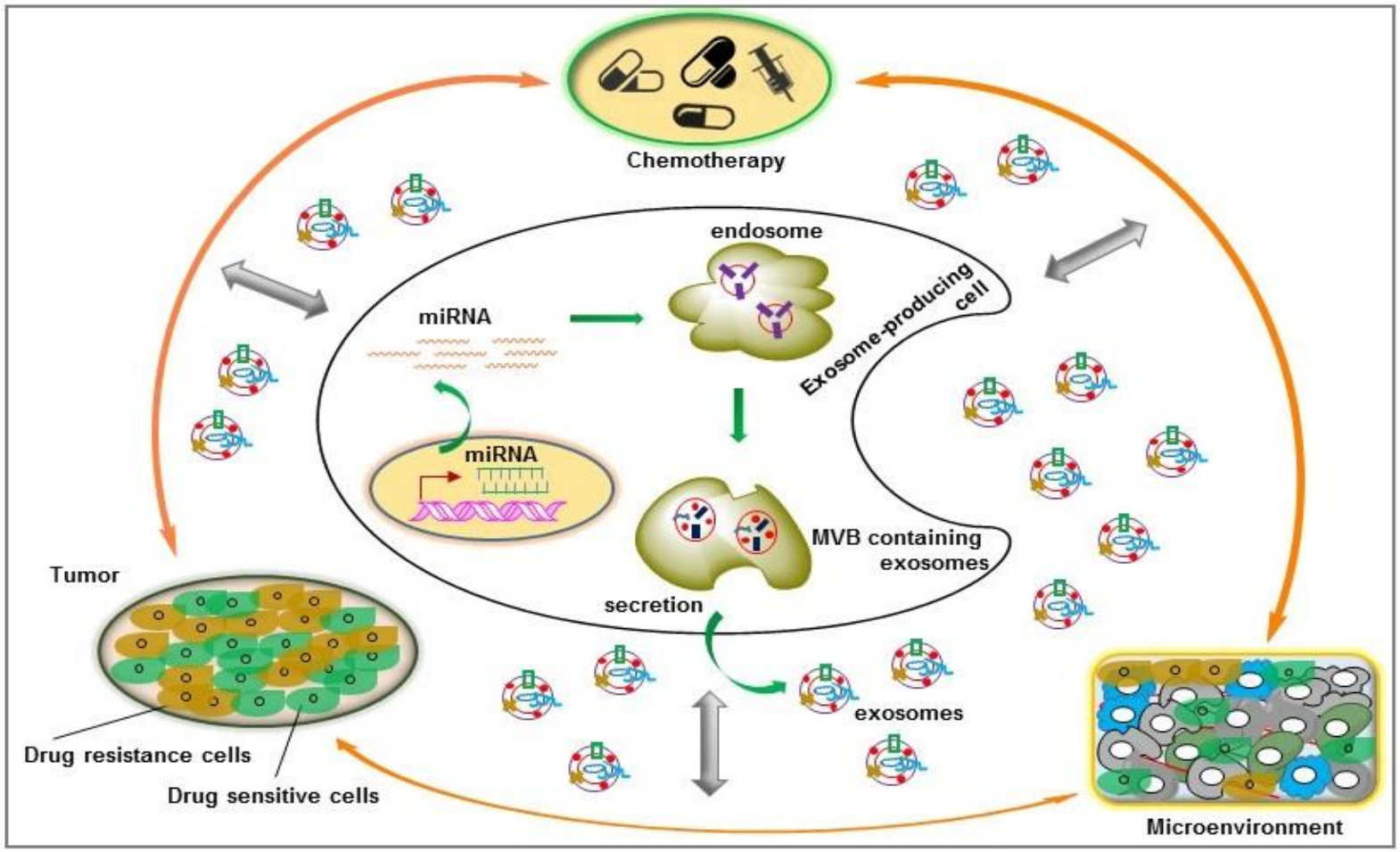

Figure 1: The proposed function of exosomal microRNA in the regulation of tumor progression and chemotherapy resistance (Bach et al., 2017a).

1.1.3 The association of bone morphogenetic proteins with miRNAs and drug-resistance of cancer cells

Bone morphogenetic proteins (BMPs), originally disclosed as an osteogenic factor in 1965 (Urist, 1965), are considered a unique extracellular multifunctional signaling cytokine and represent part of the transforming growth factor-β (TGF-β) superfamily (Guo and Wang, 2009) (Figure 2). The identification of BMPs has increasingly attracted much attention due to their functions not only in embryonic and postnatal development but also in tumor development and dissemination (Hardwick et al., 2008). These roles of BMPs are also highly correlated to various aspects of carcinogenesis, such as angiogenesis, epithelial-mesenchymal transition and cancer stem cells.

1.1.3.1 Negative modulation of BMPs by miRNAs

Additionally, various tumor microenvironment factors that strongly affect tumorigenesis interact with BMPs, such as microRNAs (miRNAs), mutations or drug treatment. miRNAs, small molecules of approximately 18 – 25 nucleotides in length, can modulate gene expression through translational repression and their critical roles in cancer progression and osteogenesis were recently manifested (Bach et al., 2017a; Wu et al., 2012). The molecular mechanisms involved in the negative regulation of BMP activity by miRNAs are also evident. Braig *et al* determined the molecular mechanisms leading to the overexpression of BMP4 in melanoma cells compared to normal melanocytes and identified miR-196a as a BMP4-negative regulator that directly suppresses BMP4 in malignant melanoma (Braig et al., 2010). Similarly, by profiling miRNAs during BMP2-stimulated osteogenesis of C2L12 mesenchymal cells, Li *et al* characterized two representative miRNAs and showed that miR-133 directly targets Runx2, an early BMP response gene essential for bone formation, and that miR-135 may also target SMAD5, a key transducer of the BMP2 osteogenic signal (Li et al., 2008). Rai *et al* employed unbiased genome-wide approaches in diffuse large B cell lymphoma and found that miR-155 directly targets the BMP-responsive transcriptional factor, SMAD5 (Rai et al., 2010). miR-155 overexpression suppressed SMAD5 expression and disrupted its activity (Rai et al., 2010). In 100 hepatocellular carcinoma tissues, Li *et al* found that miR-148a directly inhibited the expression level of activin A receptor type 1 (ACVR1), a key receptor in the BMP signaling pathway (Li et al., 2015). They also determined that this miRNA is related to cancer development and metastasis via the ACVR1/BMP/Wnt pathway (Li et al., 2015). In primary mouse keratinocytes following BMP4

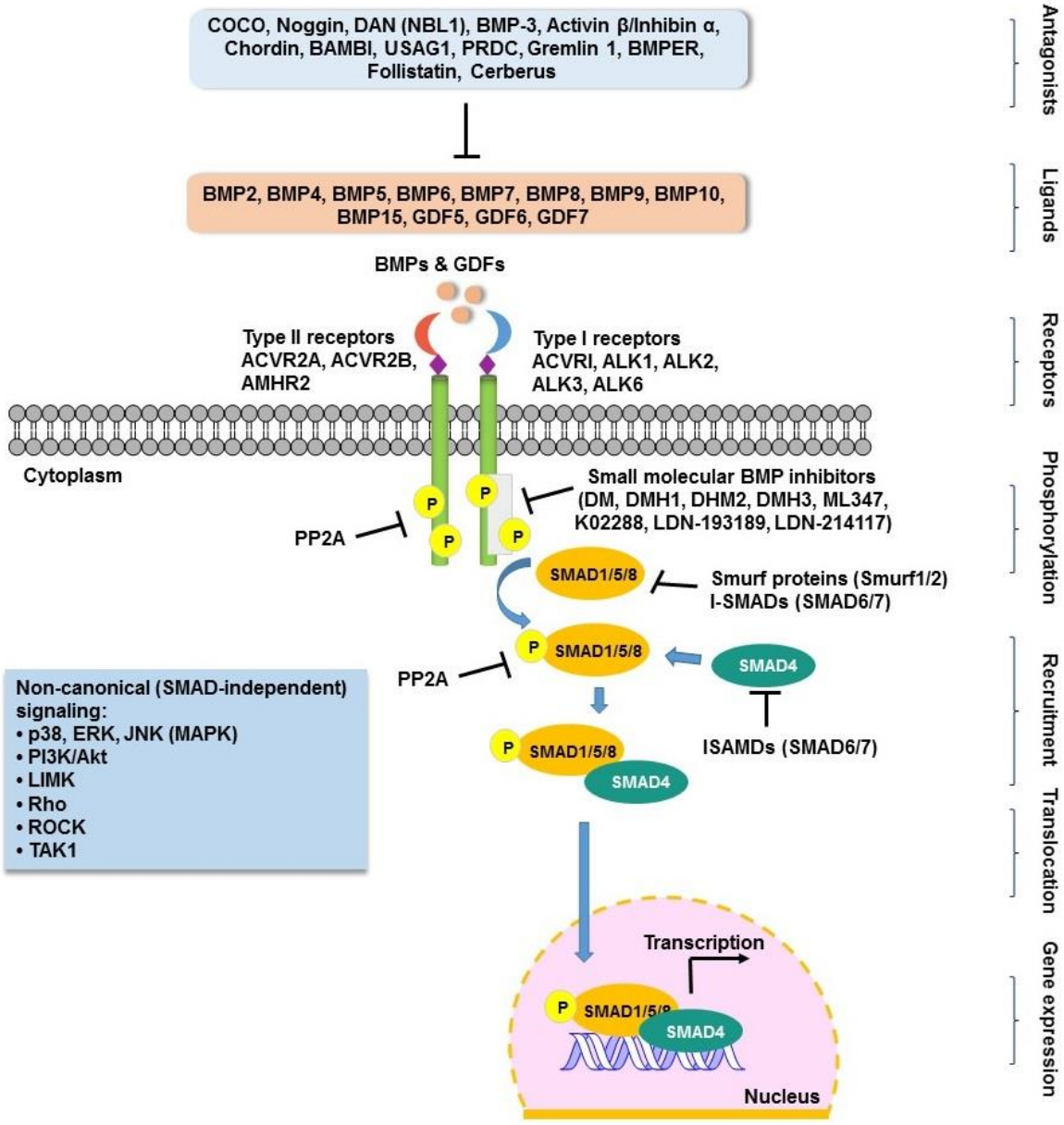

Figure 2. BMP-mediated signaling pathways. The type-II receptor *trans*-phosphorylates the type-I receptor which, in turn, stimulates transcriptional regulators called SMADs, which transduce the signal to the nucleus to modify gene expression (Bach et al., 2018b).

treatment, Ahmed *et al* identified miR-21, which is significantly suppressed by BMP4 (Ahmed et al., 2011). They also found that miR-21 regulates two groups of BMP4 target genes, including tissue inhibitors of metalloproteinases (TIMP)1, TIMP3 and programmed cell death 4. In primary keratinocytes and HaCaT cells, miR-21 can also prevent the inhibitory effects of BMP4 on cell migration and proliferation (Ahmed et al., 2011). Consistent with this observation, Qin *et al* also showed that bone morphogenetic protein receptor II (BMPRII) is a direct target of miR-21 in PC3 and LnCap prostate cancer cells (Qin et al., 2009). Together, these studies indicate the existence of an additional level of complexity in the modulation of the BMP pathway.

1.1.3.2 BMPs and drug resistance in cancer

Cancer cell chemoresistance is considered as a major impediment in medical oncology. Emerging studies indicated that drug resistance of cancer cell is able to be related to various factors such as epigenetics, miRNAs and cytokines (Bach et al., 2017a; Easwaran et al., 2014; Jones et al., 2016). Such a phenomenon has been indicated for the superfamily member TGFβ, which is suggested as an emerging player in drug resistance (Brunen et al., 2013), BMPs and their components have been also implicanted to various different drug resistance of cancer. Indeed, Wang *et al* recently demonstrated that the resistance of lung squamous cell carcinoma patients with EGFR mutations to EGFR-TKIs was, in part, due to activation of the BMP-BMPR-SMAD1/5 signaling pathway (Wang et al., 2015). Subsequently, the combined treatment of these cancer cells together with inhibitors specific to BMPR may overcome the resistance to EGFR-TKIs (Wang et al., 2015). Xian *et al* enrolled 938 patients with stage III or IV NSCLC and reported that patients with high-level expression of BMP4 had a significantly higher chance of being resistant to chemotherapy than those with low BMP4 expression (Xian et al., 2014). Du *et al* reported that knockdown of BMP2 increased chemoresistance of the MCF-7 breast cancer cell line (Du et al., 2014). Similarly, Liu *et al* also suggested that hypermethylation contributed to the regulation of BMP6 during the acquisition of drug resistance in breast cancer cells (Liu et al., 2014). BMP6 was recently indicated to induce castration resistance in prostate cancer cells via tumor-infiltrating macrophages (Lee et al., 2013). Choi *et al* also demonstrated that treatment with BMP2 *in vivo* leads to increased tumor growth and chemotherapy resistance (Choi et al., 2015). Octamer-binding transcription factor (Oct)4 and nestin, stem cell markers that promote cell survival, are highly associated with resistance to chemotherapeutic agents, suggesting that the failure of cancer treatment and BMP

signaling is a growth stimulator in cancer cells expressing Oct4 or nestin (Bourguignon et al., 2012; Wang et al., 2013; Wen et al., 2013). Langenfeld *et al* employed DMH2, a small molecule BMP inhibitor, and found that DMH2 also significantly suppressed cell growth of nestin/green fluorescent protein (GFP) or Oct4/GFP-expressing cells (Langenfeld et al., 2013). Similarly, Coffman *et al* found that human ovarian carcinoma-associated mesenchymal stem cells (CA-MSCs) promote chemotherapy resistance of ovarian cancer by stimulating the BMP4/Hedgehog (HH) signaling pathway (Coffman et al., 2016). However, employing the HH inhibitor, IPI-926, prevented CA-MSC-mediated increases in chemotherapy resistance and tumor growth (Coffman et al., 2016).

Conversely, Persano *et al* reported that BMP2-based treatment increased the Temozolomide response in hypoxic drug-resistant glioblastoma multiforme (GBM)-derived cells (Persano et al., 2012). Eramo *et al* indicated that chemotherapy resistance is one of the leading reasons for poor GBM (Eramo et al., 2006) among the most aggressive tumor types. However, Tate *et al* found that a BMP7 variant may reduce tumor growth and stem cell marker expression in subcutaneous and orthotopic glioblastoma stem-like xenografts (Tate et al., 2012). Lian *et al* also demonstrated that knockdown of BMP6 in breast cancer cells increased chemoresistance to doxorubicin by upregulating multiple drug resistance-1/P-glycoprotein expression and activating the ERK signaling pathway (Lian et al., 2013). Overall, BMPs and their involvements highly related to drug resistance of cancer cells and employing BMP family inhibitors may promisingly enhance efficiency of cancer treatment.

1.1.3.3 Bioactive compounds targeting the BMP pathway

Natural compounds have been employed to cancer treatment for thounsands of years and therefore, targeting BMPs with dietary natural product-derived compounds is considered one of several therapeutic strategies in preventing cancer progression. To illustrate, Craft *et al* demonstrated that genistein, a component of soybean, therapeutically induces reversion to a low-motility phenotype in aggressive endoglin-deficient human prostate cancer cells by activating anaplastic lymphoma kinase (ALK)2-SMAD1 endoglin-associated signaling (Craft et al., 2008). Hallahan *et al* indicated that retinoid treatment may abrogate tumor growth in medulloblastoma xenografts (Hallahan et al., 2003). Using specific retinoid receptor agonists and gene expression arrays, they identified BMP2 as a candidate mediator of retinoid activity (Hallahan et al., 2003). Retinoid-stimulated expression

of BMP2 is subsequently important and sufficient for apoptosis of retinoid-responsive cells and the expression level of BMP2 by retinoid-sensitive cells is sufficient to promote apoptosis in surrounding retinoid-resistant cells (Hallahan et al., 2003). Kodach *et al* also reported that statins, which induce apoptosis in colorectal cancer (CRC) cells via stimulation of BMP2, may only be effective in SMAD4-expressing CRCs and have adverse effects in SMAD4-negative tumors (Kodach et al., 2007). Subsequently, based on these possible effects of statins on bone tissue, Chen *et al* found that simvastatin induces osteoblast viability and differentiation via the RAS/SMAD/ERK/BMP2 signaling pathway (Chen et al., 2010).

Additionally, by employing *in silico* screening, Ahmed *et al* attempted to identify new low-molecular-weight drug-like compounds with high theoretical scores to bind to Noggin to suppress the BMP-Noggin interaction (Ahmed et al., 2010). Sanvitale *et al* also identified a new small molecule inhibitor of BMP signaling, K02288, a highly selective 2-aminopyridine-based inhibitor with *in vitro* activity against ALK2 at lower concentrations, similar to the current lead compound, LDN-193189, by screening a panel of 250 recombinant human kinases (Chen et al., 2010). In conclusion, the identifying bioactive compounds that specifically target BMPs and their involvement will provide the promising for high-through screening in a range of *in vitro* and *in vivo* models of disease where BMP functions are implicated. The progression of this study will drive towards clinical trials for new potential inhibitors of BMPs and their involvements in cancer treatment.

1.1.4 Nicotinamide N-methyltransferase in cancer

Deregulated metabolic pathways could affect cancer cell biology in various different ways that extend beyond simply providing primary building blocks and energy to support tumorigenesis (Ulanovskaya et al., 2013). Nicotinamide (NCA) N-methyltransferase (NNMT, EC 2.1.1.1), a cancer-associated metabolic enzyme, that can catalyze the transfer of the methyl group from S-adenosyl methionine (SAM) to NCA, generating S-adenosylhomocysteine (SAH) and 1-methylnicotinamide (1-MNA) (Ulanovskaya et al., 2013) is commonly overexpressed in various human tumors (Bach et al., 2018a). NNMT is implicated in various disease conditions such as metabolic disorders, neurodegenerative diseases and cancer, and tissue NNMT expression or plasma levels of its product MNA have been proposed as cancer biomarkers for these conditions (Kannt et al., 2018). NNMT exhibits a high expression levels in the liver and follows a bimodal frequency distribution which might results in differences among individuals in the metabolism and therapeutic effect of drugs (Zhang et al., 2014a). NNMT also can promote epithelial-mesenchymal transition in gastric cancer cells through stimulating TGF-β1 expression (Liang et al., 2018) while NNMT silencing can stimulate tumor suppressor PP2A, inactive oncogenic serine/threonine kinases, and suppress tumor forming ability (Palanichamy et al., 2017).

In drug resistance cells, NNMT might enhance resistance to 5-fluororacil in colorectal cancer cells through suppression of the ASK1-p38 mitogen-activated protein kinase pathway (Xie et al., 2016). Williams et al. also indicated that NNMT overexpression might contribute all fundamental events, in which NCA appears to be involved. NCA is suggested as a part of the NAD molecule, which participates in a wide range of biological processes, including cellular resistance and energy production (Williams and Ramsden, 2005).

1.1.5 Yuanhuadine

Yuanhuadine (YD), is a natural product and a daphnane-type diterpenoid that has been isolated from the flower buds of Daphne genkwa (Thymelaeceae), a medicinal plant widely distributed in Korea and China (Hong et al., 2011; Zhang et al., 2007). A recent study indicated that YD could strongly suppress lung cancer cells compared to other cancer cell lines without cytotoxic against MRC-5 normal lung epithelial cells (Hong et al., 2011). Hong et al. further found that YD can contribute the cell cycle and suppress Akt/mTOR and EGFR signaling pathways in A549 cells and the antitumor activity of YD has been confirmed in an A549 cell-implanted xenograft model (Hong et al., 2011).

In drug resistance of NSCLC studies, Bae et al. attempted to enhance AXL degradation to overcome acquired gefitinib-resistance by the treatment of gefitinib-resistant NSCLC cells with YD, a potent antitumor agent in NSCLC (Bae et al., 2015). They found that treatment with YD effectively could suppress the cancer cell survival *in vitro* and *in vivo*. Mechanistically, YD could accelerate the turnover of AXL by presenilin-dependent regulated intramembrane proteolysis and result in the down-regulation of the full-length AXL. Recently, Bae et al. also employed YD in drug resistance of NSCLC cells and found that treatment with YD could effectively elevate Serpin B2 levels and suppress invasive properties in H292-Gef cells (Bae et al., 2016).

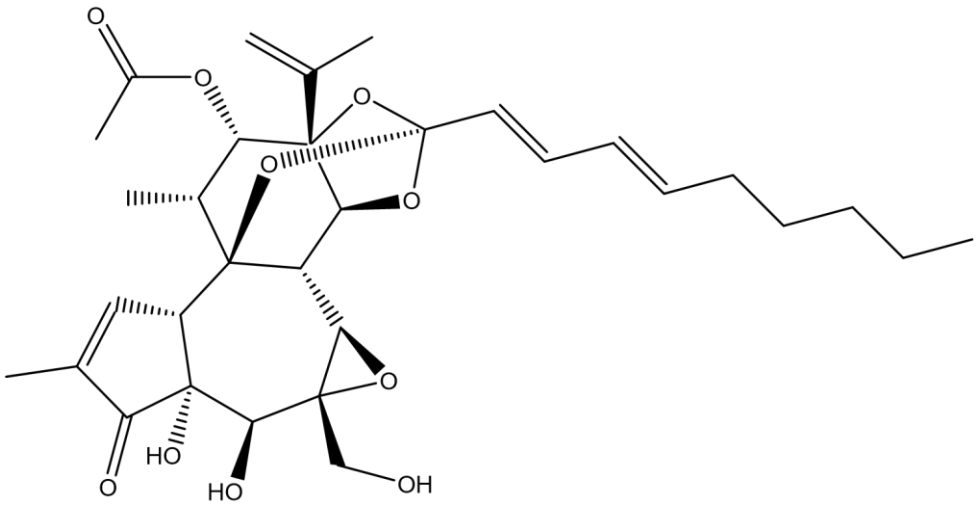

Figure 3: Chemical structure of yuanhuadine.

1.2 The purpose of this study

Even though YD showed a therapeutic promise against cancer growth in both parental lung cancer and drug resistance of NSCLC cells studies, therapeutic effects of this natural product on miRNAs in EGFR-TKI-resistant NSCLC cells remain poorly understood. Besides, based on the significance of investigating resistance mechanisms in EGFR-TKI treatment, the present study also attempts to explore the novel mechanisms of resistance in drug-resistant NSCLC cells. Subsequently, this study focused on several cancer biomarkers such as miRNAs, BMP4 and NNMT and also employed YD to this drug resistance of NSCLC cells to overcome the resistance. Detailed descriptions are found in the introductions of Part 2 and Part 3. Activation of NNMT has not been reported as a resistance mechanism of EGFR-TKIs in NSCLC yet, and the cause of this activation is unclear also. High BMP4 expression has been indicated as a poor prognostic marker in lung cancer. However, the relationship between BMP4 and EGFR-TKI resistance has not been reported yet.

In the present study, it was proven that up-regulation of NNMT and BMP4 and down-regulation of miR-139-5p and miR-449a result in gefitinib resistance. Subsequently, targeting these resistance mechanisms may serve as possible therapeutic strategies. Moreover, it is suggested that YD, a daphnane-type diterpene antitumor agent isolated from *Daphne genkwa*, has also the potential to reverse these mechanisms to overcome resistance.

[Chapter 2] Targeting Nicotinamide *N*-methyltransferase and miR-449a in EGFR-TKI-resistant non-small cell lung cancer cells

2. 1 Introduction

Lung cancer remains the leading cause of cancer death worldwide, with two main histological groups: small cell lung cancer cells and non-small-cell lung cancer (NSCLC), which presents 85% of all lung cancer cases (Molina et al., 2008). Despite process in therapeutic strategies for advanced NSCLC, the curative effects seem to have reached a plateau, and patient prognosis has remained poor. Moreover, studies examining the activation of specific genes in EGFR-TKI-resistant NSCLC cells, and the treatment of those overexpressed genes, have been thoroughly investigated. Subsequently, novel therapeutic approaches are necessarily required to elucidate the molecular mechanisms in drug-resistant cancer cells.

Accumulating evidence suggests that the deregulation of metabolic enzymes might frequently have pro-tumorigenic effects. Nicotinamide (NCA) N-methyltransferase (NNMT) is a cytosolic enzyme that catalyzes the transfer of the methyl group from S-adenosyl methionine (SAM) to NCA, generating S-adenosylhomocysteine (SAH) and 1-methylnicotinamide (1-MNA) (Ulanovskaya et al., 2013). NNMT is overexpressed in a variety of cancers, including liver, kidney, bladder, and colon, and has been shown to promote the migration, invasion, proliferation, and survival of cancer cells (Roessler et al., 2005; Tang et al., 2011; Tomida et al., 2008). Despite considerable experimental evidence that NNMT induces tumorigenesis and may thus represent a potential anticancer target, the actual functions of this enzyme in chemo-resistant tumors have not yet been fully investigated, especially in EGFR-TKI acquired resistant NSCLC cells.

A large body of evidence suggests the critical function of microRNAs (miRNAs) in epigenetically modulating different phenotypic stages in drug-resistant tumors (Engelman and Settleman, 2008; Holohan et al., 2013; Migliore and Giordano, 2013). Our recent study also described the role of miRNAs in the regulation of various aspects of tumor progression associated with drug resistance (Bach et al., 2017a; Bach and Lee, 2018). The small, non-coding molecules known as miRNAs elicit their regulatory effects by binding imperfectly to the 3’ UTR of their target mRNA, leading either to degradation of the mRNA or suppression of its translation into functional protein (Liu et al., 2005; Saxena et al., 2003). Moreover, the aberrant expression of miRNAs is highly correlated with cancer development (Bach et al., 2017a; Bach and Lee, 2018).

In general, antitumor agents can suppress cancer cell growth through the regulation of cell signal transduction or proliferation (Bachegowda et al., 2016; Kim et al., 2017; Weir et al., 2016; Yu et al., 2016). Importantly, we have previously found that natural product-derived compounds,

including the antitumor agent yuanhuadine (YD), could enhance the antitumor activity of chemotherapeutic agents through different mechanisms (Bae et al., 2015; Hong et al., 2011), suggesting that these compounds could exert their pleiotropic effects on cancer treatment by regulating various cell signaling pathways. Herein, we attempted to elucidate the role of NNMT in EGFR-TKI resistance in NSCLC cells and the dynamic interactions of NNMT with miR-449a in tumor microenvironment. Further studies also indicated that YD can modulate to both NNMT and miR-449a expression and therefore overcome drug resistance. These findings will highlight potential new strategies for the treatment of cancer patients with EGFR-TKI-resistant NSCLC.

2.2 Materials and methods

2.2.1 Reagents

RPMI 1640 medium and Opti-MEM Reduced Serum Medium were purchased from Invitrogen (Invitrogen, CA, USA). Mouse anti-β-actin and anti-NNMT (G-4) were purchased from Santa Cruz Biotechnology (Santa Cruz, CA, USA). Rabbit anti-Akt, anti-phospho-Akt (Ser^{473}), and anti-PTEN were purchased from Cell Signaling Technology (Danvers, MA, USA). Yuanhuadine (YD; purity > 98.5%) was isolated and identified from a $CHCl_2$-soluble fraction of the flowers of *Daphne genkwa*, as described previously (Bae et al., 2015; Hong et al., 2011).

2.2.2 Cell culture and establishment of EGFR-TKI resistance of NSCLC cells

Human lung carcinoma H292 and H1993 cells were obtained from the American Type Culture Collection (Manassas, VA, USA). The cell lines were cultured in RPMI 1640 medium supplemented with 10% FBS and antibiotics-antimycotics (PSF; 100 unit/mL penicillin G sodium, 100 μg/mL streptomycin, and 250 ng/mL amphotericin B). Gefitinib (gef)-resistant H292 (H292-Gef) cells were developed by our group as described previously (Bae et al., 2015), while erlotinib (erl)-resistant H292 (H292-Erl) cells were developed from the parental H292 cells though continuous exposure to gradually increasing concentrations of erl (Selleckchem. Houston, TX, USA) and maintained in RPMI 1640 medium containing 1 μM erl. Similarly, to establish gef-resistant H1993 cells (H1993-Gef) and erl-resistant H1993 cells (H1993-Erl), H1993 cells were continuously exposed to increasing drug doses up to 10 μM of gef and erl. Subsequently, H1993 cells with established resistance were maintained in medium containing 10 μM of gef and erl. All

cells were incubated at 37ºC in a humidified atmosphere containing 5% CO_2 and sub-cultured at least twice a week. Cells passaged more than three times were used for the experiments.

2.2.3 Transfection of small interfering RNAs and microRNA

The small interfering RNA (siRNA) sequences (Stealth RNAi siRNA, Invitrogen) targeting NNMT (siNNMT-1: Cat. No. HSS181544, siNNMT-2: Cat. No. HSS107222, siNNMT-3: Cat. No. HSS107223), the negative control (NC) (Negative Universal Control™ Med Cat. No. 46-2001), the miR-449a mimic (mirVana miRNA Mimic, assay ID MC11127) and the NC (mirVana miRNA Mimic NC No. 1, Applied Biosystems) were transfected into the cell lines by electroporation using Lipofectamine RNAiMAX (Invitrogen, CA, USA) according to the manufacturer's recommendations. The cells were harvested for subsequent experiments 24 h and 48 h post-transfection for real-time PCR and western blot analysis, respectively.

2.2.4 RNA extraction and real-time polymerase chain reaction (PCR)

RT-PCR was used to determine the gene expression. Briefly, the indicated cells were cultured in 36-mm dishes for 24 h. The cells were then treated with various indicated concentrations of YD for an additional 24 h. Total cellular RNA was extracted with TRIzol reagent according to the manufacturer's instructions. The total RNA (1 μg) that was isolated from the cells was used for reverse transcription reaction with Reverse Transcription Reagents. The cDNA was reverse transcribed at 42 °C for 60 min with 0.5 μg of oligo $(dT)_{15}$ in a reaction volume of 20 μL using the reverse transcription system (Promega, MI, USA). Gene-specific primers for real-time PCR were synthesized by Bioneer Corporation (Daejeon, Korea): human NNMT sense: 5′-TGTGTGATCTTGAAGGGAACAG-3′, antisense: 5′-CTTGACCGCCTGTCTCAAC-3′; human β-actin sense: 5′-AGCACAATGAAGATCAAGAT-3′, antisense: 5′-TGTAACGCAACTAAGTCATA-3′. Real-time PCR was conducted using a MiniOpticon system (Bio-Rad, Hercules, CA, USA); each PCR amplification included 5 μL of reverse transcription product, iQ SYBR Green Supermix (Bio-Rad, Hercules, CA, USA), and primers in a total volume of 20 μL. The following standard thermo cycler conditions were employed: 95 °C for 20 s prior to the first cycle; 40 cycles of 95 °C for 20 s, 56 °C for 20 s, and 72 °C for 30 s; 95 °C for 1 min; and 55 °C for 1 min. The threshold cycle (C_T), indicating the fractional cycle number at which the amount of amplified target gene reached a fixed threshold for each well, was determined using the

MJ Opticon Monitor software package (Bio-Rad, Hercules, CA, USA). Relative quantification, representing the change in gene expression in real-time quantitative PCR experiments between a sample-treated group and the untreated control group, was calculated by the comparative C_T method in accordance with previously described methods (Bach et al., 2017b; Bach et al., 2015). The data were analyzed by evaluating the expression $2^{-\Delta\Delta CT}$, where $\Delta\Delta C_T$ = (C_T of target gene − C_T of housekeeping gene) treated group − (C_T of target gene − C_T of housekeeping gene) untreated control group. For the treated samples, the evaluation of $2^{-\Delta\Delta CT}$ represents the fold change in gene expression relative to the untreated control, normalized to a housekeeping gene.

2.2.5 Plasmid transfection

FuGENE HD Transfection Reagent (Roche Applied Science) was used to transfect plasmid pcDNA™3.1(+)-NNMT (#RG200641 from Origene) or pCMV6-AC-GFP (#PS 100010) control vector into parental NSCLC cells. All transfections procedures were performed according to the protocol provided by the manufacturer. After transfection for 48 h, NSCLC cells were harvested and extracted for protein isolation.

2.2.6 miRNA quantitative polymerase chain reaction (PCR)

To determine the expression of miR-449a in NSCLC cells, we used the TaqMan® MiRNA Assay kit (Applied Biosystems) (Cat. No. 4427975) following the manufacturer's protocol. In detail, miRNA expression was determined by collecting total RNA from 90% confluent cells. Total RNA was isolated using TRIzol (Invitrogen, CA, USA) and then converted to cDNA using the TaqMan® MiRNA Assay (Part No. 4366596) according to the manufacturer's protocol. The specific primer for mature miRNA was hsa-miR-449a (5′-UGGCAGUGUAUUGUUAGCUGGU-3′). The miR-449a (Assay ID: 001030) expression levels were analyzed using Taqman quantitative real-time PCR (TaqMan MicroRNA Assay, Applied Biosystems) and normalized to the RNU6B, an endogenous control (Assay ID: 001093). All reactions were performed in triplicate.

2.2.7 Cell proliferation assay

The indicated cells were seeded in 96-well plates with various concentrations of YD and incubated at 37 °C in a humidified atmosphere with 5% CO_2. After incubation, the cells were fixed with a 50% trichloroacetic acid (TCA) solution for 1 h, and cellular proteins were stained with 0.4%

sulforhodamine B (SRB) in 1% acetic acid. The stained cells were dissolved in 10 mM Tris buffer (pH 10.0). The effect of SA on cell proliferation was calculated as a percentage relative to a solvent-treated control, and the IC_{50} values were evaluated using nonlinear regression analysis (percent survival *versus* concentration).

2.2.8 Flow cytometry for cell cycle analysis

The indicated cells were plated in a 36-mm culture dish and incubated for 24 h. Following a 24 or 48 h treatment, the cells were harvested (via trypsinization and centrifugation), rinsed twice with pre-cooled phosphate buffered saline (PBS), and prepared for apoptosis and cell cycle analysis.

For cell cycle analysis, 1 mL of pre-cooled 70% ethanol was added, and the cells were fixed overnight at −20 °C. Next, fixed cells were washed with PBS and incubated with a staining solution containing RNase A (50 μg/mL) and propidium iodide (PI) (50 μg/mL) in PBS for 30 min at room temperature. The cellular DNA content was analyzed with a FACSCalibur® flow cytometer (BD Biosciences, San Jose, CA, USA). At least 10,000 cells were used for each analysis, and the distribution of cells in each phase of the cell cycle was displayed using histograms.

2.2.9 Analysis of drug combination

The cells were post-transfected with siNNMT and/or miR-449a and their scramble siRNA and/or NC miRNA, then, the transfected cells were determined using the SRB assay. The combination effect was evaluated as described previously (Bae et al., 2015) and the CI values were compared to the reference values reported by Chou (Chou, 2006).

2.2.10 Western blot analysis

The indicated cells were placed in a 36-mm culture dish and incubated for 24 h. After treatment, the protein was extracted with lysis buffer, and the protein concentrations were determined using the bicinchoninic acid (BCA) method. A 40 μg protein sample was collected from each group, boiled for 10 min, loaded onto 10% SDS-PAGE gels, and then transferred to PVDF membranes with electroblotting. Membranes were blocked for 1 h with 5% fat-free milk at room temperature, rinsed with PBS, and incubated with diluted primary antibodies 1:1000 or 1:500 overnight at 4 °C. Then, the membranes were incubated with specific secondary antibodies (1:1000) for 2 h and rinsed with PBS. The expression of β-actin was used as an internal standard. Proteins were detected

with an enhanced chemiluminescence detection kit from GE Healthcare (Little Chalfont, UK) and an LAS-4000 Imager (Fuji Film Corp., Tokyo, Japan).

2.2.11 Methylation-specific PCR

The methylation status of the PTEN promoter was determined by methylation-specific PCR after bisulfite-modification. The methylation sites of the PTEN gene promoter involved region sites MF (5′ – TTCGTTCGTCGTCGTCGTATTT – 3′), MR (5′ – GCCGCTTAACTCTAAACCGCAA – 3′), UF (5′ – GTGTTGGTGGAGGTAGTTGTTT – 3′), and UR (5′ – ACCACTTAACTCTAAACCACAACCA – 3′). Genomic DNA was isolated and modified by bisulfite using an EpiTect Bisulfite kit (Qiagen, Valencia, CA). Then, the Epitect Methylight PCR kit (Cat. No. 59496, Qiagen, Valencia, CA) was employed for quantitative, real-time probe-based PCR analysis of methylation status. Methylated and un-methylated genomic regions can be amplified by PCR using each sequence-specific pair of primers.

2.2.12 NNMT enzyme assay

The NNMT enzyme activity was measured using S-adenosyl methionine (SAM) as the methyl group donor and nicotinamide as the substrate from Biovision (Milpitas, CA, USA) (Cat No. K822-100) according to the manufacturer's instructions.

2.2.13 5-Aza-2'-deoxycytidine treatment

A stock solution of 10 mM 5-Aza-2'-deoxycytidine (5-Aza) obtained from Sigma was prepared in DMSO. H292-Gef, H1993-Gef, HCC-Gef and PC-9-Gef cells were treated for 24 h with 10 μM 5-Aza, and total protein or RNA was extracted for western blotting or qRT-PCR, respectively.

2.2.14 Colony formation assay

Resistant NSCLC cells were plated in a 35-mm culture dish at a density of 100 cells/dish. Twenty-four hours later, fresh medium containing NNMT siRNA or control siRNA was added to culture dishes. Forty-eight hours post-transfection with NNMT siRNA, the cells were washed with PBS or treated with gef for an additional 24 h and allowed to grow in plasmid-free medium for 14 days (37ºC, 100% humidity, 5% CO_2 atmosphere). Cell colonies were fixed with 2% paraformaldehyde,

stained with crystal violet (0.5% w/v), and then counted visually or by using ImageJ software. The percentage of cells surviving the treatment relative to solvent-treatment controls was calculated.

2.2.15 cDNA microarray expression analysis

The cDNA array was continuously employed as described previously (Bae et al., 2016) to analyze and compare H292-Gef cells treated with YD (10 nM) and non-treated H292-Gef cells.

2.2.16 *In vivo* tumor xenograft model

All animal experiments and care were conducted in a manner that conformed to the Guidelines of the Institutional Animal Care and Use Committee at Seoul National University and were approved by the Korean Association of Laboratory Animal Care (Permission number: SNU-161117-1).

For the nucleic acid *in vivo* study, miR-449a, control miRNA, siNNMT and control siRNA were purchased from Bioneer Corporation (Daejeon, Korea). These miRNAs and siRNAs were conjugated to *in vivo*-jetPEI transfection reagent (Polyplus-transfection Inc., New York, NY, USA) according to the manufacturer's instructions. Male mice aged 4 – 6 weeks were purchased from the National Laboratory Animal Centre. These mice received 200 μl subcutaneous transplants that consisted of 1×10^7 cells of PC-9-Gef. On day 14 post-implantation, the mice were randomly divided into four groups (n = 5 per group): (1) Control miRNA + control siRNA, (2) control miRNA + siNNMT, (3) control siRNA + miR-449a, and (4) miR-449a + siNNMT treated with multipoint intratumoral injection (10 μg per 100 μl per tumor for siRNAs two times per week and 20 μg per 100 μl per tumor for miRNAs three times per week) of these nucleic acids complexed with *in vivo*-jetPEI in 5% glucose for 3 weeks. After completion of the treatment over 1 additional week, the mice were sacrificed, and the mouse weight, tumor weight, number of nodules, and distribution of the tumors were recorded.

H1993-Gef and PC9-Gef cells were injected subcutaneously into the flanks of the mice (1×10^7 cells in 200 μL of medium), and tumors were allowed to grow. When the tumor volume reached approximately 400 mm^3 (H1993-Gef) and 150 mm^3 (PC9-Gef), the mice were randomized into vehicle control and treatment groups (n = 5). YD (1 mg/kg) or Gef (10 kg/mg) dissolved in a volume of 150 μL of vehicle solution (Tween 80-ethanol-H_2O), 1:1:98) was administrated orally once a day for 22 days. The control group was treated with an equal volume of vehicle. The tumor volume was monitored two times per week for 22 days using calipers and estimated using the

following formula: tumor volume (mm^3) = (width) × (length) × (high) × π/6. The body weight of each mouse was also monitored for toxicity.

2.2.17 Immunohistochemistry of human cancer tissues

The excised tumors were fixed in 4% paraformaldehyde (PFA) and embedded in paraffin. Sectioned slides of the embedded specimens were serially deparaffinized, and the samples were rehydrated and subjected to antigen retrieval. The slides were incubated overnight with the indicated antibody at 4ºC. After washing with PBS, the sections were incubated with HRP-conjugated anti-rabbit IgG for 30 min, washed with PBS, and then detected using the LSAB^{TM}+ System-HRP kit from Dako (Glostrup, Denmark) and counterstained with hematoxylin and eosin (H&E). Finally, the stained sections were observed and photographed under an inverted phase-contrast microscope.

2.2.18 *Ex vivo* biochemical analysis of tumors

A portion of frozen tumors excised from each nude mouse was thawed on ice and homogenized using a hand-held homogenizer in Complete Lysis Buffer (Active Motif, Carlsbad, CA, USA). Aliquots were stored at -80ºC, and the expression of protein, mRNA and miRNA levels of the tumor lysates were determined.

2.2.19 Molecular docking analysis

Molecular docking simulation was carried out using the SYBYL-X2.1.1 (Tripos Inc., St Louis, MO) with Surflex-Dock Geom mode. The chemical structure of yuanhuadine was prepared in a mol2 format, and the ligand was docked into chain A of the human nicotinamide N-methyltransferase downloaded from the Protein Data Bank (pdb:3ROD). Staged minimization was performed using Powell's method until the gradient converged to a value of 0.001 kcal/mol·Å. A MMFF94 force field was used with MMFF94 charges. Protomol was generated based on the location of the original ligands, S-adenosyl-L-homocysteine (SAH) and nicotinamide (NCA), with a threshold of 0.5 Å and bloat of 6 Å. The protein movement option was used to allow flexibility in the binding pocket of the protein. Docking performance was validated based on the docking scores, visual inspection, and the RMSD values of the re-docked poses compared with the original structure. Molecular interactions between the ligand and protein were further analyzed using the

Discovery studio 4.0 Visualizer (Biovia, San Diego, CA) or PyMOL-v1.0 (Schrödinger KK, Tokyo, Japan).

2.2.20 Statistical analysis

Data are expressed as means ± SD for the indicated number of independently performed experiments. Student's t-test or one-way analysis of variance (ANOVA) followed by Newman-Keuls multiple comparison test were used to examine between-group differences. Statistical significance was accepted at either * $p < 0.05$, ** $p < 0.01$, *** $p < 0.001$, *ns*: not significant. Data analyses were performed using Graphpad Prism (Version 6).

2.3 Results

2.3.1 The NNMT expression profile is inversely correlated to miR-449a expression in gef-resistant NSCLC tissues and cell lines

Previous findings suggest that the higher expression of NNMT in tumor tissues is associated with the lower overall survival rates in cancer patients. Therefore, there is an opposite correlation between the expression level of NNMT in tumor tissues and the duration of survival (http://kmplot.com/analysis/index.php?p=service&start=1). Using a cDNA microarray, we have also previously observed high expression of NNMT in EGFR-TKI-resistant cancer cells compared to their parental cells (Bae et al., 2016). These findings suggested that NNMT, one of the most over-expressed genes, might be considered a novel target gene in EGFR-TKI-resistant NSCLC cells. Consequently, we initially determined the expression level of NNMT in parental NSCLC cells, including H292 (EGFR wild-type), H1993 (MET amplification), HCC827 (EGFR mutation and MET amplification) and PC-9 (EGFR mutation), *versus* their EGFR-TKI-resistant NSCLC cells, including gefitinib (gef)- and erlotinib (erl)-acquired cells. We observed over-expression of NNMT mRNA in gef-resistant cells (H292-Gef, H1993-Gef and PC9-Gef) compared with their parental cells (Figure 4A). A similar phenomenon was also found in erl-resistant cells (H292-Erl, H1993-Erl, HCC827-Erl and PC9-Erl) (Figure 4B). To validate whether these findings might be associated with NNMT expression in EGFR-TKI-resistant tumors, the expression of NNMT in tumor tissues obtained from our previous *in vivo* studies was also investigated. Confirmation using

H292-Gef and PC9-Gef tumor tissues revealed that the levels of NNMT mRNA were also over-expressed in gef-resistant tissues (Figure 4C).

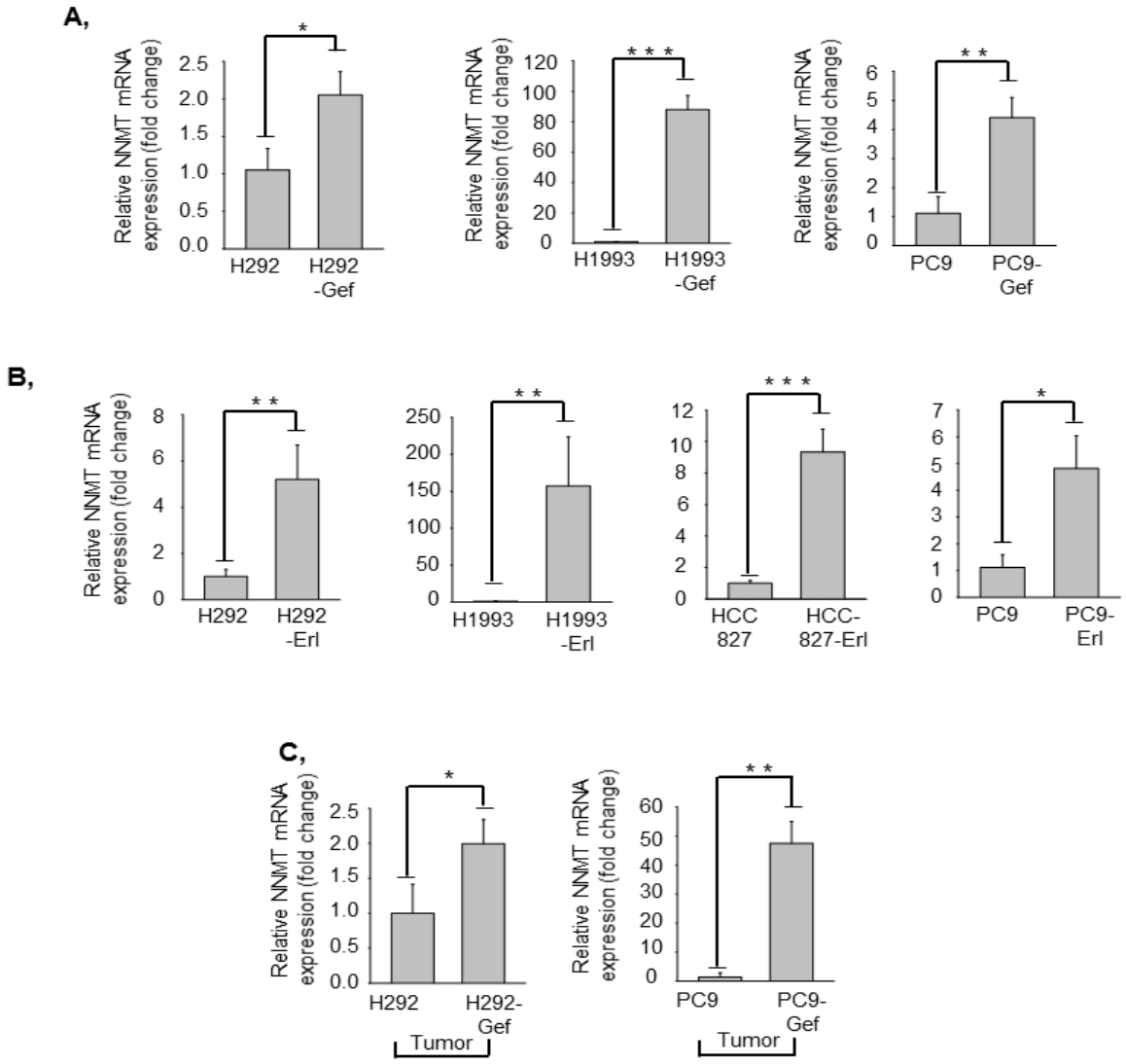

Figure 4: The expression of mRNA NNMT in gef-resistant NSCLC cell lines. (A & B) Characterization of the indicated parental or drug-resistant phenotype cell lines for NNMT expression at mRNA levels. (C) Characterization of the indicated parental or gef-resistant phenotype tissues for NNMT expression at the mRNA levels. Total RNA was isolated and analyzed by real-time PCR using NNMT-specific primers and normalized to β-actin expression.

Interestingly, we further observed that H1993 cells, which had the highest established gef and erl resistance at 10 μM drug, showed significant NNMT over-expression at both protein and mRNA levels in EGFR-TKI-resistant NSCLC cells compared with their parental cells.

Similarly, NNMT protein expression was up-regulated in H292-Gef, H1993-Gef (Figure 5A), H1993-Erl, and HCC827-Erl cells (Figure 5B) and in H292-Gef tumor tissues (Figure 5C). Immunohistochemistry (IHC) analyses also illustrated a higher NNMT level in gef-resistant tumors (H292-Gef, H1993-Gef) than in their parental tumors (Figure 6). Collectively, these data indicated that the basal levels of NNMT expression in gef- or erl-resistant NSCLC cells were over-expressed compared with their parental NSCLC cells.

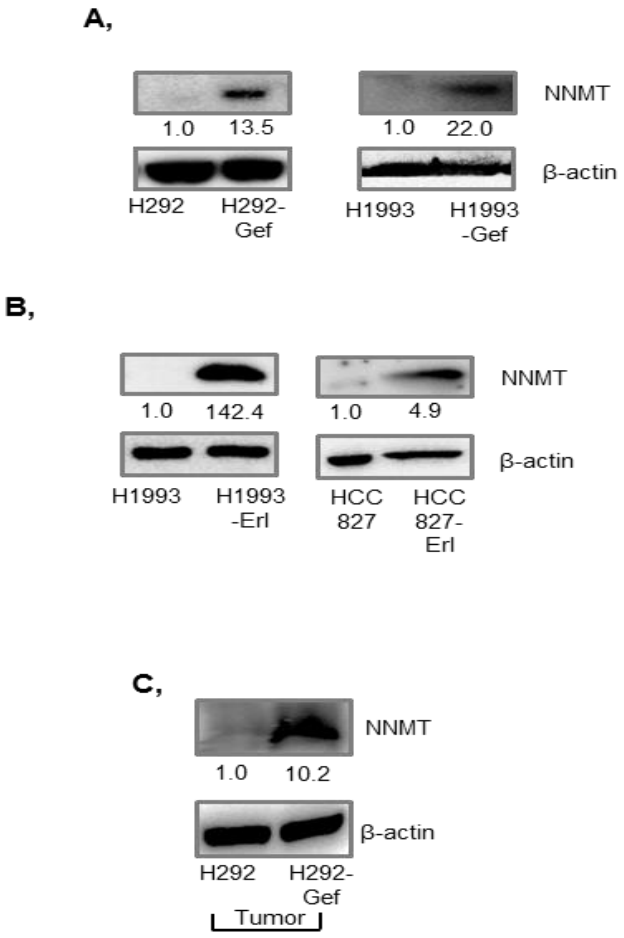

Figure 5: The expression of NNMT protein in gef-resistant NSCLC cell lines. (A & B) Confirmation of NNMT protein over-expression in drug-resistant cancer cell lines. (C) Confirmation of NNMT protein over-expression in gef-resistant tissues. The expression of NNMT protein was investigated by western blotting using β-actin as the loading control.

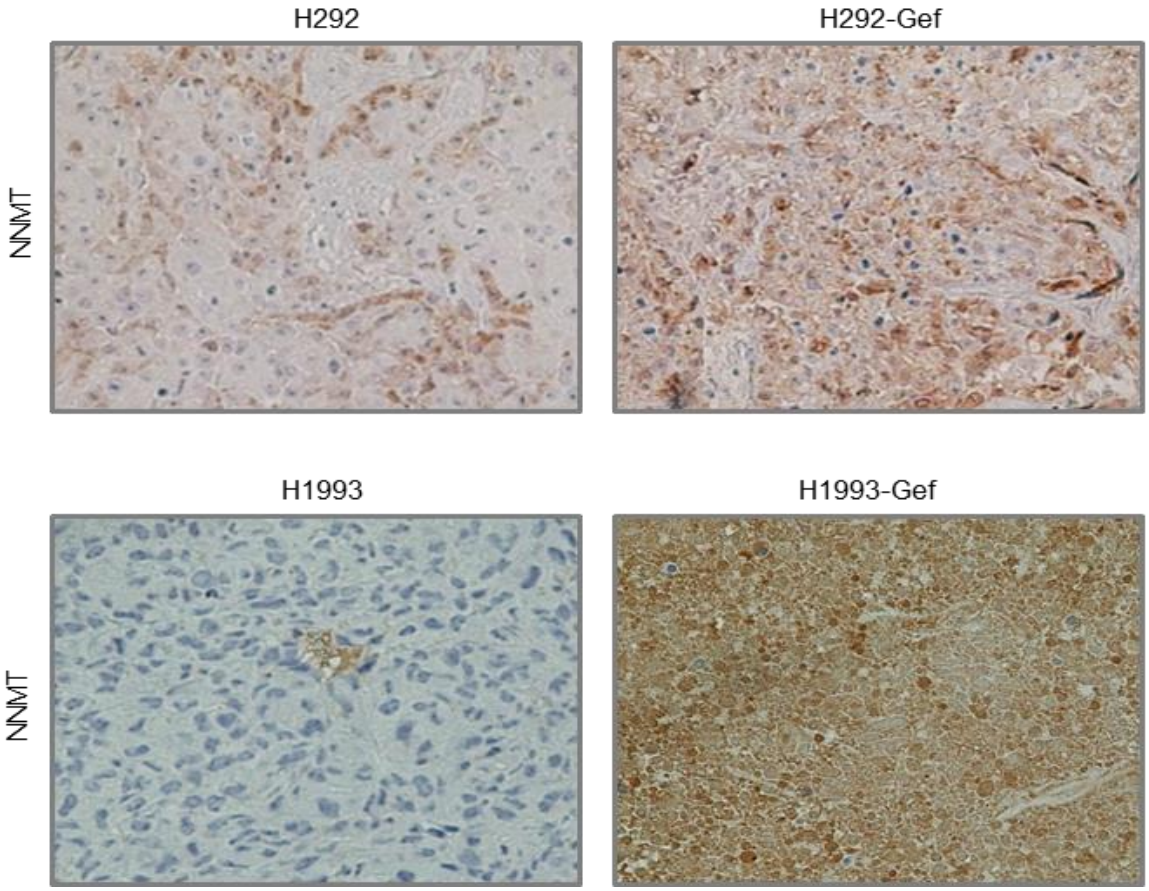

Figure 6: Immunohistochemistry of NNMT in tumor tissue sections. Immunohistochemical analysis of NNMT was performed using anti-NNMT antibody in tumor tissue sections.

Recently, miRNAs have been implicated in a wide range of cellular processes, as well as the critical function of miRNAs in the drug resistance of tumor cells, as recently reviewed by our group (Bach et al., 2017a; Bach et al., 2018b). Among various miRNAs, we initially analyzed miR-449a which has recently been described to have an important role in resistance to sunitinib, an oral multi-targeted tyrosine kinase inhibitor (TKI) (Qu et al., 2016). In addition, miR-449a is down-regulated in NSCLC and suppresses cancer cell migration and invasion (Luo et al., 2013). Subsequently, we found that miR-449a was down-regulated in gef-resistant NSCLC cells compared to their parental cells *in vitro* (Figure 7A) and *in vivo* in tumor tissues (Figure 7B). Furthermore, we observed that miR-449a was also down-regulated in H292-Erl and H1993-Erl (Figure 7C). These findings suggested that the expression of NNMT was up-regulated but miR-449a was down-regulated in EGFR-TKI-resistant NSCLC cells.

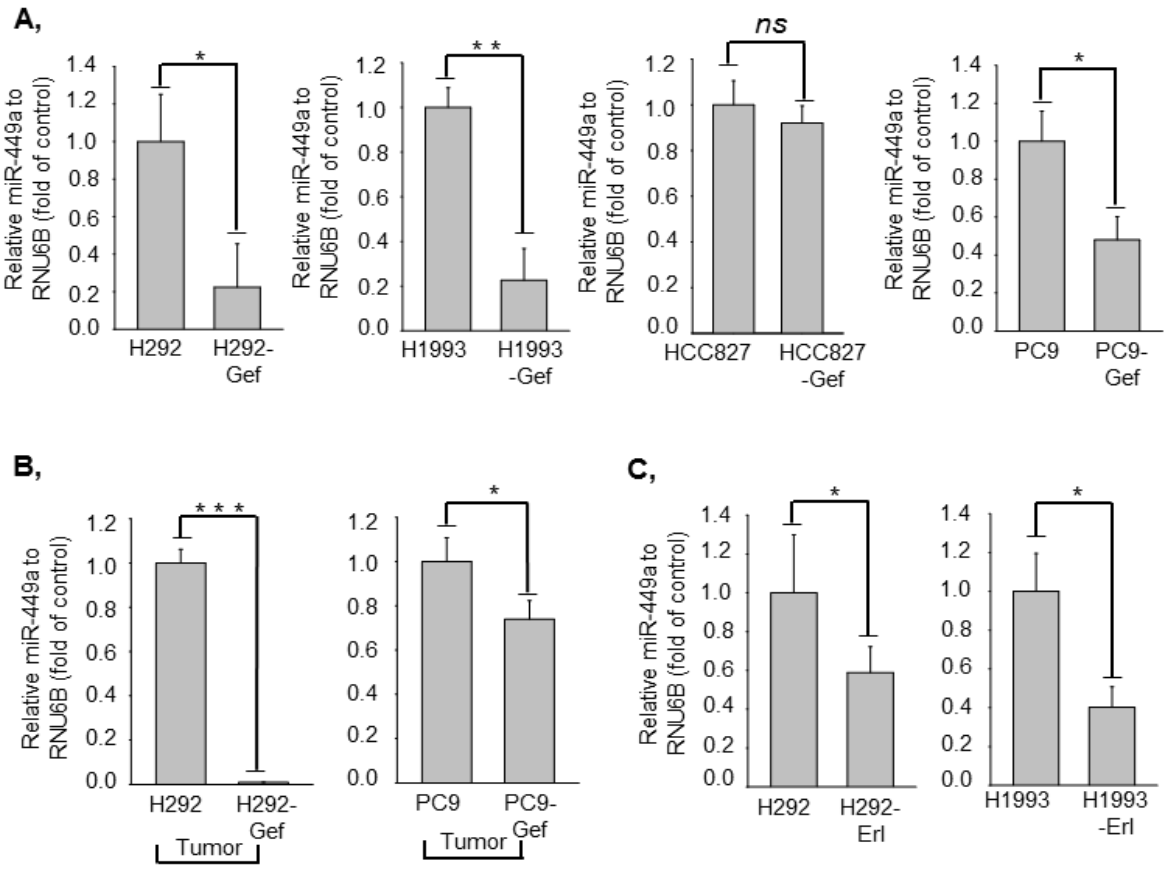

Figure 7. The expression of miR-449a in gef-resistant NSCLC tissues and cell lines. (A, B & C) Characterization of the indicated parental or drug-resistant phenotype cell lines (A & C) and tissues (B) for miR-449a expression. miR-449a levels were quantified by Taqman real-time PCR and normalized to RNU6B. Data are representative of three independent experiments. *ns*, not significant. *, $P < 0.05$; **, $P < 0.01$; ***, $P < 0.005$ by the *t*-test.

2.3.2 NNMT modulates gef-resistant NSCLC cells by interacting with miR-449a

The effects of NNMT on proliferation and metastatic potential have been reported in cancer cells (Tang et al., 2011; Yu et al., 2015). To investigate whether abnormal over-expression of NNMT is associated with the survival of gef-resistant NSCLC cells subjected to gef resistance, NNMT small interfering RNA (siRNA) was transfected into human gef-resistant NSCLC cells to knockdown intracellular NNMT expression. We found that knockdown of NNMT by siRNA interference restored gef sensitivity to gef-resistant NSCLC cells (Figure 8 and Table 1). Even though at 48 h, post-siRNA transfection had seemly no significant effects on G0/G1 phase or G2/M in cell cycle analysis (Figure 9), the treatment of NNMT siRNA effectively suppressed colony formation and enhanced activity with co-treatment of gef in gef-resistant NSCLC cells (Figure 10).

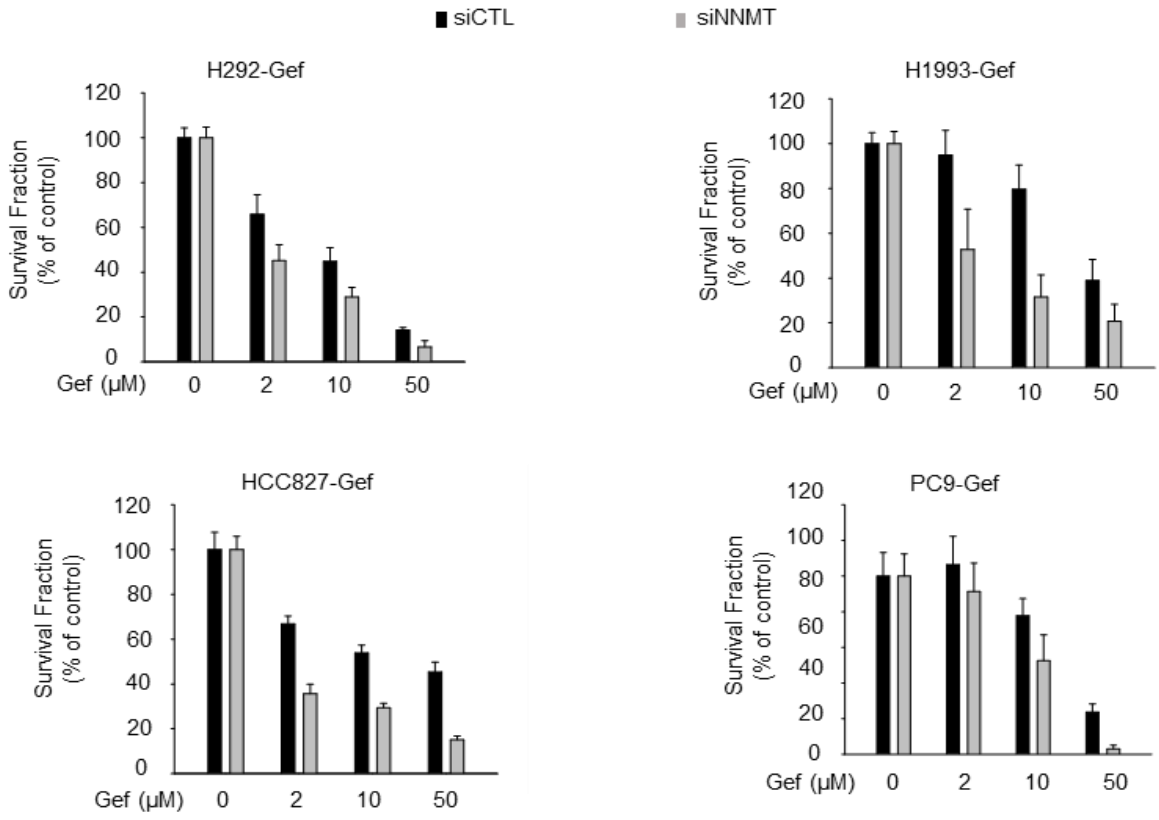

Figure 8. Effects of NNMT in gef-resistant NSCLC cell growth. Gefitinib sensitivity of the indicated gef-resistant phenotype cell lines. Cells were transiently post-transfected with scramble siRNA or NNMT siRNA for 48 h and then incubated with the indicated concentrations of gef. Cell viability was assessed by the SRB assay.

Table 1: Effects of gefitinib on the cell proliferation of NSCLC cells.

Cell line	IC_{50} of Gefitinib (μM)	
	siCTL	siNNMT
H292-Gef	7.6	0.5
H1993-Gef	13.1	2.3
HCC827-Gef	3.9	0.4
PC-9-Gef	5.5	2.1

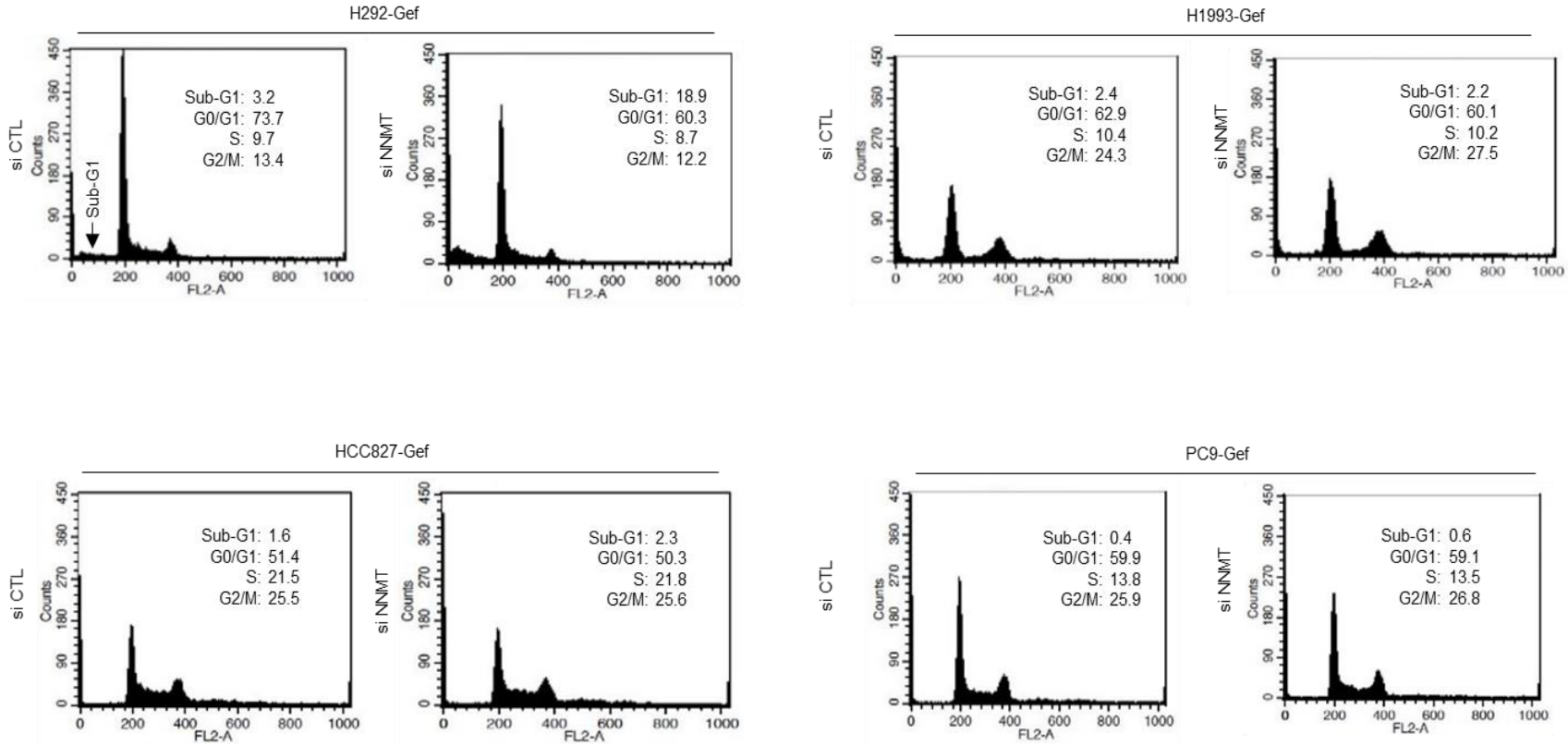

Figure 9. Cell cycle progression of gef-resistant phenotype cell lines. Cells were transiently transfected with either scramble siRNA or NNMT siRNA for 48 h. Transfected cells were subjected to FACS analysis.

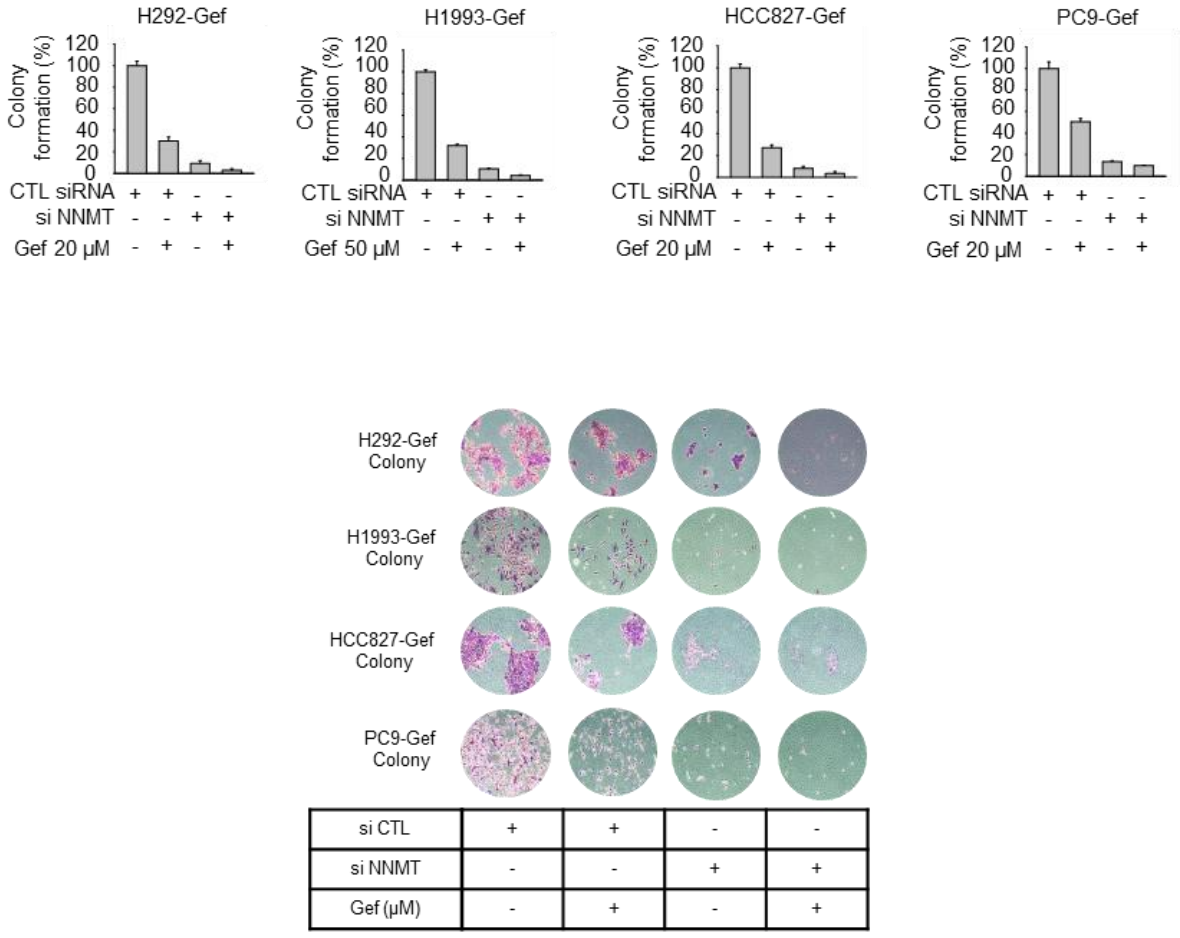

Figure 10: Colony formation of gef-resistant phenotype cell lines. Cells were transiently post-transfected with either scramble siRNA or NNMT siRNA for 48 h and then cultured with the indicated concentrations of gef and subjected to colony formations assays.

We further assessed the effects of miR-449a on cancer cell growth to determine whether miR-449a expression could alter gef sensitivity in resistant cells. When gef-resistant NSCLC cells were treated with exogenous miR-449a, the cellular level of miR-449a was significantly enhanced (Figure 11A). miR-449a-treated gef-resistant NSCLC cells were cultured in various concentrations of gefitinib (0.4 - 50 μM gef). As a result, miR-449a transduction significantly increased the gef sensitivity, with at least a 2-fold change in the IC_{50} for gef (Figure 11B & Table 2). These data indicated that the level of miR-449a expression affected the gef sensitivity in cancer cells.

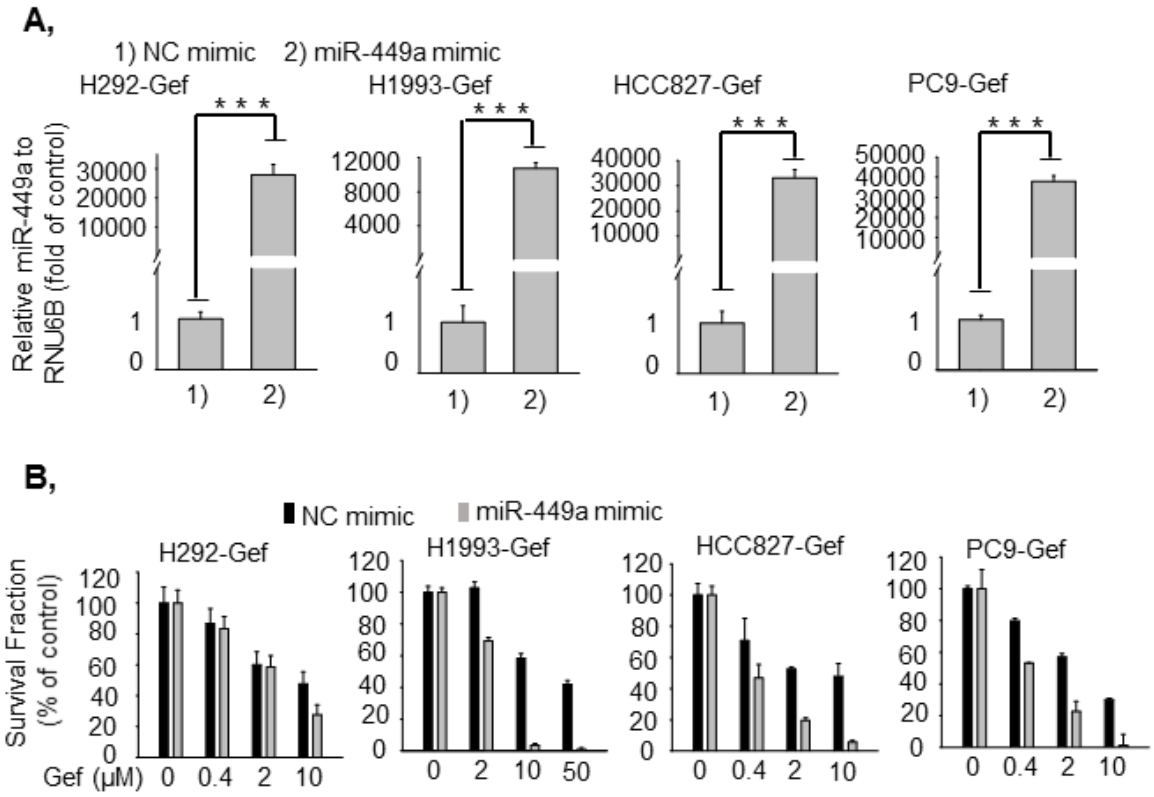

Figure 11: Effects of miR-449a mimic on the miR-449a expression in gef-resistant cell lines. (A) The indicated gef-resistant cell lines were cultured in six-well plates and then transfected with NC miRNA or miR-449a for 48 h (50 *p*mole/well). The levels of miR-449a expression were determined by Taqman real-time PCR with specific primers for mature miR-449a. Samples were normalized to RNU6B. (B) Gefitinib sensitivity of the indicated gef-resistant phenotype cell lines. Cells were transiently post-transfected with NC miRNA or miR-449a for 48 h and then incubated with the indicated concentrations of gef. Cell viability was assessed by the SRB assay.

Table 2: Effects of gefitinib on the cell proliferation of resistance NSCLC cells.

Cell line	IC_{50} of gefitinib (μM)	
	NC mimic	miR-449a mimic
H292-Gef	6.8	3.2
H1993-Gef	14.3	2.1
HCC827-Gef	2.7	0.3
PC-9-Gef	2.8	0.4

To further investigate the possible pathological relevance of the relationship between miR-449a and NNMT in gef-resistant NSCLC cells, we next assumed that the over-expression of NNMT could alleviate the expression of miR-449a in gef-resistant NSCLC cells. Subsequently, bio-informatics analysis (targetscan.org) led us to focus on NNMT as a possible predicted target of miR-449a *via* their potential bindings (Figure 12A). When we knocked down NNMT expression by its siRNA, the expression of miR-449a was up-regulated in gef-resistant NSCLC cells (Figure 12B). Collectively, these data suggested that NNMT was critical for the suppression of miR-449a in gef-resistant NSCLC cells. Based on these findings, we sought to experimentally determine whether dual inhibition of NNMT by NNMT siRNA and miR-449a exhibited a synergistic antitumor efficacy. The combination of NNMT siRNA and miR-449a showed significantly different p values compared with each treatment of NNMT siRNA or miR-449a, particularly the combination index (CI) was 0.285 at Gef 10 μM (synergism), which led to a remarkable inhibition of cell proliferation in PC9-Gef cells (Figure 12C).

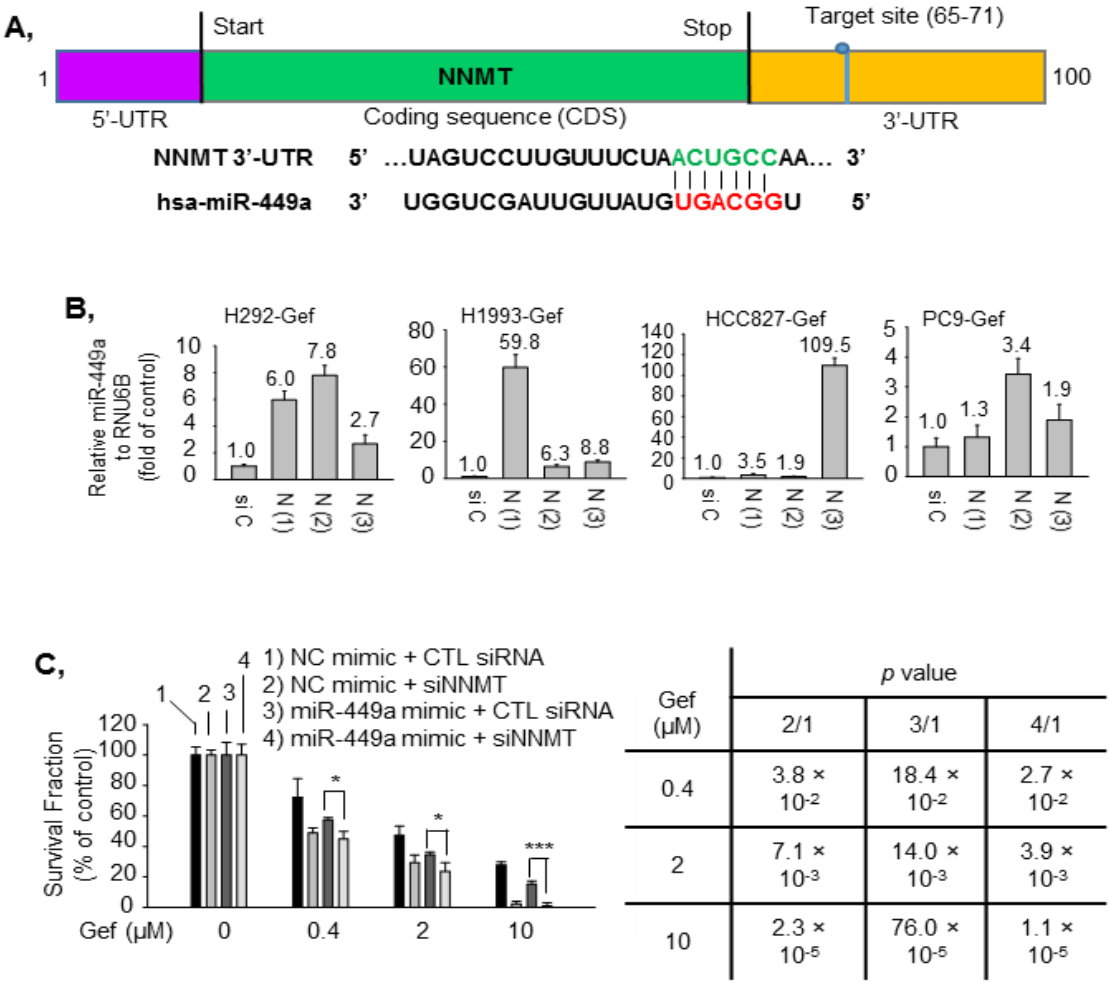

Gef (μM)	*p* value		
	2/1	3/1	4/1
0.4	3.8×10^{-2}	18.4×10^{-2}	2.7×10^{-2}
2	7.1×10^{-3}	14.0×10^{-3}	3.9×10^{-3}
10	2.3×10^{-5}	76.0×10^{-5}	1.1×10^{-5}

Figure 12: The potential interactions between NNMT and miR-449a. (A) Bioinformatics analysis. The possible binding sites between NNMT and hsa-miR-449a were determined using a bioinformatics tool (targetscan.com). (B) Effects of siNNMTs on miR-449a expression by transfection with siNNMTs (N(1): siNNMT #1; N(2): siNNMT #2; N(3): siNNMT #3). (C) Effects of siNNMT and/or miR-449a on cell proliferation by transfection with miR-449a and/or siNNMT in PC9-Gef cells. The combination effect was measured by calculating CI values.

Consequently, this combination was applied in additional functional studies. We found that *in vivo*, the miR-449a/siRNA NNMT (siNNMT) combination showed an enhanced antitumor activity compared with each treatment (Figure 13A). We next examined the effects of dual therapy on antitumor activity in *in vivo* models. Staining with Ki67, a biomarker of cell proliferation, also revealed that miR-449a or siNNMT suppressed the expression of Ki67 (Figure 13B). Taken together, the *in vitro* and *in vivo* data confirmed the therapeutic efficiency and antitumor activity of combined miRNA and siRNA therapy compared with the individual treatments in gef-resistant cells.

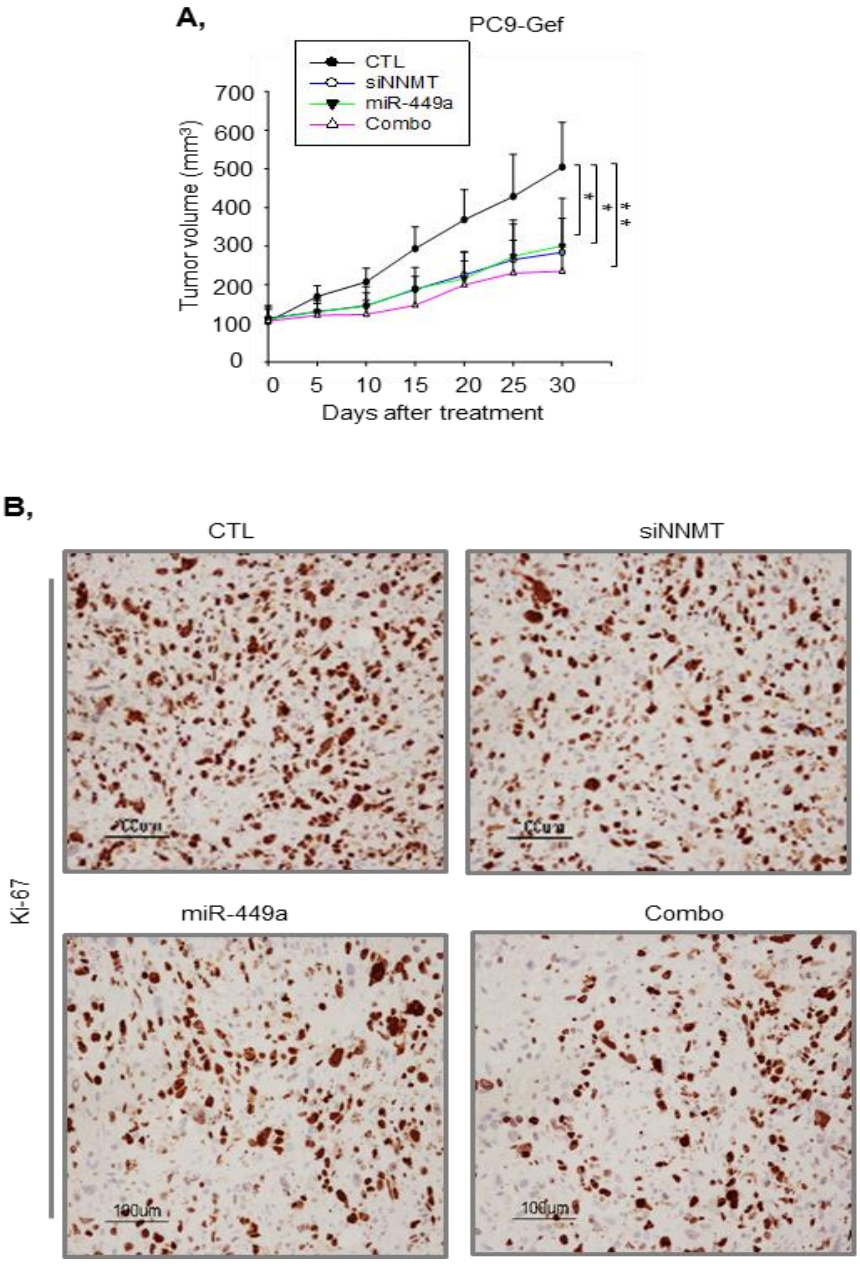

Figure 13: Effects of dual therapy on antitumor activity in *in vivo* models. (A) Effects of miR-449a and/or siNNMT on tumor growth in PC9-Gef cells. (B) Immunohistochemistry of Ki-67 in tumor tissue sections.

2.3.3 Reversal of PTEN promoter methylation by miR-449a in gef-Resistant NSCLC cells

PTEN plays an important role in cancer development and sensitivity to chemotherapy and loss or decreased expression of PTEN has been correlated to acquired resistance (Bach et al., 2017a; Sos et al., 2009; Yamasaki et al., 2007). While gef and erl, which target the EGFR, are approved for the treatment of patients with advanced NSCLC, PTEN loss is also associated with resistance to small molecule EGFR inhibitors including gef (Kokubo et al., 2005). A previous study reported that PTEN is down-regulated in PC9-Gef compared with parental PC9 cells (Yamamoto et al., 2010). In the present study, we also confirmed and continuously investigated the expression of PTEN in four cell lines with two different levels of EGFR-TKI resistance, including gef and erl. PTEN loss was observed in all EGFR-TKI-resistant NSCLC cells by western blotting (Figure 14A) and confirmed by IHC analysis (Figure 14B).

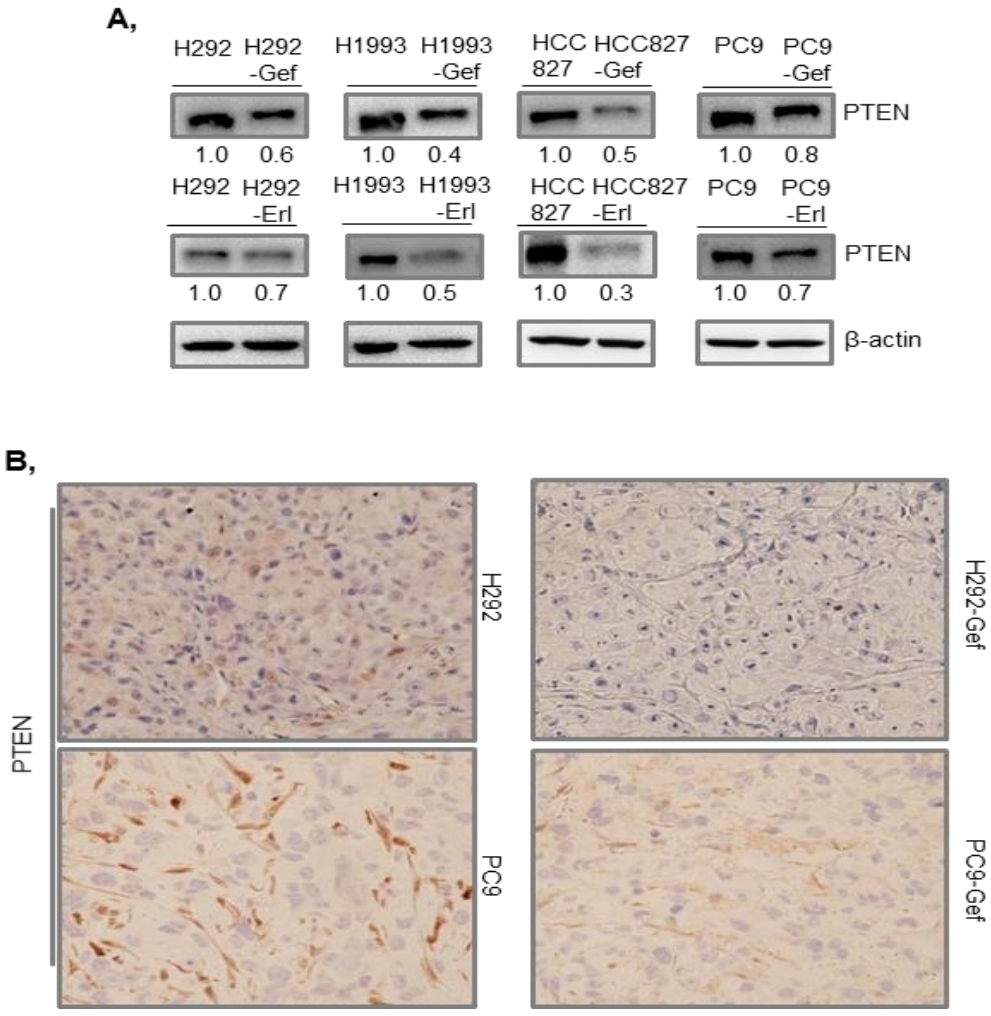

Figure 14: The expression of PTEN in gef-resistant NSCLC cells. (A) Characterization of the indicated parental or drug-resistant phenotype cell lines for PTEN expression at protein levels. (B) Immunohistochemistry of PTEN in tumor tissue sections. Immunohistochemical analysis of PTEN was performed using anti-PTEN antibody in tumor tissue sections.

Alternations in DNA methylation have been common and extensively studied in many cancers (McCubrey et al., 2011). While Ulanovskaya *et al* found no significant NNMT-dependent changes in global cytosine, protein methylation was found to be markedly lower in cells with increased NNMT levels (Ulanovskaya et al., 2013). Subsequently, 5-Aza, a DNA methylation inhibitor, was employed to investigate its effect on PTEN and miR-449a. We found that 5-Aza suppressed the levels of NNMT protein expression (Figure 15A), while 5-Aza induced PTEN expression as reported previously (Maeda et al., 2015; Mao et al., 2013) and stimulated the levels of miR-449a (Figure 15B). These data suggested that PTEN and miR-449a loss might be closely related to DNA methylation in gef-resistant NSCLC cells. Therefore, we further investigated the effect of miR-449a on PTEN promoter methylation, in which the promoter region contains the methylation site (Figure 15C, *top* panel) (Hino et al., 2009). The H292-Gef cells showed a significant down-regulation of the expression level of miR-449a both *in vitro* and *in vivo* compared with the H292 cells employed in this study. Using Epitect Methylight assays, we found that miR-449a suppressed PTEN methylation, with approximately 3-fold changes compared with the control (Figure 15C, *bottom-right* panel). Using methyl-specific PCR assays, we further confirmed that miR-449a induced PTEN un-methylation and suppressed PTEN methylation (Figure 15C, *bottom-left* panel). These results indicated that miR-449a transduction was associated with aberrant methylation of the PTEN promoter site in gef-resistant NSCLC cells. Western blot analysis also revealed that miR-449a over-expression increased PTEN expression (Figure 15D).

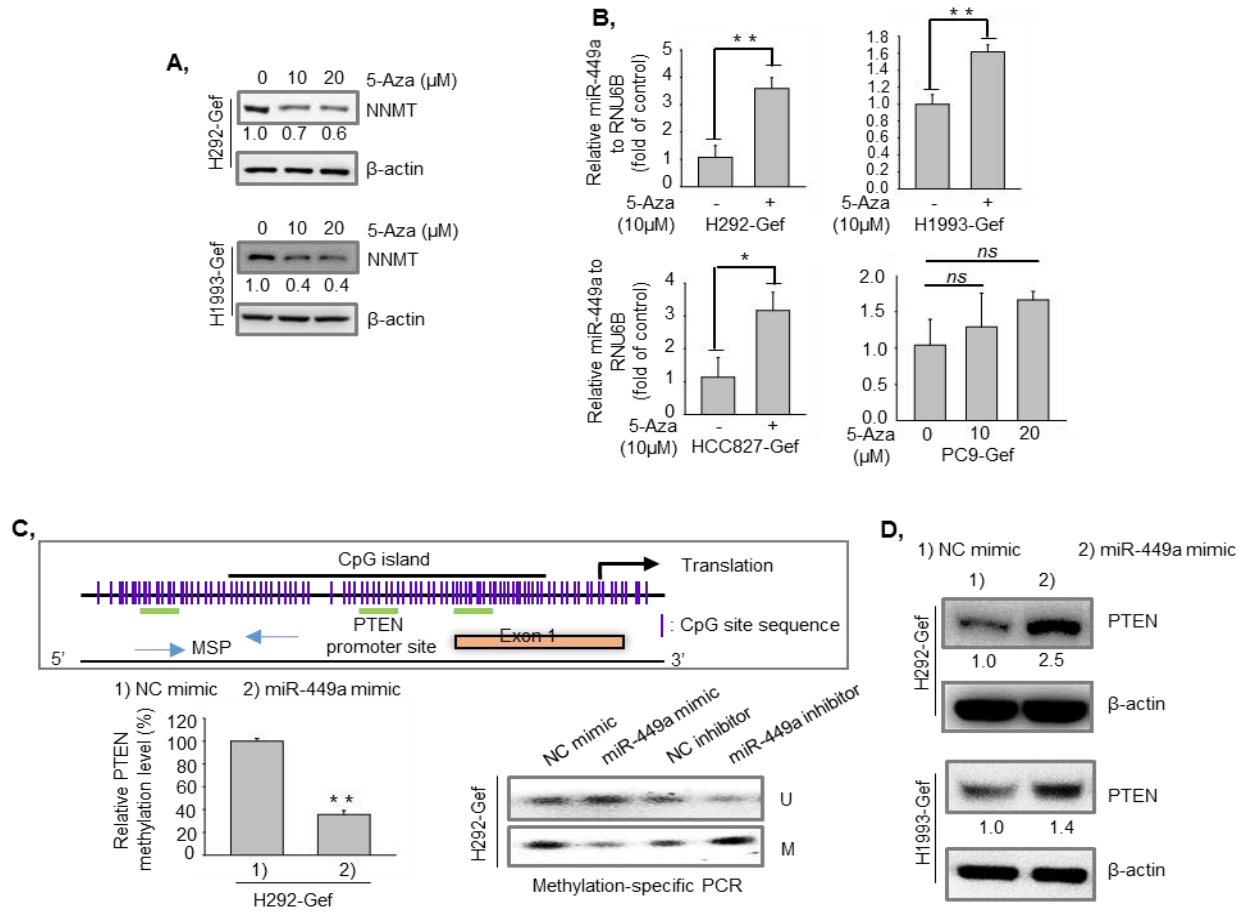

Figure 15: Effects of miR-449a on PTEN methylation and PTEN expression. (A & B) Effects of 5-Aza on the levels of NNMT and miR-449a expression. The drug-resistant cell lines were incubated in the presence or absence of 5-Aza (10 or 20 μM) for 24 h. (C) Reversal of PTEN promoter methylation by miR-449a in gef-resistant cells. *Top*, MSP analysis of the PTEN gene and map of the promoter region of the PTEN gene. *Bottom,* Methylation-specific PCR analysis of the PTEN gene in H292-Gef cells. *Bottom-right*, Cells were transfected with or without miR-449a (50 *p*mole/well) and furthered analyzed by using EpiTect Methylight PCR kit as described in Methods part. *Bottom-left*, Results of MSP analysis of PTEN gene in H292-Gef cells after post-transfection with or without miR-449a mimic & miR-449a inhibitor (50 *p*mole/well). M and U represent PCR products of methylated and unmethylated alleles, respectively. (D) Effects of miR-449a on the protein expression of PTEN. The gef-resistant cells were transfected with NC miR-449a or miR-449a for 48 h. PTEN protein levels were determined from cell lysates by immunoblotting.

Activation of the PI3K/Akt pathway is reported to associate with drug resistance to chemotherapeutic drugs (Bach et al., 2017a; Bach and Lee, 2018). Therefore, targeting Akt might modulate the drug resistance in cancer cells (Chiarini et al., 2008; Tazzari et al., 2007; Tazzari et al., 2008). The PI3K/Akt pathway was also previously reported to participate in NNMT-dependent MMP2 activation and cellular invasion (Tang et al., 2011). Therefore, we further clarified the correlations between PTEN/PI3K/Akt and NNMT in gef-resistant NSCLC cells. Knockdown of PTEN (siPTEN) was found to increase the levels of p-Akt (Ser^{473}) protein expression (Figure 16A). Employing LY294002, a PI3K inhibitor, suppression of NNMT was also observed in gef-resistant cells (Figure 16B). Next, we further elucidated the possible crosstalk between the miR-449a level and PI3K activity in gef-resistant NSCLC cells. We determined the levels of miR-449a in gef-resistant NSCLC cells in the presence of LY294002 and found that miR-449a expression was increased by PI3K inhibition (Figure 16C).

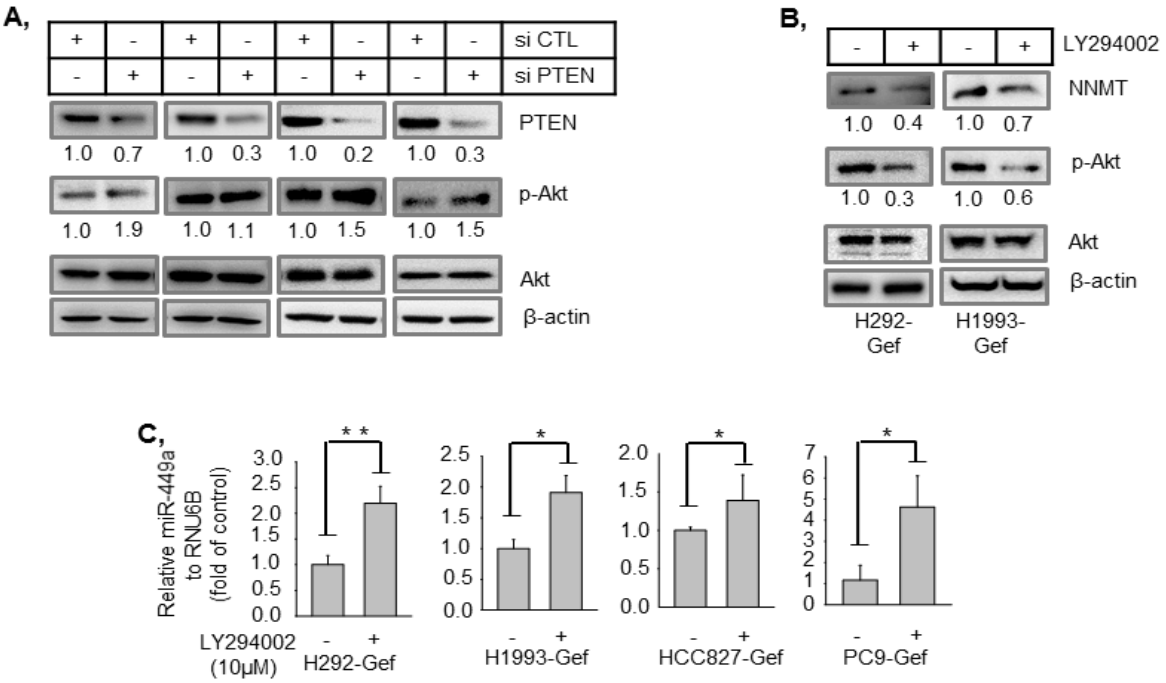

Figure 16: The associations between miR-449a and PI3K/Akt pathway in gef-resistant NSCLC cells. (A) Effects of PTEN siRNA on the Akt pathway. The drug-resistant cell lines were incubated with scramble siRNA or PTEN siRNA for 48 h and then analyzed by western blotting. (B) Effects of PI3K inhibitor on the Akt pathway. Cells were incubated with PI3K inhibitor (LY294002, 20 μM) for 24 h and then analyzed by immunoblotting. (C) Effects of PI3K inhibitor on miR-449a. The gef-resistant cell lines were incubated with LY294002 for 24 h, and then the levels of miR-449a were determined using Taqman real-time PCR.

We also found that knockdown of NNMT expression by treatment with NNMT siRNA decreased the levels of active Akt *in vitro* (Figure 17A) and *in vivo* (Figure 17B). In contrast, transfection with NNMT plasmid up-regulated the levels of p-Akt in gef-resistant cells (Figure 17C). Taken together, these data raise the possibility that a positive feedback loop of miR-449a with NNMT and PI3K guarantees the sustained activation in the resistance of NSCLC cells, which is essential for the over-expression of NNMT.

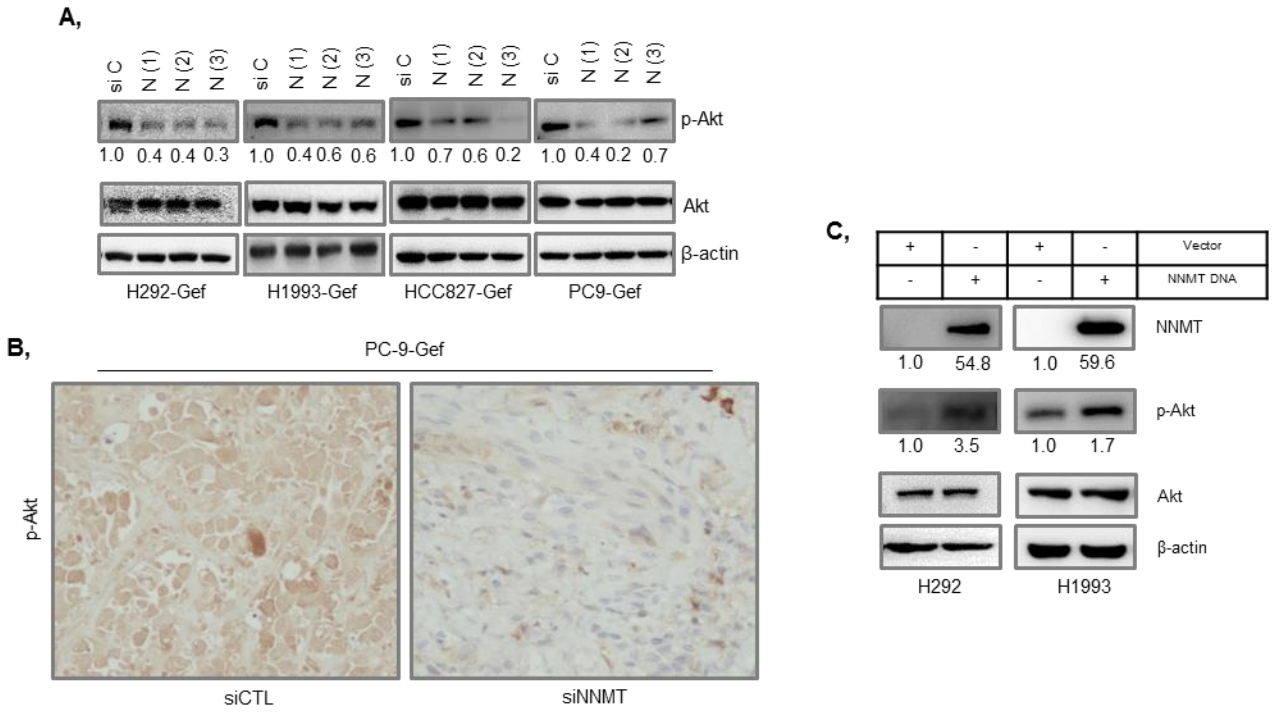

Figure 17: The associations between NNMT and PI3K/Akt pathway in gef-resistant NSCLC cells. (A) Effects of NNMT siRNA on the Akt pathway. The gef-resistant cell lines were incubated with scramble siRNA or NNMT siRNA for 48 h, and then the indicated protein levels were further analyzed by immunoblotting. (B) Immunohistochemistry of p-Akt in tumor tissue sections. Immunohistochemical analysis of p-Akt was performed using anti-p-Akt antibody in tumor tissue sections with or without NNMT siRNA. (C) Effects of NNMT plasmid on the Akt pathway. NNMT plasmid was transfected to the indicated parental cells within 48 h, and then further immunoblotting was performed to detect protein expressions.

2.3.4 Yuanhuadine leads to reversal of miR-449a and NNMT expression in EGFR-TKI-resistant NSCLC cells

Based on the correlation between miR-449a and NNMT expression in resistant cancer cells, we assumed that an agent with the potential to reverse miR-449a and NNMT expression might be a drug candidate to overcome EGFR-TKI-resistant cancers. Natural products have emerged as an important source of agents in drug discovery and development (Bach et al., 2015; Bae et al., 2015; Kim et al., 2017; Um et al., 2016). Our previous study revealed that the expression of NNMT levels in H292-Gef was approximately 4.3-fold higher than that in H292 cells based on a cDNA array analysis (Bae et al., 2016). Therefore, to confirm our hypothesis and explore the potential to overcome the resistance by regulating the expression of NNMT and miR-449a, we applied yuanhuadine (YD), a natural product-derived antitumor agent that was shown to be more sensitive to lung cancer cells (Hong et al., 2011). As shown in Table 3, employing cDNA array analysis with using the standard 2-fold change in expression as our threshold criterion revealed that NNMT was one of the most over-expressed genes in H292-Gef cells compared with H292 cells, and YD (10 nM) effectively suppressed the expression of NNMT with a 2.5-fold change.

Table 3: Effects of Yuanhuadine (10 nM) and Gefitinib (50 nM) on Gene Expression in H292-Gef Cells (FC, fold change; R, H292-Gef; H, H292; YD, yuanhuadine; Gef, gefitinib; +, up-regulated; -, down-regulated).

No.	Accession	FC (R CTL /H CTL)	FC (R YD /R CTL)	FC (R Gef /R CTL)	Gene Symbol	Description
1	NM_006169.2	+ 4.33	-2.55	-	NNMT	Nicotinamide N-methyltransferase
2	NM_002543.3	+ 3.79	-2.31	-	OLR1	Oxidized low density lipoprotein (lectin-like) receptor 1
3	XM_034819.6	+ 2.39	-2.1	-	ZNF629	Zinc finger protein 629
4	NM_000600.1	+ 2.39	-3.3	-	IL6	Interleukin 6 (interferon, beta 2)
5	NM_016352.2	+ 2.32	-3.41	-	CPA4	Carboxypeptidase A4
6	NM_001360.2	+ 2.29	-2.34	-	DHCR7	7-dehydrocholesterol reductase
7	NM_003238.1	+ 2.21	-2.1	-	TGFB2	Transforming growth factor, beta 2
8	NM_005585.3	+ 2.07	-3.63	-	SMAD6	SAMD family member 6
1	NM_002575.1	-21.64	+ 20.75	-2.69	SERPINB2	Serpin peptidase inhibitor, clade B (ovalbumin), member 2
2	NM_007036.3	-6.79	+ 3.69	-	ESM1	Endothelial cell-specific molecule 1
3	NM_198129.1	-6.45	+ 4.82	-	LAMA3	Laminin, alpha 3
4	NM_005554.3	-5.62	+ 3.98	-	KRT6A	Keratin 6A
5	NM_139314.1	-4.82	+ 2.75	-3.28	ANGPLT4	Angiopoietin-like 4
6	NM_005562.1	-4.32	+ 3.41	-	LAMC2	Laminin, gamma 2

7	NM_004029.2	-4.15	+ 2.17	-	IRF7	Interferon regulatory factor 7
8	NM_000024.4	-4.08	+ 2.5	-	ADRB2	Adrenergic, beta-2 receptor
9	NM_000240.2	-3.84	+ 3.84	-	MAOA	Monoamine oxidase A
10	NM_000963.1	-3.83	+ 5.65	-3.01	PTGS2	Prostaglandin-endoperoxide synthase 2
11	NM_006850.2	-3.76	+ 15.87	-3.3	IL24	Interleukin 24
12	NM_058172.3	-3.29	+ 2.77	-	ANTXR2	Anthrax toxin receptor 2
14	NM_002658.2	-2.84	+ 10.67	-	PLAU	Plasminogen activation urokinase
15	NM_173343.1	-2.73	+ 6.67	-	IL1R2	Interleukin 1 receptor, type II
16	NM_000584.2	-2.63	+ 4.99	-3.84	IL8	Interleukin 8
17	NM_031892.1	-2.62	+ 2.34	-	SH3KBP1	SH3-domain kinase binding protein 1
18	NM_005555.3	-2.45	+ 4.11	-	KRT6B	Keratin 6B
19	NM_002203.3	-2.42	+ 4.95	-2.07	ITGA2	Intergrin, alpha 2
20	NM_005863.3	-2.35	+ 2.52	-	NET1	Neuroepithelial cell transforming 1
21	NM_005318.2	-2.32	+ 2.56	-	H1F0	H1 histone family, member 0
22	NM_002153.1	-2.26	+ 6.99	-	HSD17B2	Hydroxysteroid (17-beta) dehydrogenase 2
23	NM_001109.3	-2.26	+ 3.77	-2.63	ADAM8	ADAM metallopeptidase domain 8
25	NM_000228.2	-2.21	+ 2.17	-	LAMB3	Laminin, beta 3
26	NM_006238.3	-2.21	+ 3.54	-	PPARD	Peroxisome proliferative activated receptor, delta
27	NM_004431.2	-2.17	+ 2.31	-2.07	EPHA2	EPH receptor A2

28	NM_004029.2	-2.07	+ 2.17	-	IRF7	Interferon regulatory factor 7
29	NM_014631.2	-2.07	+ 2.47	-	SH3PXD2A	SH3 and PX domains 2A
30	NM_000611.4	-2.02	+ 2.28	-	CD59	CD59 molecule, complement regulatory protein
31	NM_006244.2	-2.01	+ 2.51	-	PPP2R5B	Protein phosphatase 2, regulatory subunit B, beta isoform

A subsequent analysis also confirmed that treatment with YD suppressed NNMT expression in gef-resistant NSCLC cells. YD down-regulated the expression levels of NNMT protein, NNMT-related protein (p-Akt, Ser^{473}) and NNMT mRNA in a concentration-dependent manner (Figure 18A & 18B). Interestingly, YD also effectively restored the decreased level of miR-449a in all gef-resistant cells in a concentration-dependent manner (Figure 18C). In addition, the anti-tumor activity of YD was evaluated in nude mouse xenograft models implanted with MET amplification (H1993-Gef) and EGFR mutation (PC9-Gef) cell lines. As depicted in Figure 19A & 19B, YD (1 mg/kg) efficiently inhibited tumor growth in H1993-Gef and PC9-Gef cells and was superior to gef in H1993-Gef and PC9-Gef cells. Interestingly, we also found that the suppression of NNMT by YD was higher than gef both *in vitro* and *in vivo* (Figure 20A, *left* & *right* & 20B). IHC analysis confirmed that the expression of NNMT was suppressed in tumor tissues in the YD-treated groups (Figure 20C). In addition, YD was able to suppress NNMT mRNA expression in tumor tissues (Figure 20D) while concurrently inducing the levels of miR-449a expression (Figure 20E). Taken together, these findings were consistent with the changes in expression of miR-449a and NNMT *in vitro*, suggesting that both YD and miR-449a could regulate the expression of NNMT and indeed could be useful for the suppression of NNMT over-expression, which could lead to improved sensitivity of gef in gef-resistant cancer cells.

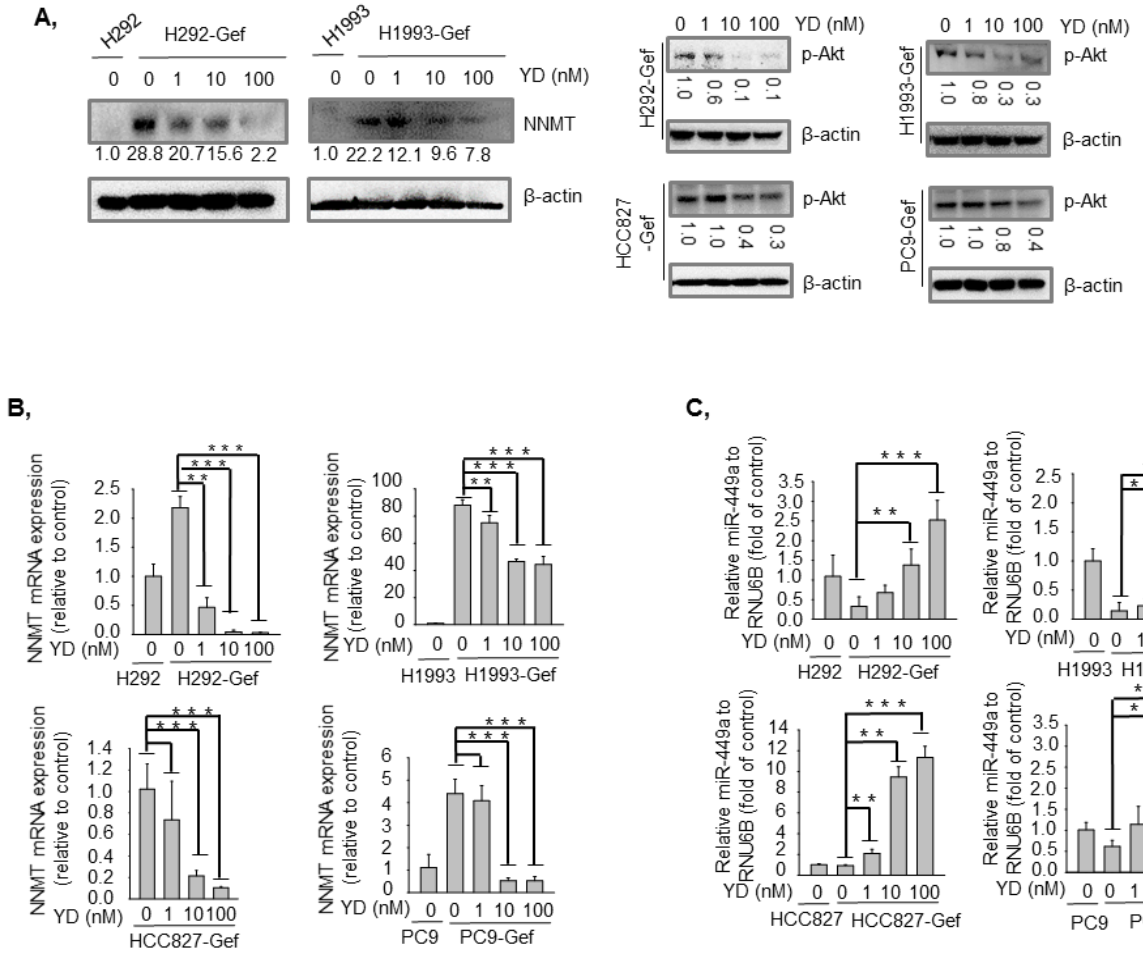

Figure 18. Effects of YD on miR-449a and NNMT over-expression in gef-resistant NSCLC cells. (A) Effects of YD on NNMT and the related protein expression. NNMT, p-Akt, Akt, and β-actin protein levels in cell lysates were assayed by immunoblotting after 24 h of YD treatment. (B) Effects of YD on NNMT mRNA expression. NNMT mRNA expression was evaluated by real-time PCR after 24 h of YD treatment. (C) Effects of YD on miR-449a expression. miR-449a levels were further analyzed using the Taqman PCR kit after 24 h of YD treatment.

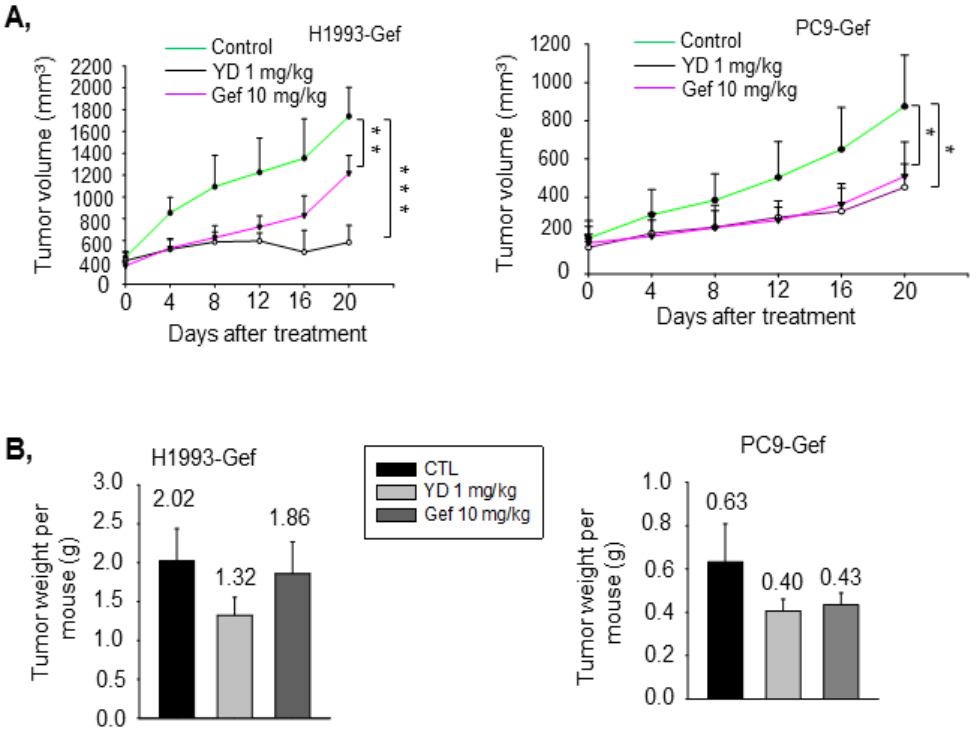

Figure 19: Effects of YD on gef-resistant NSCLC *in vivo* models. (A) The indicated cells were implanted subcutaneously into the flanks of BALB/c nude mice. Dosing of YD (1 mg/kg body weight) or gef (10 mg/kg body weight) was initiated when the tumor volumes reached approximately 400 mm^3 for H1993-Gef cells or 150 mm^3 for PC9-Gef cells. YD and gef were administrated orally once daily for 21 days continuously. The tumor volumes were measured every 4 days (n = 5 mice per group). The error bars represent the means ± SD. (B) H1993-Gef and PC9-Gef tumors were excised from animals on day 21 after treatment, and tumor weights were calculated.

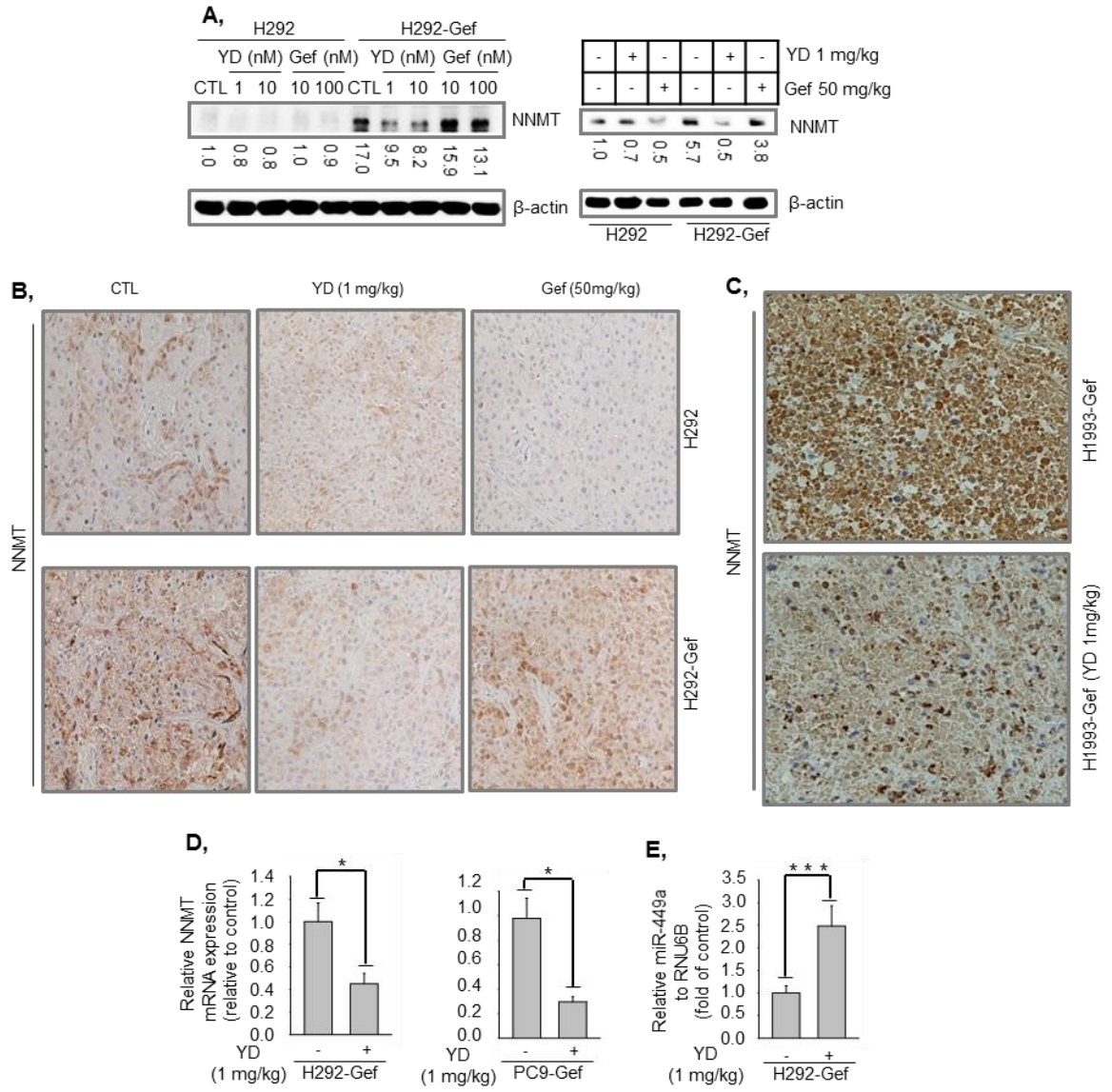

Figure 20: Effects of YD on gef-resistant NSCLC *ex vivo* analysis. (A) Protein expression levels of NNMT. The proteins from cell lysates (*Right panel*) or small portions of tumors from each group were homogenized in Complete Lysis Buffer (Active Motif) (*Left panel*) for immunoblotting. β-actin was used as an internal standard. (B & C) Immunohistochemistry of NNMT in tumor tissue sections. Immunohistochemical analysis of NNMT was performed using anti-NNMT antibody in each of the indicated groups. (D & E) Relative expression of NNMT and miRNA-449a in tumor transcripts of the indicated xenograft tissues. The levels of NNMT (D) or miR-449a (E) expression were analyzed by real-time PCR or with the Taqman PCR kit using specific primers, respectively.

2.3.5 YD suppresses NNMT activity *via* the interacting pocket of the enzyme

To date, there have been very few reports about NNMT inhibitors, especially from natural products. Herein, in an effort to identify the interactions between YD and NNMT, the ability of YD to inhibit NNMT enzyme activity was initially determined using a biochemical *in vitro* assay. The analysis revealed an inhibitory activity of the NNMT enzyme by YD with an IC_{50} of 0.4 µM. As a positive control, 1-MNA was used for *in vitro* NNMT inhibition (Figure 21A). To understand the potential interactions of YD in the binding site of NNMT, we used the published crystal structure of human NNMT complexed with SAH and NCA for the docking study (pdb:3ROD). Due to the low similarity between the original ligands (SAH and NCA) and YD, the majority of the interactions observed in the original pdb structure (Figure 21B) were changed. The structure of the NNMT-YD complex with the highest docking score is shown in Figure 21C. YD, which possesses 10 oxygen atoms including three hydroxyl groups, exhibits several hydrogen bonds and van der Waals interactions with NNMT in the binding site. Hydrogen bonds were observed between 1) the acetyl group of YD and the hydroxyl group of Tyr20, 2) the hydroxyl group of YD and the backbone amide of Tyr86 as well as the side chain of Asn90, 3) the primary alcohol of YD and the side chain amide of Gln89, 4) the oxygen atom of the dioxolane ring and the hydroxyl group of Tyr204. Among them, the interaction with Tyr20 was an important element for the reported ligand (SAH) (Peng et al., 2011). Residues with hydrophobic interactions are shown in Figure 21D. A portion of the clustered conserved aromatic residues (Phe15, Tyr20, Tyr86, and Tyr204) reported previously are shown in spheres (Peng et al., 2011). Tyr86, which interacted with the adenine ring in the original structure, displayed a pi-alkyl interaction with the alkyl side chain of YD. Tyr204 and Leu164, residues that form a sandwiched hydrophobic interaction for the nicotinamide ring, exhibited pi-alkyl and alkyl hydrophobic interactions with the propylene group of YD, respectively.

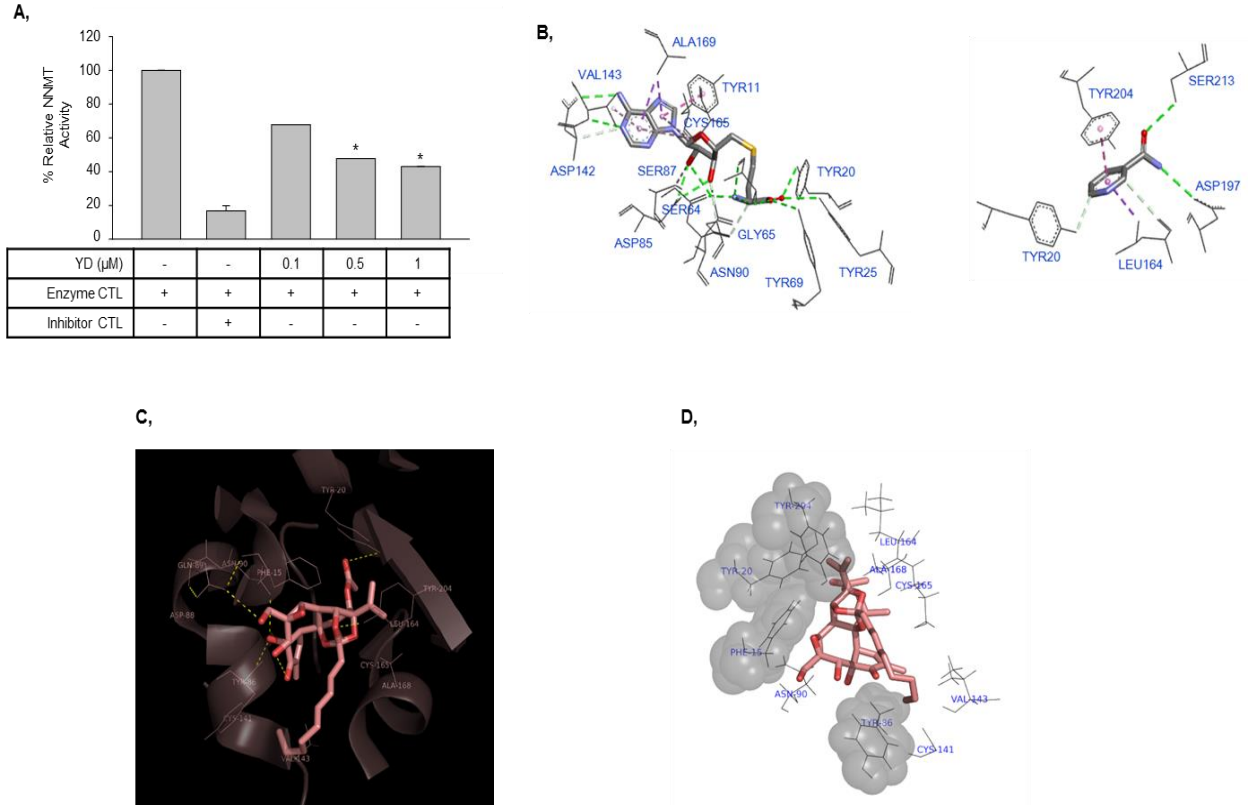

Figure 21. YD interacts with the binding site of NNMT. (A) *In vitro* activity of purified NNMT was assessed in the presence of increasing concentrations of YD. Data are reported as a percentage of NNMT activity with respect to the control. Histograms represent the mean ± SD of three independent experiments. (B) Binding site of hNNMT complexed with S-adenosyl-L-homocysteine (SAH) and nicotinamide (NCA). C) Docked pose of YD with the highest binding score. Hydrogen bonds within the binding site are shown as yellow lines. D) Residues forming hydrophobic interactions with YD are shown as grey lines. Among them, previously reported conserved aromatic residues (Phe15, Tyr20, Tyr86, and Tyr204) are presented as spheres.

2.3.6 Discussion

Clinically, advanced NSCLC patients who suffer EGFR-TKI resistance currently have limited therapeutic options. Improved detection methods for cancer diagnosis are crucial for early and reliable prognosis and treatment (Santarelli et al., 2011). Therefore, molecular profiling and gene expression analysis are considered useful tools for improving outcomes and minimizing side effects. We investigated the expression profiles of NNMT and miR-449a and their possible interactions both *in vitro* and *in vivo* in EGFR-TKI-resistant NSCLC cells. The association between miR-449a and c-MET expression has also been previously elicited in sunitinib-resistant renal cell carcinoma (Qu et al., 2016) and amplification of c-MET has been implicated in resistance to therapies targeting the EGFR (Zhang et al., 2010). In the present study, we observed that the NNMT protein and mRNA were over-expressed, while miR-449a was significantly down-regulated in EGFR-TKI-resistant NSCLC cells compared with their parental cells, especially with H1993, a high-c-MET-expressing NSCLC cell line. Subsequently, further study about the plausible association between MET amplification and NNMT/miR-449a expression can be potentially needed. We further employed bioinformatics tools and found possible correlations between NNMT and miR-449a. Moreover, knockdown of NNMT induced the expression of miR-449a in drug-resistant NSCLC cells. These findings suggested that the mechanism underlying the miR-449a down-regulation might be related to the up-regulated NNMT expression in resistant NSCLC cells. It is possible that NNMT-mediated down-regulation of miR-449a is impaired in drug-resistant cancer cells.

The regulation of PTEN expression is a critical strategy for therapeutic sensitivity, and its dysregulation is often associated with cancer drug resistance. Our group has newly described a significant function of PTEN in regulating tumor progression (Bach et al., 2017a). Moreover, variation in NNMT enzyme activity could lead to toxicological and pharmacological consequences. In fact, methylation is a fundamental process in the biotransformation of many drugs and xenobiotic compounds, and NNMT, which catalyzes the N-methylation of pyridines that are structurally related to nicotinamide, has a primary role in detoxifying many xenobiotics (Ulanovskaya et al., 2013). Therefore, we employed 5-Aza, a methylation inhibitor, and found that it suppressed NNMT expression while inducing the expression of miR-449a in gef-resistant NSCLC cells. This finding led us to investigate the methylation status of the PTEN promoter in miR-449a-over-expression resistant NSCLC cells. The over-expression of miR-449a was able to

suppress the methylation intensity of the PTEN promoter and restore the expression of PTEN in EGFR-TKI-resistant NSCLC cells. This result suggests that miR-449a-dominated NNMT expression is crucial for PTEN expression in drug-resistant NSCLC cells. In addition, PTEN may also exert its role as a tumor suppressor by negatively regulating the PI3K/Akt pathway, which determines cell growth, survival and inhibition in both cancer and normal cells (Fry, 2001; Stambolic et al., 1998). Thereby, we further employed LY294002, a PI3K inhibitor, and found that PI3K suppression by LY294002 treatment suppressed NNMT expression and also restored the expression of miR-449a in gef-resistant NSCLC cells. These results imply that constitutive activation of the PI3K/Akt pathway is also involved in the control of miR-449a-mediated NNMT expression in the resistance of NSCLC cells. Hence, a positive feedback loop between the PTEN-controlled PI3K/Akt pathway and miR-449a-mediated NNMT expression in drug resistance of NSCLC cells seems to be crucial for the enhanced cell proliferation and decreased gef sensitivity. Although the role of NNMT in drug resistance has been emerging, there are few reports of NNMT inhibitors in cancer cells. Employing cDNA analysis with YD and *in vitro* results, we found that the down-regulation of NNMT by YD enhanced the sensitivity of gef in gef-resistant cells. We also found that the expression of miR-449a could be significantly up-regulated by YD, suggesting that the growth of gef-resistant NSCLC cells could be reverted by treating EGFR-TKI-resistant NSCLC cells with YD. This significant point could be exploited for the future design of novel strategies for the prevention or tumor progression and/or treatment of lung cancer using the combination of YD and miR-449a. Although studies of the interactions between YD and NNMT are limited, we revealed interactions between the active sites of this enzyme with YD. Further analyses of NNMT and YD interactions will be essential to design and develop new NNMT inhibitors.

In summary, we suggest that the over-expression of NNMT in gef-resistant cells is caused by the deregulation of its positive feedback loop between the PTEN/PI3K/Akt pathway and miR-449a and employing YD can overcome this resistance *via* modulation of NNMT and miR-449a in NSCLC (Figure 22). These findings indicate that targeting the NNMT over-expression mechanism might be a novel therapeutic strategy in EGFR-TKI-resistant NSCLC patients.

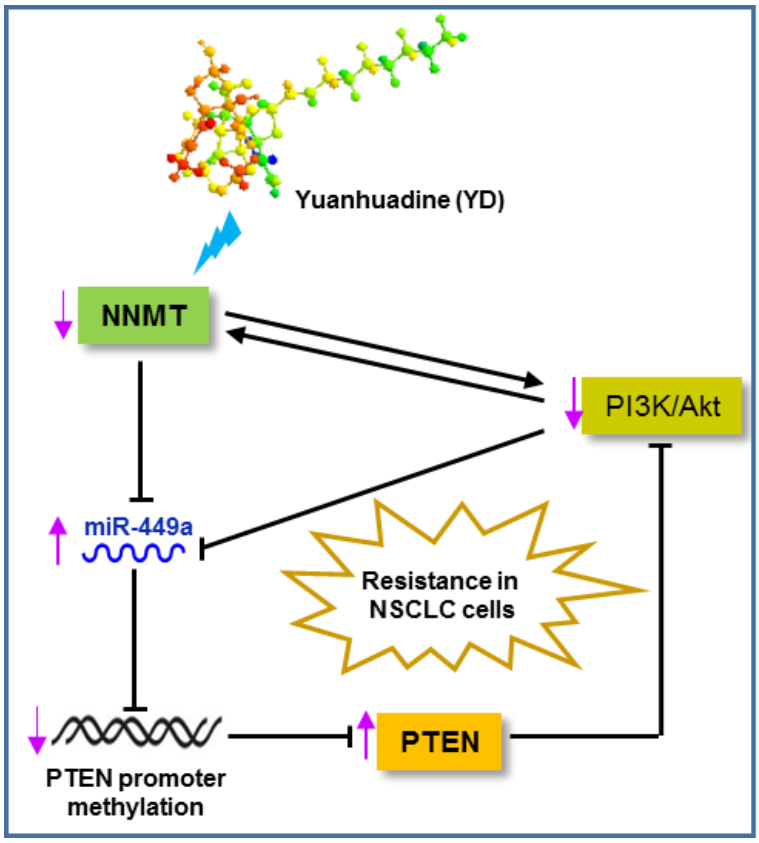

Figure 22: Scheme of the mechanism of action EGFR-TKI-resistant NSCLC cells by miR-449a and NNMT.

[Chapter 3] BMP4 is associated with acquired drug resistance and regulation of fatty acid metabolism in EGFR-mutant non-small cell lung cancer cells

3.1 Introduction

The rapid emergence of resistance to chemotherapy and molecular targeted therapies is currently considered a major reason for treatment failure in cancer patients (Diaz Jr et al., 2012; Engelman and Settleman, 2008; Holohan et al., 2013). Various molecular mechanisms that contribute to drug resistance have been investigated, including those that are both non-mutational (presumably epigenetic) and mutational (genetic). Somatic mutations in the epidermal growth factor receptor (EGFR) gene such as T790M mutation, deletion in exon 19 or wild-type EGFR amplification (Nakata and Gotoh, 2012) are highly correlated to favorable response to the EGFR tyrosine kinase inhibitor (EGFR-TKI), gefitinib (Sharma et al., 2007), a pioneer targeted drug that has been used as the first-line treatment for patients with EGFR mutations (Mok et al., 2009). Targeting gene aberrances, such as EGFR mutations, has significantly enhanced the prognosis for advanced non-small cell lung cancer (NSCLC) patients (Maemondo et al., 2010; Mok et al., 2009). Therefore, EGFR mutational status has been considered a significant biomarker and rational target for chemotherapy in advanced NSCLC patients (Chan and Hughes, 2015; Gazdar, 2009; Sharma et al., 2007).

Accumulating evidence also suggests that microRNAs (miRNAs) play a significant role in epigenetically modulating various phenotypic changes in cancer cells (Bach et al., 2017a; Bach and Lee, 2018; Bach et al., 2018b; Cho et al., 2017; Zhou et al., 2017). Indeed, miRNAs may affect genetic programs through post-transcriptional silencing of target genes, either by inhibiting the translation of target mRNAs or by promoting their degradation (Bartel, 2004, 2009). These actions may lead to the regulation of numerous aspects of cancer biology, including drug resistance, epithelial-to-mesenchymal transition and metastasis (Bach et al., 2018a; Bartel, 2004, 2009).

Bone morphogenetic proteins (BMPs) are a family of signaling molecules that belong to the transforming growth factor-β (TGF-β) superfamily (Wang et al., 2014). Many processes, such as cell differentiation, early development and tumor growth are also dependent on BMP signaling (Bach et al., 2018b). Wang *et al* recently reported that activation of the BMP-BMPR pathway conferred resistance to EGFR-TKIs in lung cancer patients harboring EGFR mutations (Wang et al., 2015). We have also recently addressed the role of BMPs in cancer and have emphasized their function in association with miRNAs, drug resistance and mutations (Bach et al., 2018b). Recent studies have also suggested the possibility that small-molecule BMP4 antagonists, such as LDN-

193189, were able to effectively inhibit the growth of lung cancer cells and chemotherapy-resistant cancer cells (Ali et al., 2015; Wang et al., 2015).

In the present study, we established gefitinib-resistant NSCLC cells to investigate novel mechanisms of resistance to EGFR-TKI. In comparison with the gene expression pattern of parental NSCLC cells, acquired gefitinib-resistant cell lines displayed that BMP4 gene was up-regulated in the gefitinib-resistant cell lines. We continuously attempted to elucidate the role of BMP4 in EGFR-TKI resistance in NSCLC cells and the dynamic interactions of BMP4 with the tumor microenvironment such as miRNA or fatty acids. These findings will highlight potential new strategies for the treatment of cancer patients, especially in cases of EGFR-TKI-resistant NSCLC by targeting BMP4.

3.2 Materials and Methods

3.2.1 Cancer cell lines and reagents

H1993 human lung carcinoma cells were obtained from the American Type Culture Collection (Manassas, VA, USA). Gefitinib-resistant cells were developed as previously described (Bae et al., 2015) and all cells were cultured as previously described (Bach et al., 2015; Bae et al., 2015). In brief, gefitinib (gef)-resistant H1993 and erlotinib (erl)-resistant H1993 cells were developed from the parental H1993 cells through continuous exposure to gradually increasing drug dosages up to 10 μM each of gef and erl. Subsequently, resistant H1993 cells were maintained in medium containing 10 μM of gef or erl. LDN-193189 was purchased from Selleckchem (Houston, TX, USA).

3.2.2 Establishing stable cell lines

Murine BMP4 shRNAs (EZWC0CL102, TF306390A, CCN 185819 – A; EZWB0CL101, TF306390B, CCN 185818 – B; EZWA0CL101, TF306390C, CCN 185817 – C; EZVZ0CL101, TF306390D, CCN 185816 – D) and control shRNA (TR30015, Lot #0116) were purchased from Origene (Rockville MD, USA) and introduced into the indicated cells by viral infection. Stable cell lines were established following greater than 2 weeks of antibiotic selection according to the manufacturer's instructions.

3.2.3 Microarray expression analysis

3.2.3.1 *RNA quality check*

RNA purity and integrity were evaluated using the ND-1000 Spectrophotometer (NanoDrop, Wilmington, USA) and the Agilent 2100 Bioanalyzer (Agilent Technologies, Palo Alto, USA).

3.2.3.2 *Affymetrix whole transcript expression arrays*

The Affymetrix Whole Transcript Expression array procedure was executed according to the manufacturer's protocol (GeneChip Whole Transcript PLUS reagent Kit). cDNA was synthesized using the GeneChip WT (Whole Transcript) Amplification kit, as described by the manufacturer. The sense cDNA was then fragmented and biotin-labeled with TdT (terminal deoxynucleotidyl transferase) using the GeneChip WT Terminal labeling kit.

Approximately 5.5 μg of labeled DNA target was hybridized to the Affymetrix GeneChip Human 2.0 ST Array for 16 h at 45°C. Hybridized arrays were washed and stained on a GeneChip Fluidics Station 450 and scanned on a GCS3000 Scanner (Affymetrix). Signal values were computed using the Affymetrix® GeneChip™ Command Console software.

3.2.3.3 *Raw data preparation and statistical analysis*

Raw data were extracted automatically as part of the Affymetrix data extraction protocol using the Affymetrix GeneChip® Command Console® Software (AGCC). After importing CEL files, the data were summarized and normalized using the robust multi-average (RMA) method within the Affymetrix® Expression Console™ Software (EC). We exported results with gene level RMA analysis and performed differentially-expressed gene (DEG) analysis. Fold changes were used to determine statistical significance of the expression data. For each DEG set, hierarchical cluster analysis was performed using complete linkage and Euclidean distance as measures of similarity. Gene-Enrichment and Functional Annotation analysis of the list of significant genes was performed using Gene Ontology (www.geneontology.org/) and KEGG (www.genome.jp/kegg/). All data analysis and visualization of differentially expressed genes was conducted using R 3.1.2 (www.r-project.org).

3.2.4 Xenograft studies

All procedures involving animals (BALB/c nude mice, 4 – 6 weeks) were reviewed and approved by Seoul National University (permission number: SNU-161117-1).

For tumorigenicity assays in nude mice, the indicated cells were subcutaneously injected into the right axilla of BALB/c nude mice (n = 5) in a total volume of 200 μL of culture medium (5×10^6 cells). At 40 days (PC9-Gef) and 30 days (H1993-Gef) after inoculation, the mice were humanely killed and the tumors were excised and photographed.

For drug response assays, the indicated cells (5×10^6 cells in 200 μL of medium) were injected subcutaneously into the flanks of nude mice and tumors were allowed to grow. When the tumor volume reached approximately 100 mm^3 (PC9-Gef) or 160 mm^3 (H1993-Gef), the mice were randomized into vehicle control and treatment groups (n = 5). Then, these mice were treated with vehicle or LDN-193189 (4 mg/kg for PC9-Gef, 5 mg/kg for H1993-Gef) for 3 weeks (5 days on,

2 days off). Tumor volumes were determined using digital calipers using the formula (L × W × M × π)/6 as described previously.(Bae et al., 2015) The body weight of each mouse was also monitored for toxicity analyses.

3.2.5 Phospho-antibody array analysis

Phospho-antibody array analysis was performed using the Proteome Profiler Kit ARY003B (R&D Systems) according to the manufacturer's instructions. Briefly, cells were transfected with siBMP4 for 48 h. Cells were then lysed and centrifuged at 14,000 × *g* for 10 minutes. 500 μg of cellular extract was then subjected to a protein array. Phosphorylated kinases were identified by incubating arrays with biotinylated detection antibodies, streptavidin-HRP antibodies, and chemiluminescent detection reagents.

3.2.6 Metabolic analysis

3.2.6.1 *Metabolite extraction*

Metabolites were extracted from cells in 600 μL of a chilled methanol-chloroform mixture (2:1). This mixture was vortexed for 30 seconds, frozen on liquid nitrogen for 2 minutes and thawed at room temperature for 1.5 min; this process was repeated three times. Then, 200 μL chilled chloroform and 200 μL chilled water were added and the mixture was vigorously vortexed and then centrifuged at 15,000 x *g* for 20 min at 4°C. The upper aqueous phase and lower organic solvent phase were collected separately and dried with a centrifugal evaporator (Vision). The residuals were stored at -20°C until analysis.

3.2.6.2 *NMR experiments and statistical analysis*

For lipid analyses, the organic layer samples were dissolved in 500 μL deuterated chloroform and transferred into a 5 mm NMR tube. The HSQC NMR spectra were obtained using 800 MHz Bruker Avance spectrometers equipped with a cryogenic triple resonance probe at the College of Pharmacy, Seoul National University (Seoul, Korea). 2D HSQC spectra were processed and analyzed with NMRView J software (One Moon Scientific) to extract quantitative information as follows: The integrated peak area of the 2D HSQC spectra were normalized against the total peak area and then used for statistical analyses. Metabolite identification was performed using in-house and public databases (An et al., 2012).

3.2.7 Exosome isolation

Total exosomes were extracted with Invitrogen Total Exosome Isolation Reagent (Catalog number: 4478359, publication number: MAN0006949) from Invitrogen (Thermo Fisher Scientific), according to the manufacturer's instructions.

3.2.8 Immunoblot analysis

Western blot analysis was performed as described previously, using equal amounts of protein from each cell lysate (Bach et al., 2017b; Bach et al., 2015; Kim et al., 2017; Um et al., 2016). The following antibodies were used: anti-BMP4 (ab39973, Abcam, UK); anti-p53 (DO-1) (sc-126), anti-β-actin (C4) (sc-47778), (Santa Cruz Biotechnology, Santa Cruz, CA, USA); anti-p-Smad1/5 (Ser463/465) (#9516), anti-p-p53 (Ser15) (#9284) (Cell Signaling Technology, Danvers, MA, USA), anti-ACSL4 (Invitrogen, CA, USA) (PA5-27137).

3.2.9 Sulforhodamine B assay (SRB)

PC9-Gef cells and H1993-Gef cells were post-transfected with control or BMP4 siRNA for 48 h, then the indicated cells (1×10^4 cells/mL) were seeded in 96-well plates with the indicated concentrations of gefitinib and further analyzed as previously described (Bach et al., 2015). Similarly, PC9-Gef cells were also post-transfected with miRNA mimic or miR-139-5p for 48 h, and then the transfected cells were further analyzed as previously described (Bach et al., 2015).

3.2.10 Combinatorial drug analysis

The indicated cells were plated in 96-well culture plates and then exposed to various concentrations of LDN-193189 and YD (10 nM) at a 1:1 ratio. After 48 h of incubation, cell proliferation was evaluated using the SRB assay, as previously described (Bach et al., 2015).

3.2.11 Real-time polymerase chain reaction (PCR)

Total cell or tumor tissue RNA was extracted with TRI reagent (Invitrogen, Grand Island, NY, USA), and then RT-PCR analysis was carried out as described previously.(Bach et al., 2017b; Bach et al., 2015) Gene-specific primers for real-time PCR were synthesized by Bioneer Corporation (Daejeon, Korea); human ACSL4 sense: 5'-TTCATCTCTTGGACTTTGCTCA-3';

antisense: 5’-TGTACTGTACTGAAGCCCACACTT-3’, human BMP4 sense: GGGATGTTCTCCAGATGTTCTT; antisense: TCCACAGCACTGGTCTTGAG.

3.2.12 Transfection of small interfering RNAs and microRNAs

The siRNAs targeting BMP4 (siBMP4-1: 1012726, siBMP4-2: 1012728, siBMP4-3: 1012733) and ACSL4 (siACSL4-1: 1001674, siACSL4-2: 1001681, siACSL4-3: 1001676), as well as the negative control siRNA (catalog number: SN-1002), miR-139-5p mimic (mature sequence 5’-UCUACAGUGCACGUGUCUCCAGU-3’), and miRNA mimic negative control (catalog number: SMC-2002) were synthesized by Bioneer Corporation (Daejeon, Korea) and were transfected into the cell lines by electroporation using Lipofectamine RNAiMAX (Invitrogen, CA, USA) according to the manufacturer’s recommendations. The cells were post-transfected within the indicated times and harvested for further analysis.

3.2.13 Colony formation assay

The indicated cells were seeded in 24-well plates at a density of 200 cells per well. Following an overnight incubation of seeded plates, the indicated cells were transfected with the indicated siRNA or siRNA control for 48 h and were then further analyzed by colony formation assay as described previously (Bach et al., 2018a).

3.2.14 Cell migration and invasion assays

Cell invasion assays were performed in 24-well Transwell plates with polycarbonate (PVDF) filters (8 m pore size, Corning, USA), while changes in cell migration were analyzed using Transwell assays without the incorporation of Matrigel. The indicated cells were post-transfected with siBMP4 or siRNA control, and then further analyzed using cell migration and invasion assays as described previously (Bach et al., 2018a).

3.2.15 Taqman microRNA assay

To determine the expression of miRNAs in human cancer cells, we used the TaqMan® MiRNA Assay kit (Applied Biosystems) (Cat. No. 4427975) according to the manufacturer’s protocol. Mature miR-139-5p sequence: UCUACAGUGCACGUGUCUCCAG (Catalog number: 4427975, assay ID: 002289, assay type: Taqman^{TM} microRNA assay).

Mature miR-31-5p sequence: AGGCAAGAUGCUGGCAUAGCU (Catalog number: 4427975, assay ID: 002279, assay type: TaqmanTM microRNA assay). All reactions were performed in triplicate.

3.2.16 *Ex vivo* biochemical analysis of tumors

A portion of the frozen tumor excised from each nude mouse was thawed on ice and homogenized using a hand-held homogenizer in Complete Lysis Buffer (Active Motif, Carlsbad, CA, USA) as described previously (Bach et al., 2018a). The protein concentrations of the tumor lysates were calculated and aliquots were stored at –80 ˚C.

3.2.17 Immunohistochemistry

Immunohistochemical analysis of tumors was carried out as described previously, using the indicated antibodies (Bach et al., 2018a).

3.2.18 Ribonucleoprotein immunoprecipitation (RIP) assay

The RIP-Assay kit for miRNA (MBL) was employed to confirm between miR-139-5p and BMP4 interaction following the manufacturer's instructions. Briefly, fresh cellular extracts from PC9-Gef cells or H1993-Gef cells (10^6) were co-immunoprecipitated with 20 µg of RIP-certified anti-EIF2C2/AGO2 mouse monoclonal antibody (MBL) overnight at 4 ˚C, one of the RISC protein components, previously conjugated with Sepharose Protein G beads (Amersham Biosciences, GE Healthcare). Rabbit IgG was used as negative control. BMP4 and miR-139-5p expression levels were evaluated after total RNA isolation from antibody-immobilized Protein G agarose beads-RNP complexes by real-time PCR (as described in the Materials and Methods Section). Data were normalized to control samples from three independent experiments.

3.2.19 Statistical analysis

The data are presented as the mean ± SD for the indicated number of independently-performed experiments. Statistical significance ($p < 0.05$) was assessed using Student's *t*-test. All statistical tests were two-sided.

3.3. Results

3.3.1 miR-139-5p is a novel biomarker of EGFR-TKI resistance in EGFR-mutant NSCLC cells

To investigate whether miRNAs are required to establish or maintain gefitinib (gef)-resistance, we employed a miRNA array in a primary screen of EGFR mutant NSCLC cells (PC9 cells and PC9-Gef cells). Within this array, the expression of miR-139-5p, a tumor suppressor (Zhang et al., 2014b) and a modulator of chemotherapeutic sensitivity of cancer cells (Li et al., 2016), was observed to be the most significantly suppressed transcript in PC9-Gef cells compared to the parental PC9 cells (Figure 23). In addition, miR-139-5p was previously reported to be able to inhibit cell proliferation by targeting insulin-like growth factor 1 receptor (IGF1R) (Xu et al., 2015) or c-Met (Sun et al., 2015b) in NSCLC cells. Therefore, we attempted to further elucidate the role of miR-139-5p in EGFR-TKI resistance, as its function in tumorigenesis is currently unclear.

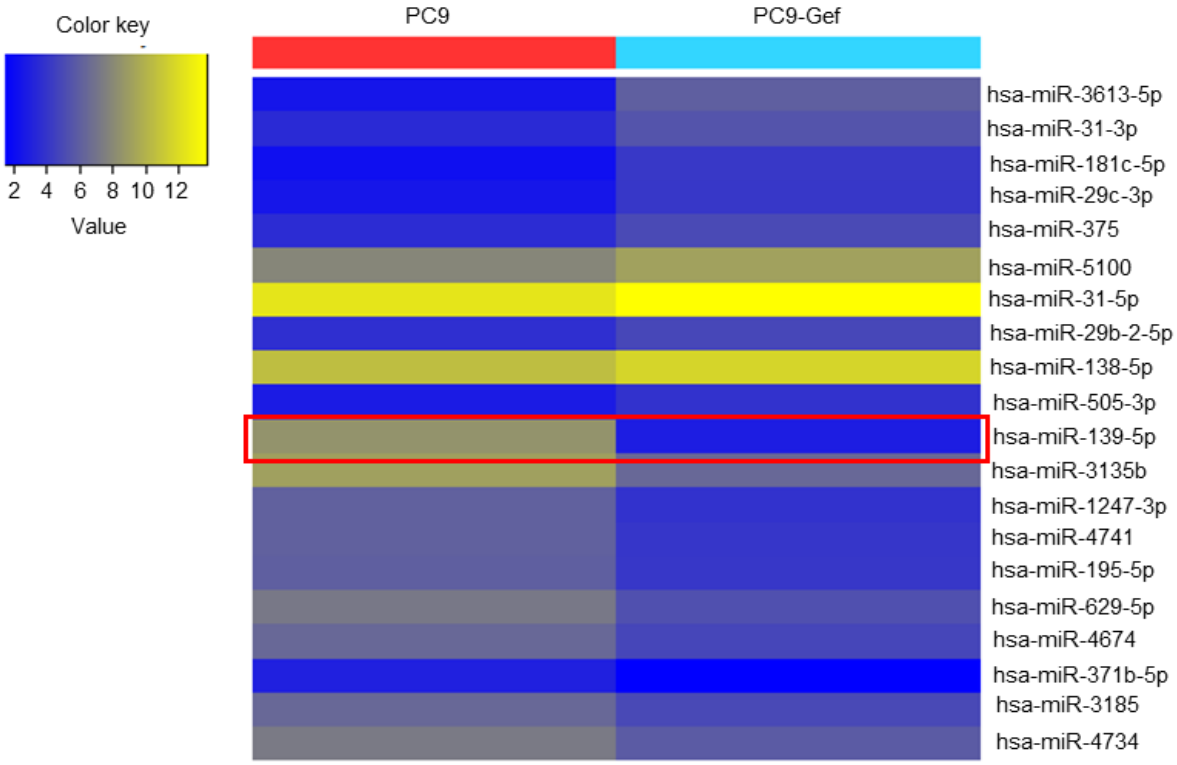

Figure 23: Heat-map representing changes in expression of top up-regulated and down-regulated miRNAs in PC9-Gef cells compared to PC9 cells. Heat-map showing relative expression between PC9 and PC9-Gef cells groups. Rows represent miRNAs and columns represent samples. Yellow blocks represent high expression and blue blocks low expression.

A Taqman assay confirmed that miR-139-5p was down-regulated in PC9-Gef cells in both *in vitro* (Figure 24A, left panel) and in tumor tissues *in vivo* (Figure 24A, right panel). In our previous review, we reported a significant relationship between exosomes and miRNAs in the drug resistance of cancer cells (Bach et al., 2017a). In the present study, we observed that the expression of exosomal miR-139-5p is also down-regulated in PC9-Gef cells compared to PC9 cells (Figure 24B). Interestingly, the expression of miR-139-5p is similarly down-regulated in other EGFR-TKI-resistant NSCLC cells, including HCC827-Gef cells (EGFR mutation) *versus* HCC827 cells (EGFR mutation) (Figure 24C, left panel), HCC827-Erl cells *versus* HCC827 cells (Figure 24C, right panel), H1993-Gef cells (EGFR wild-type) *versus* H1993 cells (EGFR wild-type) (Figure 24D, left panel), H1993-Erl cells *versus* H1993 cells (Figure 24D, right panel) and H1993-Gef tumor tissues *versus* H1993 tumor tissues (Figure 24E).

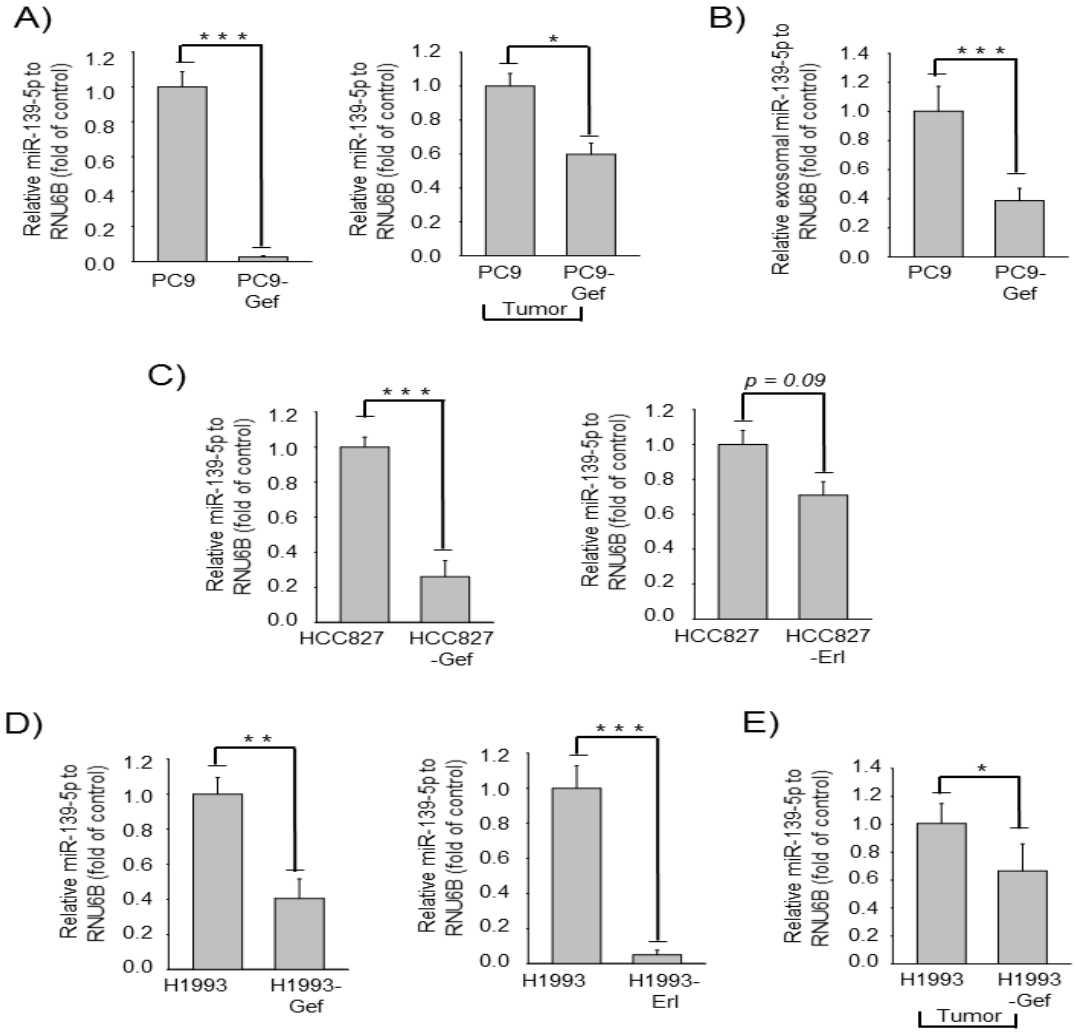

Figure 24. The expression of miR-139-5p in PC9-Gef compared to PC9 cells. (A) Characterization of PC9 cells or PC9-Gef cells (left panel) and tissues (right panel) for miR-139-5p expression. miR-139-5p levels were quantified by Taqman assay and normalized to U6 snRNA levels. (B) Characterization of total exosome isolation from PC9 cells and PC9-Gef cells for miR-139-5p. miR-139-5p levels were quantified by Taqman assay as described in Materials and Methods. (C, D, E) Characterization of indicated cells (C, D) and tissues (E) for miR-139-5p expression. miR-139-5p levels were quantified by Taqman assay as described in Materials and Methods.

To further identify and validate miRNAs that are specifically affected by yuanhuadine (YD), an antitumor agent (Bach et al., 2018a; Bae et al., 2015) we performed a miRNA array with PC9-Gef cells in the presence or absence of a 24 h YD treatment. Interestingly, we found that miR-139-5p was also up-regulated by YD in PC9-Gef cells (Figure 25). Therefore, miR-139-5p which was mostly down-regulated in gef-resistant cell lines can be a novel biomarker in drug resistance cells and thereby primarily chose miR-139-5p as a promising candidate biomarker compared to the miR-4485.

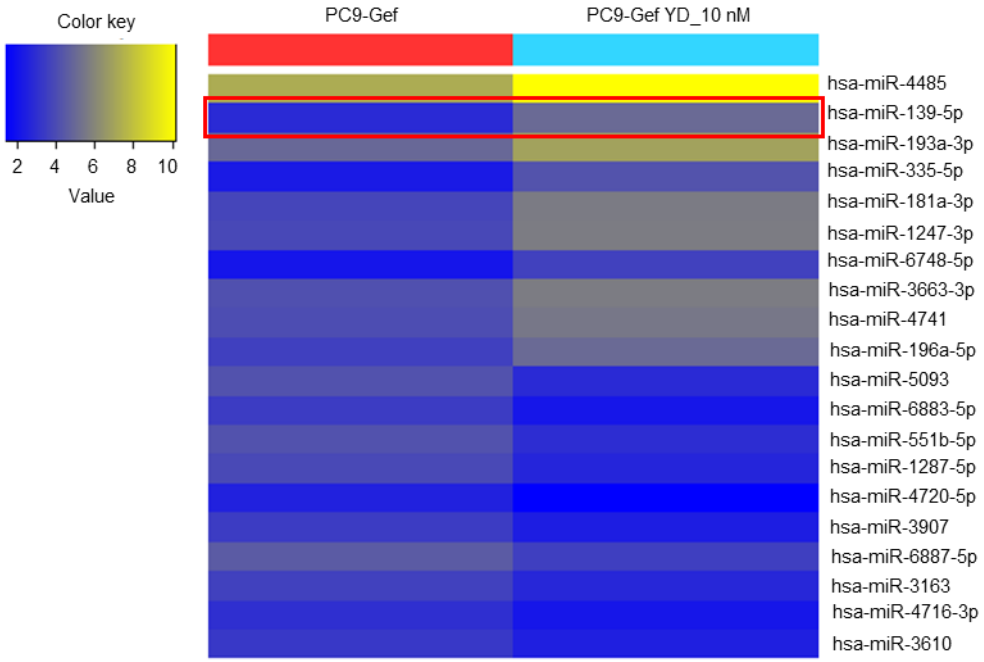

Figure 25: Heat-map showing changes in expression of top up-regulated and down-regulated miRNAs in PC9-Gef cells treated with control or YD (10 nM) for 24 h. Heat-map showing relative expression between the indicated groups. PC9-Gef cells were treated for 24 h with 10 nM YD or vehicle control. Rows represent miRNAs and columns represent samples. Yellow blocks represent high expression and blue blocks low expression relative to control cells.

Subsequently, we further confirmed the effects of YD on miR-139-5p and observed that YD is able to enhance the expression of miR-139-5p not only in PC9-Gef (Figure 26A, left panel) and PC9-Erl (Figure 26A, right panel) cells but also in other drug resistant NSCLC cells, including HCC827-Gef (Figure 26B, left panel), HCC827-Erl (Figure 26B, right panel), H1993-Gef (Figure 26C, left panel), H1993-Erl (Figure 26C, right panel), and H1993-Gef tissues *in vivo* (Figure 26D). Taken together, these findings indicated that miR-139-5p might be considered a novel biomarker associated with EGFR-TKI resistance in NSCLC cells. In addition, YD, an antitumor agent, could effectively modulate the expression of the tumor suppressor miR-139-5p in NSCLC cells with acquired resistance to EGFR-TKIs.

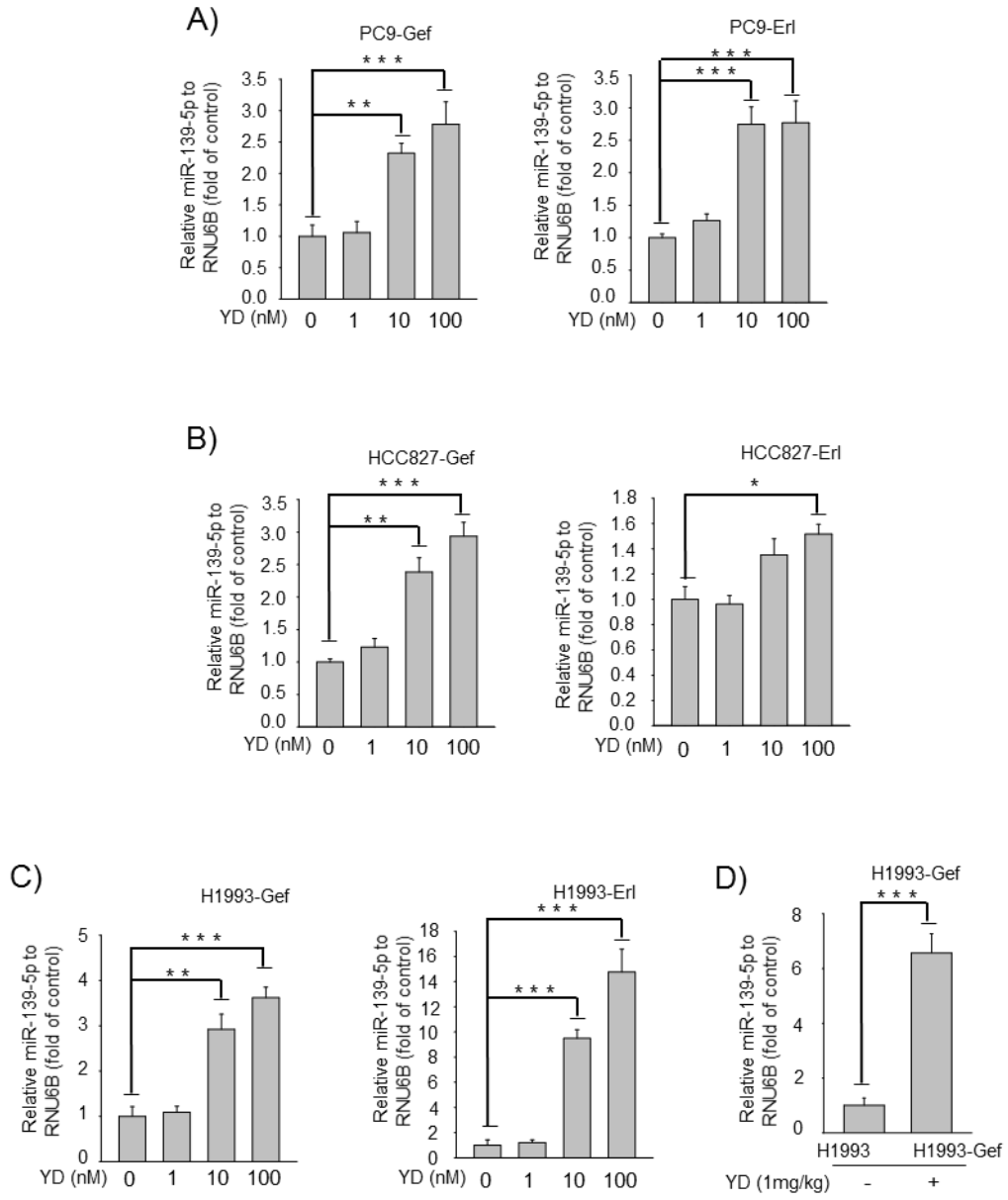

Figure 26. Effects of YD on miR-139-5p expression in gef-resistant NSCLC cells. (A, B & C) The indicated cells were treated with YD for 24 h, and then miR-139-5p levels were analyzed by Taqman assay as described in Materials and Methods. (D) Relative expression of miR-139-5p in the indicated xenografts. The levels of miR-139-5p were analyzed by Taqman assay as described in Materials and Methods. Each assay was performed in triplicate and the expression of miR-139-5p was normalized to snRNA RNU6B.

3.3.2 BMP4 is a candidate biomarker in EGFR-TKI-resistant NSCLC cells

To identify the candidate gene markers associated with acquired resistance to EGFR-TKIs in EGFR-mutant NSCLC cells, we initially performed cDNA arrays in two different groups, as depicted in Figure 27. BMP4 was observed to be one of the most overexpressed genes in PC9-Gef cells compared to PC9 cells. Furthermore, BMP4 was effectively suppressed by YD (Figure 27, left panel) and miR-139-5p (Figure 27, right panel) in PC9-Gef cells (Table 1). We further confirmed that BMP4 was up-regulated in PC9-Gef cells compared to parental cells both *in vitro* (Figure 28A) and in tumor tissues *in vivo* (Figure 28B) at both the protein (upper panel) and mRNA levels (lower panel). Interestingly, we also observed that BMP4 was overexpressed in H1993-Gef (Figure 28C, left panel) and H1993-Erl cells (Figure 28C, right panel) compared to their parental cells.

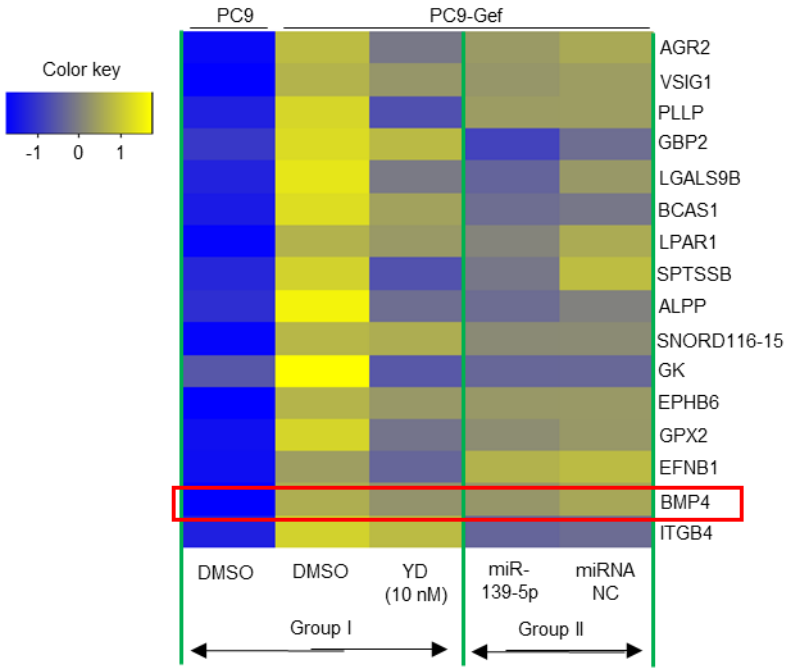

Figure 27. BMP4 is identified by combining target arrays. Heat-map showing relative expression among all groups. Left panel, PC9-Gef cells were treated for 24 h with 10 nM YD or vehicle control. Right panel, PC9-Gef cells were transfected with miR-139-5p or miRNA mimic for 48 h. Rows represent genes and columns represent samples. Yellow blocks represent high expression and blue blocks low expression relative to control cells.

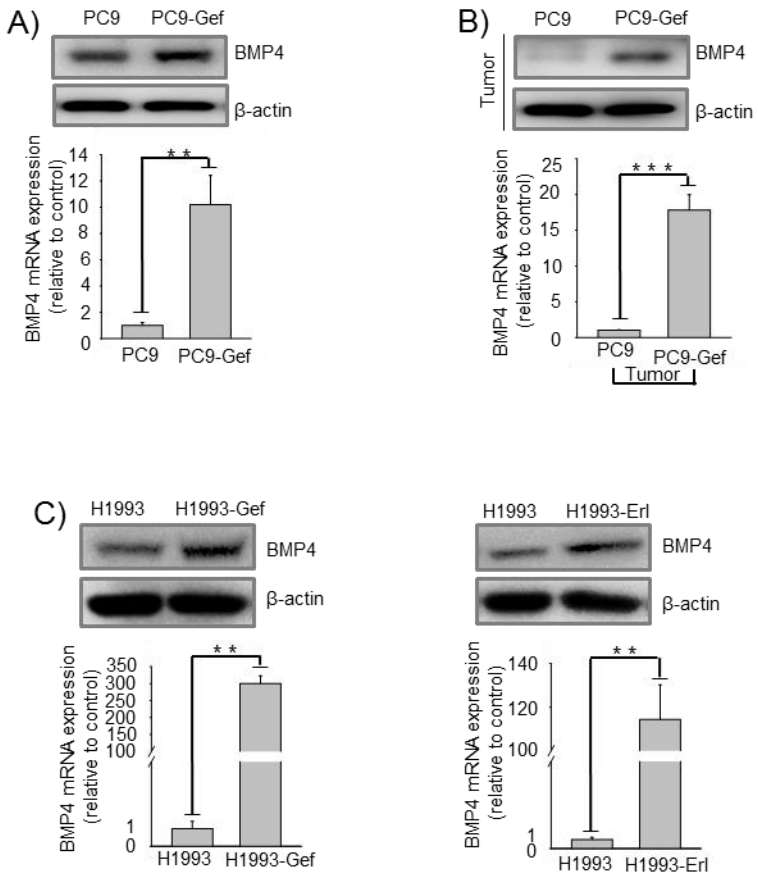

Figure 28: Characterization of indicated parental or drug-resistant cell lines and tissues for BMP4 expression at both the protein and mRNA levels. (A) PC9-Gef cells compared to PC9 cells *in vitro*. (B) PC9-Gef cells compared to PC9 cells *in vivo*. (C) H1993-Gef cells compared to H1993 cells *in vitro* (left panel) and in vivo (right panel).

Next, we transfected miR-139-5p into the resistant cells and observed the effects of miR-139-5p and/or YD on the expression of BMP4. When PC9-Gef, HCC827-Gef or H1993-Gef cells were transduced with exogenous miR-139-5p, the cellular level of miR-139-5p was significantly enhanced in these indicated cells (Figure 29A). As shown in Figure 29B, transfection with miR-139-5p effectively suppressed the expression of BMP4 and co-treatment with YD enhanced this suppression. In addition, to determine whether miR-139-5p binds directly to BMP4 mRNA, we performed ribonucleoprotein immunoprecipitation assay (RIP assay) to pull down miRNAs associated with RNA-induced silencing complex (RISC). An anti-AGO2 antibody was used to isolate miRNAs and mRNAs that were incorporated in RISC. In H1993-Gef cells that were stably over-expression miR-139-5p, BMP4 mRNA was enriched in RISC as compared with the IgG control (Figure 30A). Anti-AGO-2 antibody also significantly enriched miR-139-5p as detected by Taqman PCR, compared with NC mimic in PC9-Gef and H1993-Gef cells (Figure 30B), indicating that miR-139-5p directly interacts with BMP4 mRNA. The expression of BMP4 was also effectively suppressed by YD in *in vivo* tumor tissues analyzed by real-time PCR (Figure 31A, upper panel), immunoblotting (Figure 31A, lower panel) and immunohistochemistry (IHC) (Figure 31B). Taken together, these data suggest that BMP4 is a novel marker associated with acquired EGFR-TKI resistance in EGFR-mutant NSCLC cells and that BMP4 expression can be effectively suppressed by miR-139-5p and/or YD treatment in order to overcome resistance in these cells.

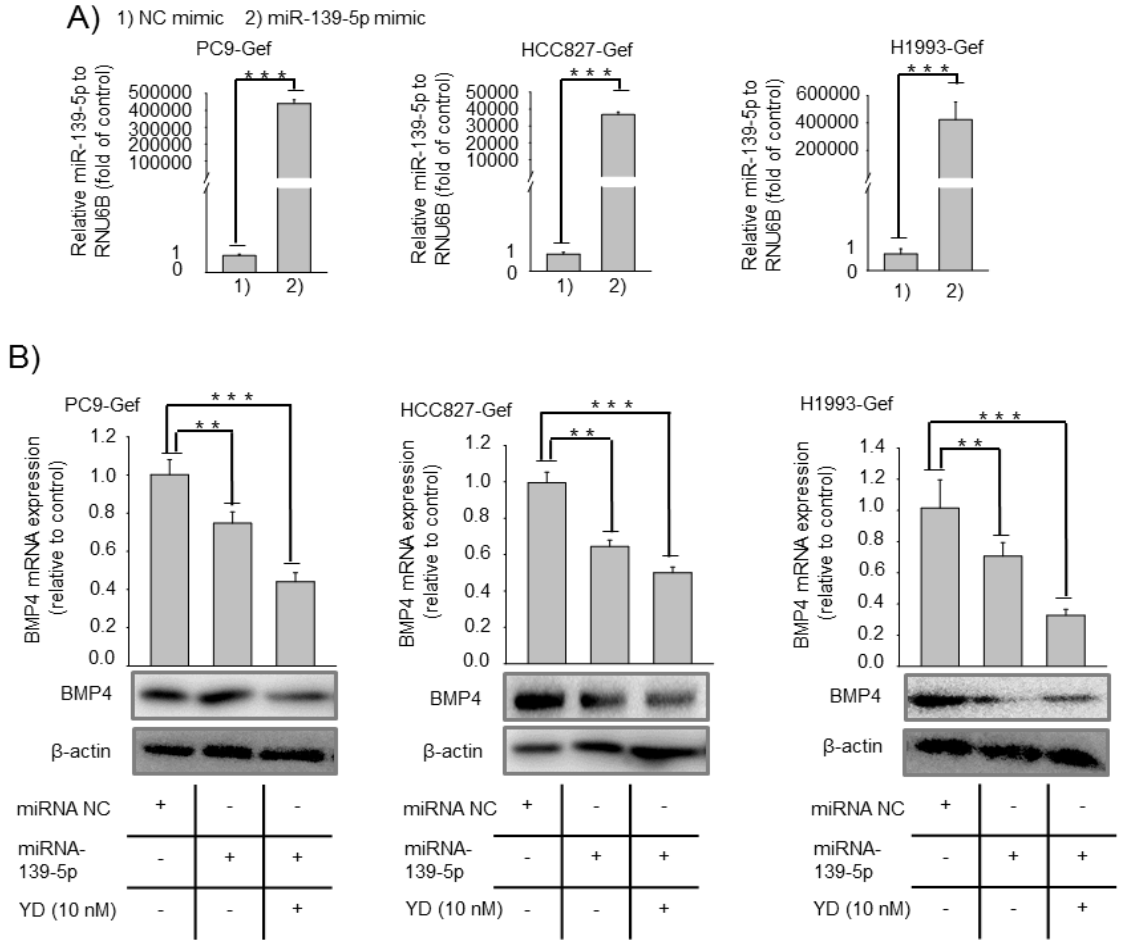

Figure 29: Effects of miR-139-5p and YD on BMP4 in gef-resistant NSCLC cells. (A) Effects of miR-139-5p mimic on miR-139-5p expression in the indicated gef-resistant cell lines. The indicated gef-resistant cell lines were cultured in 6-well plates and then transfected with negative control mimic or miR-139-5p for 48 h (50 *p*mole/well). The expression levels of miR-139-5p were determined by Taqman assay with specific primers for mature miR-139-5p. Expression levels in each sample were normalized to levels of U6 snRNA. (B) The indicated cells were post-transfected with miR-139-5p for 24 h. Then, the indicated cells were further treated with YD (10 nM) for 24 h. The cell lysates were subsequently analyzed by real-time PCR and immunoblotting, as described in Materials and Methods.

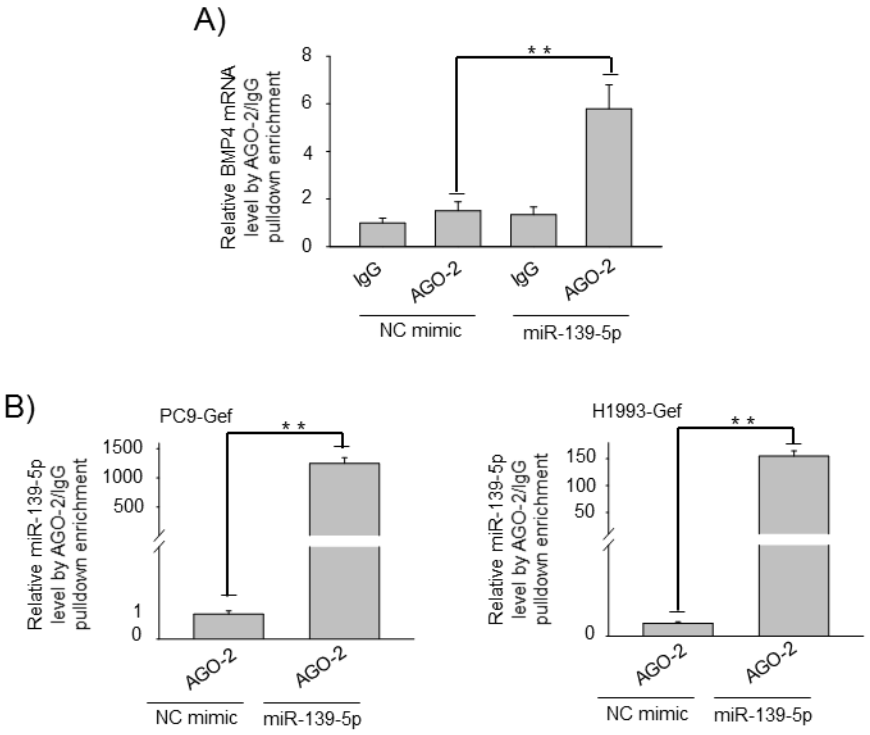

Figure 30: RIP assay of miR-139-5p interaction with BMP4 mRNA. Co-immunoprecipitated BMP4 mRNA (A) and miR-139-5p (B) by anti-AGO-2 RIP are shown. The data were normalized to β–actin or U6 snRNA, respectively. NC, negative control.

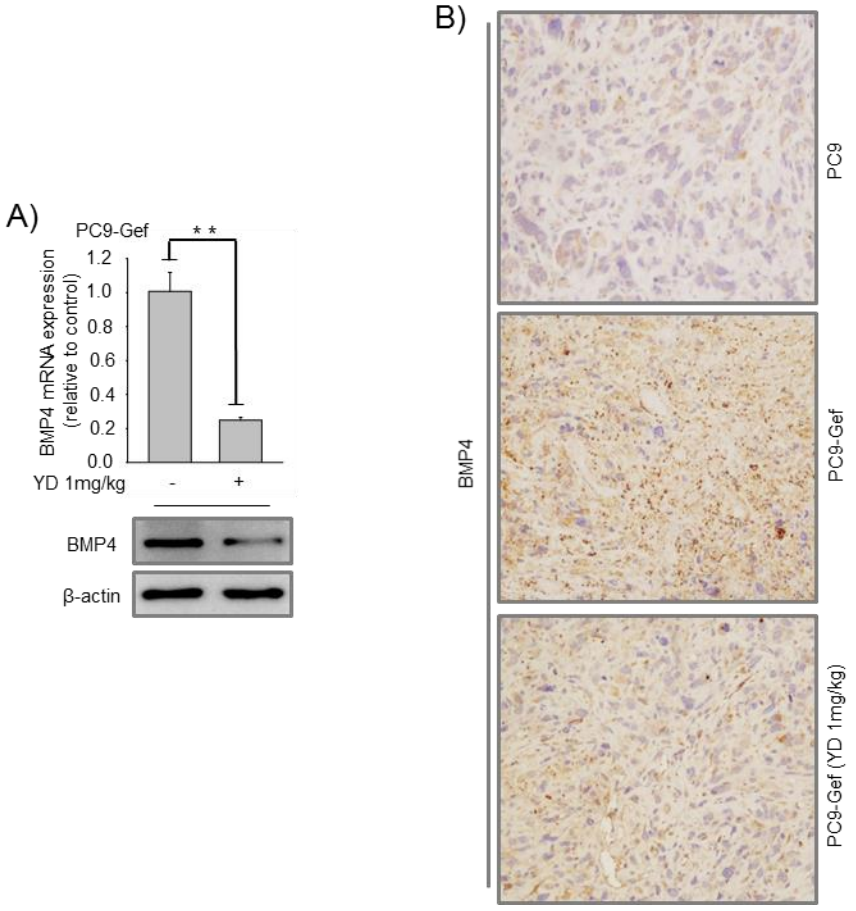

Figure 31: Effects of YD on BMP4 *ex vivo* models. (A) Relative expression of BMP4 in the indicated xenograft tumors. The levels of BMP4 were analyzed by real-time PCR (upper panel) or immunoblotting (lower panel), as described in Materials and Methods. (B) Immunohistochemical analysis for BMP4 in indicated tumor tissue sections.

3.3.3 BMP4 affects the growth of EGFR-TKI-resistant NSCLC cells

The critical function of BMPs in cancer is still unclear, as discussed in a recent review by our group (Bach et al., 2018b). However, in human NSCLC, blockage of BMP signaling is considered an effective therapeutic approach for lung cancer patients (Hao et al., 2014). Kim *et al* recently reported that BMP4 depletion might suppress tumorigenesis and metastasis in lung adenocarcinoma cells (Kim et al., 2015). Furthermore, the growth and metastasis of lung adenocarcinoma was potentiated by BMP4-mediated immunosuppression (Chen et al., 2016). Therefore, we determined whether the knockdown of BMP4 by siRNA affects the growth of the EGFR-TKI-resistant NSCLC cells. We first measured the knockdown efficiency of various siBMP4s and selected specific siRNAs for further study in the resistant cells (Figure 32A and 32B). As depicted in Figure 32C, knockdown of BMP4 enhanced the growth-inhibitory activity of gefitinib in PC9-Gef and H1993-Gef cells (Figure 32C). In addition, the knockdown of BMP4 also significantly suppressed colony formation in PC9-Gef and H1993-Gef cells (Figure 33A). Similarly, knockdown of BMP4 also inhibited cell invasion (Figure 33B) and migration (Figure 33C) in PC9-Gef cells.

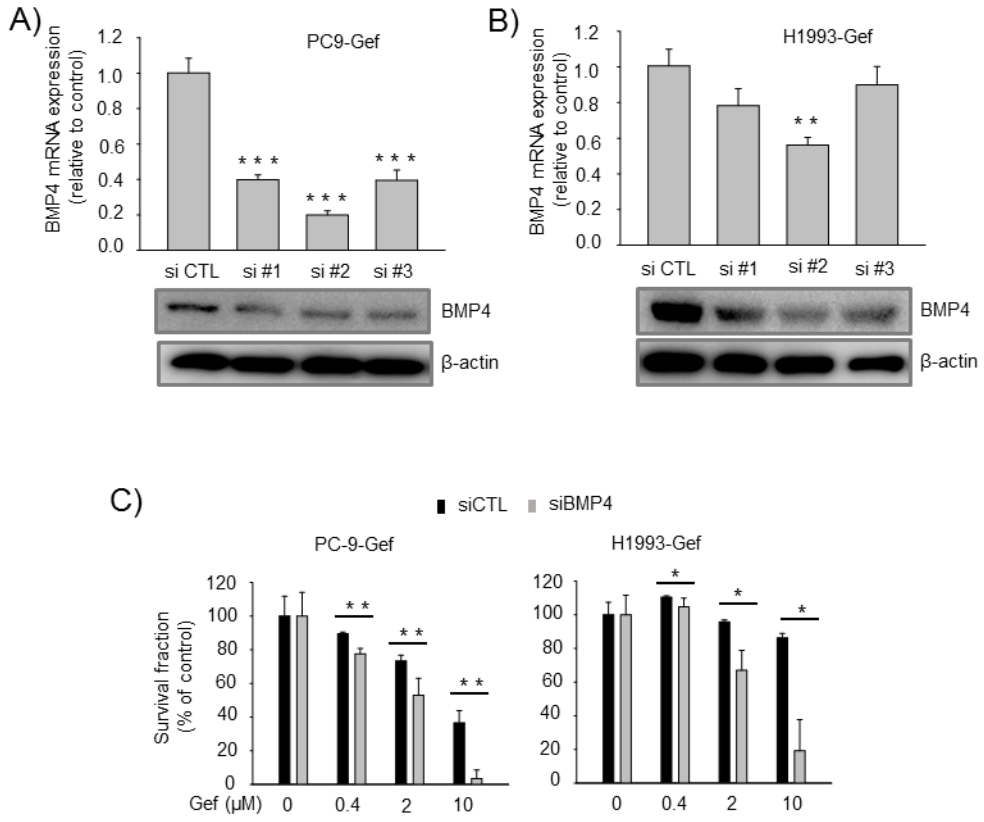

Figure 32. Effects of BMP4 on the growth of EGFR-TKI-resistant NSCLC cells *in vitro*. (A & B) Confirmation of BMP4 knockdown efficiency at the mRNA (upper panels) and protein levels (lower panels) in PC9-Gef (A) and H1993-Gef (B) cells. (C) Cells were transiently post-transfected with control or BMP4 #2 siRNA for 48 h, and then incubated with the indicated concentrations of gef. Cell viability was further assessed by SRB assay as described in Materials and Methods.

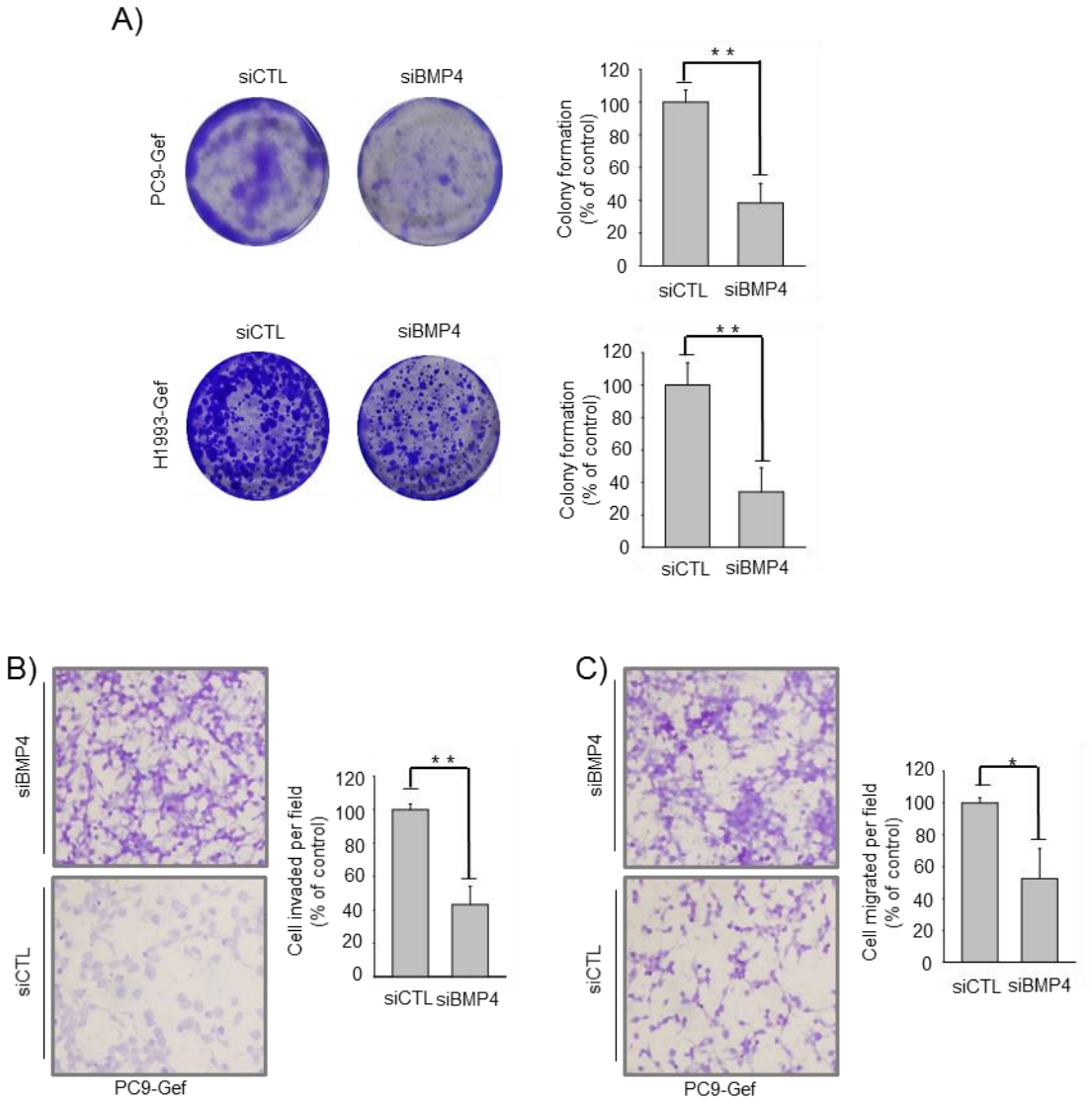

Figure 33. Effects of BMP4 on colony, migration and invasion of EGFR-TKI-resistant NSCLC cells. (A) The indicated cells were transiently post-transfected with either scramble siRNA or BMP4 #2 siRNA for 48 h, then cultured for colony formation assays as described in Materials and Methods. (B & C) PC9-Gef cells were transiently post-transfected with either scramble siRNA or BMP4 #2 siRNA for 48 h, then cultured for invasion and migration assays as described in Materials and Methods.

The *in vivo* effects of BMP4 on tumor growth were subsequently investigated in BALB/c nude mouse xenograft models implanted with gef-resistant NSCLC cells. The gef-resistant cells were initially established as stable BMP4-knockout cells. As shown in Figures 34A and 34B, shBMP4-A and shBMP4-D were the most efficient in knocking down BMP4 expression in PC9-Gef and H1993-Gef cells compared to shBMP4-B and shBMP4-C. Mice were then subcutaneously injected in the right axilla with empty vector-transfected PC9-Gef cells and H1993-Gef cells, or stable BMP4-A or BMP4-D knockout PC9-Gef and H1993-Gef cells. At 40 days (PC9-Gef) and 30 days (H1993-Gef) after inoculation, the mice were sacrificed, and the tumors in each mouse were excised and photographed. As shown in Figures 35A and 35B, the tumors in the stable BMP4 knockout group were smaller than those in the vector-treated groups, demonstrating that BMP4 is able to enhance the growth of gef-resistant NSCLC cells.

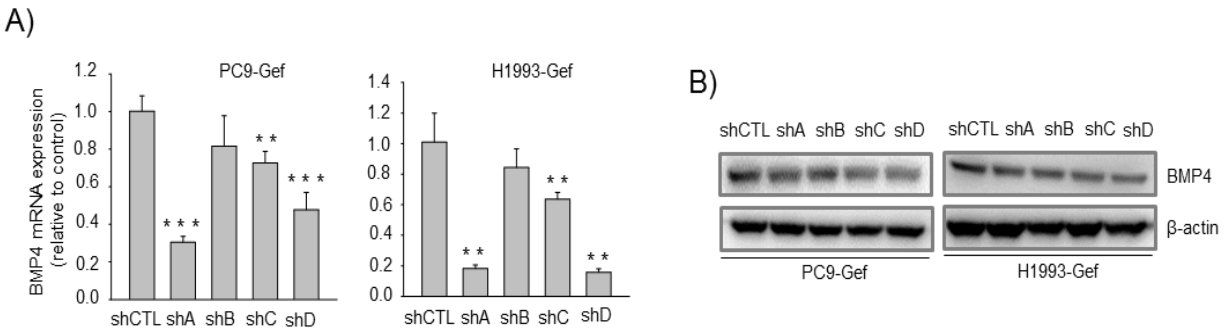

Figure 34: Establishing stable knock-down BMP4 cell lines. (A & B) Confirmation of BMP4 knockdown efficiency by shRNA at both the mRNA (A) and protein (B) levels in stable knockout PC9-Gef and H1993-Gef cells as described in Materials and Methods.

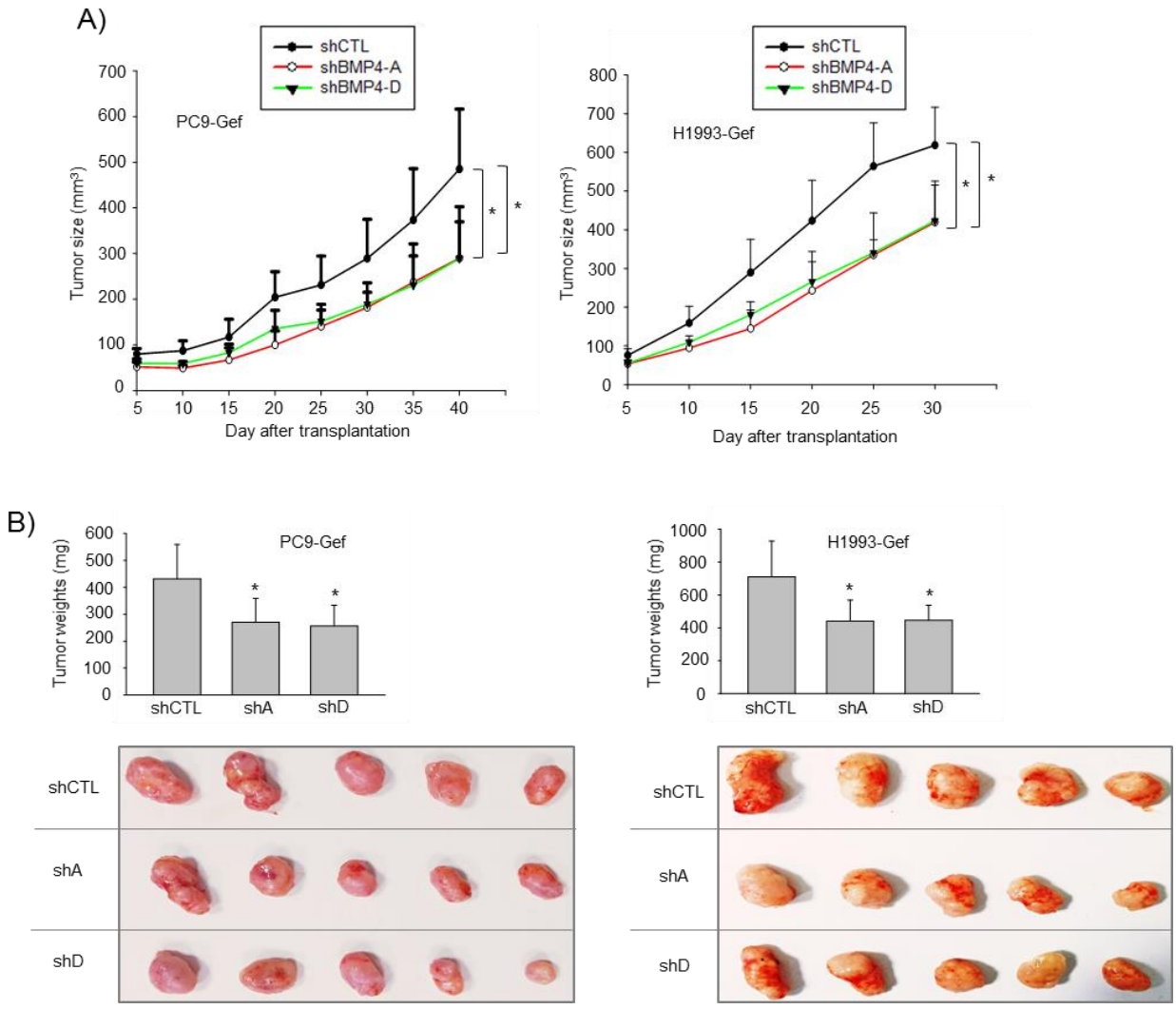

Figure 35: Effects of BMP4 on the growth of gef-resistant NSCLC cells *in vivo* models. (A & B) Tumor-forming ability of BMP4-silenced gef-resistant NSCLC cells. BALB/c nude mice received subcutaneous transplants of PC9-Gef-sh control (n = 5) and PC9-Gef-shBMP4 (shA or shD) (n = 5) cells or H1993-Gef-sh control (n = 5) and H1993-Gef-shBMP4 (shA or shD) (n = 5) cells. (A) Tumor volumes at the indicated time points. (B) Tumor weights (upper panels) and representative photographs 40 days (PC9-Gef) and 30 days (H1993-Gef) after injection (lower panels).

3.3.4 BMP4 affects cancer cell metabolism via modulation of ACSL4 and p53

To further investigate the downstream targets of BMP4 and its functional activity in cancer cells, a cDNA microarray was performed on BMP4-depleted EGFR-TKI-resistant NSCLC cells. Genes associated with cell metabolism were the genes most affected by BMP4 depletion (Figure 36). Among these genes, Acyl-CoA synthetase long-chain family member 4 (ACSL4) was highly suppressed in PC9-Gef cells (Figure 37A). Previous studies suggested that ACSL enzymatic activity plays a significant role in the maintenance of mutant lung cancer; furthermore, fatty acid oxidation mediated by ACSL enzymes is required for mutant lung tumorigenesis (Padanad et al., 2016; Phan et al., 2017). In addition, BMP4 depletion suppresses ACSL4 expression at both the mRNA (Figure 37B, upper panels) and protein levels (Figure 37C, lower panels). However, ACSL4 knockdown did not affect BMP4 expression at both the mRNA (Figure 38, upper panels) and protein levels (Figure 38, lower panels). These data indicate that ACSL4 seems to be one of downstream target proteins mediated by BMP4.

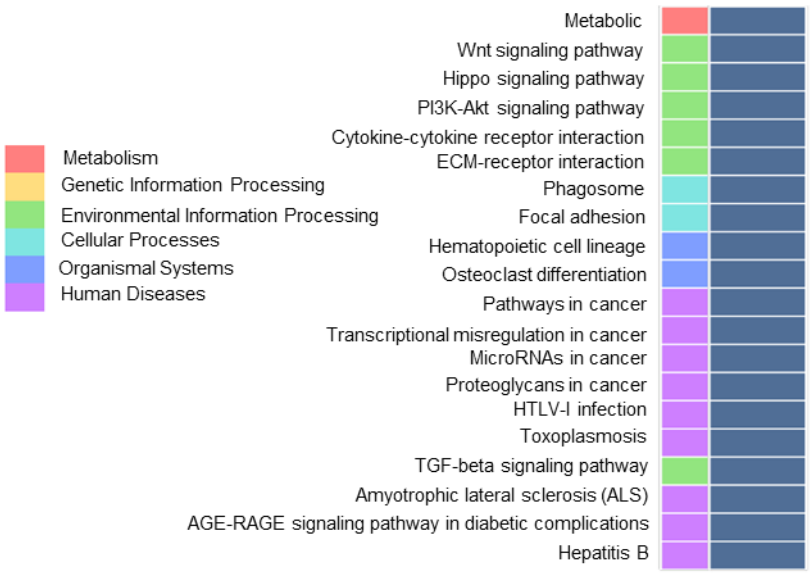

Figure 36. Effects of BMP4 on top 20 terms in enrichment. Heat-map showing and comparing top enriched terms. Enrichment test based on the Gene Ontology (GO, http://geneontology.org/) database was conducted using the significant gene list. Significant enrichments are displayed in blue (p-value = 0.0001).

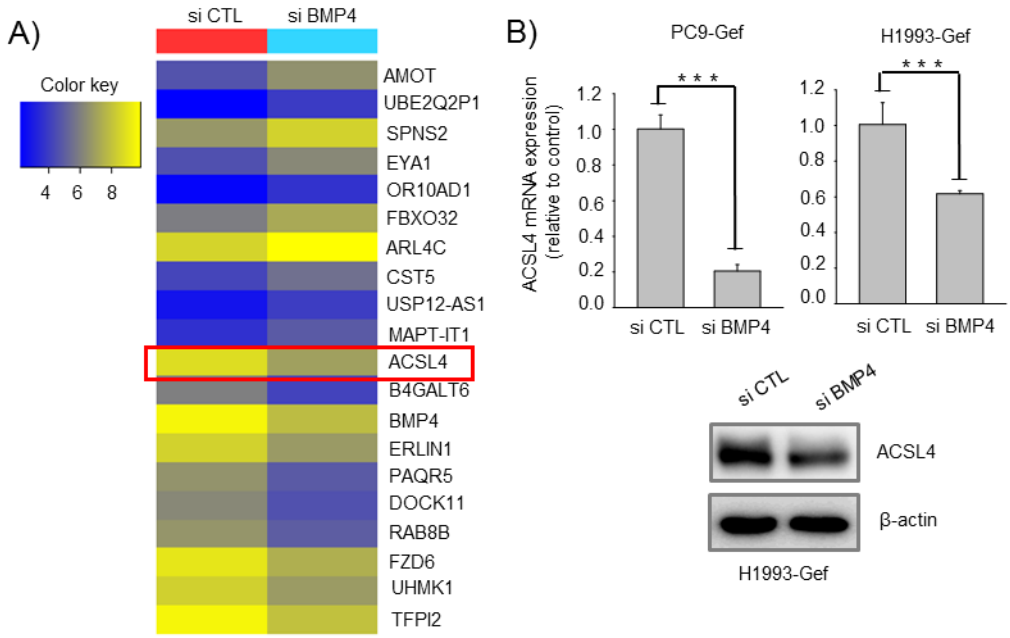

Figure 37: Effects of BMP4 on ACSL4 in gef-resistant NSCLC cells. (A) Heat-map representing changes in expression of top up-regulated and down-regulated genes in PC9-Gef cells transfected with control or BMP4 #2 siRNA. (B) PC9-Gef and H1993-Gef cells were transfected with control or BMP4 siRNA for 48 h, then cell lysates were subjected to real-time PCR (*top panels*) or immunoblotting (*bottom panels*).

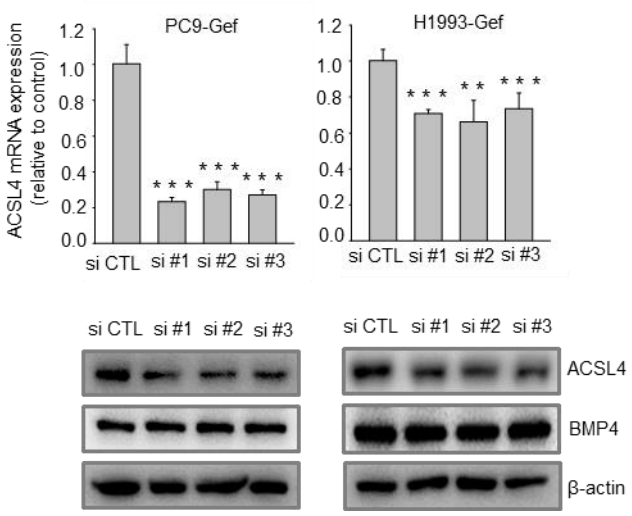

Figure 38: Effects of ACSL4 on BMP4 in gef-resistant NSCLC cells. PC9-Gef and H1993-Gef cells were transfected with control or ACSL4 siRNA for 48 h, then cell lysates were subjected to real-time PCR (*top panels*) or immunoblotting (*bottom panels*).

Interestingly, ACSL4 is considered an important enzyme in energy metabolism (Maloberti et al., 2010; Miyares et al., 2013; Sanchez-Martinez et al., 2015) and BMP4 is also associated with oxidative metabolism in cells (Modica and Wolfrum, 2017; Qian et al., 2013; Tang et al., 2016), as depicted in Figure 39A. Therefore, we determined whether the effects of BMP4 on the production of main energy metabolites were catalyzed by ACSL4. We found that BMP4 depletion suppressed the enzymatic activity of ACSL4 and thus restored metabolites, including fatty acids ($-CH_3$), triglycerides and cholesterol esters, in the resistant cells (Figure 39B). We also found that BMP4 depletion stimulated p-p53 expression, as shown by phosphor-kinase array (Figure 39C). This up-regulation of p-p53 (Ser15) was confirmed by Western blot analysis (Figure 39D) in PC9-Gef cells. Recent findings suggest that the tumor suppressor p53 is also related to the regulation of lipid metabolism, including enhancing fatty acid oxidation and suppressing fatty acid synthesis (Liang et al., 2013; Liu et al., 2015). Therefore, the activation of p53 expression by BMP4 depletion might affect lipid metabolism catalyzed by ACSL4. Taken together, BMP4 seems to be associated with cancer cell metabolism through the regulation of ACSL4 and the tumor suppressor p53.

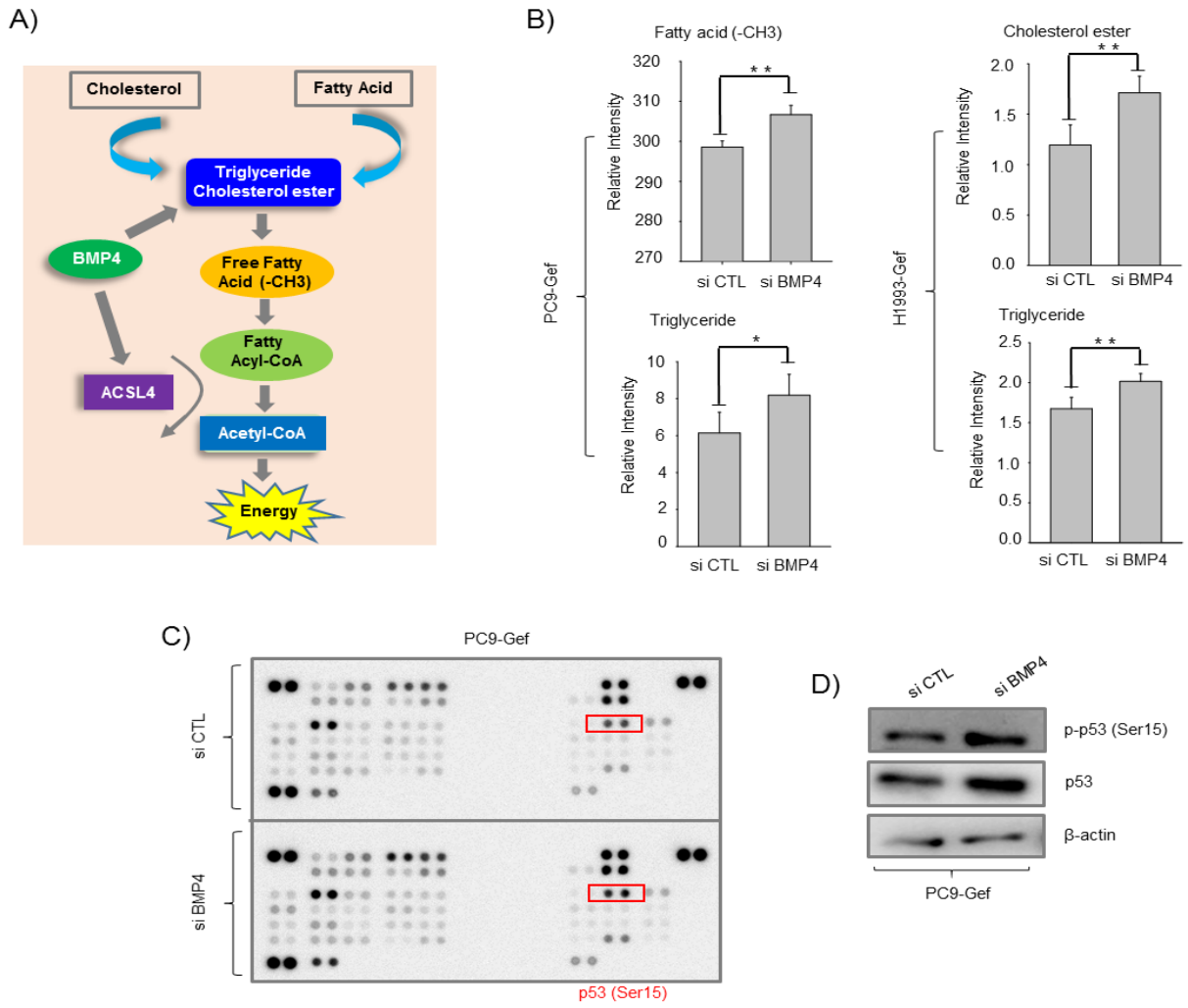

Figure 39: Effects of BMP4 on fatty acid metabolism in gef-resistant NSCLC cells. (A) Schematic diagram illustrating the proposed BMP4 pathway modulating energy metabolism through ACSL4 and triglycerides. (B) PC9-Gef and H1993-Gef cells were transfected with control and BMP4 #2 siRNA for 48 h, and then cell lysates were further processed for metabolic analyses as described in Materials and Methods. (C) PC9-Gef cells were transfected with control or siBMP4 #2 siRNA for 48 h, and cell lysates were subjected to the phosphor-kinase array. p-p53 (Ser15) expression levels are indicated. (D) Indicated cells were transfected with either siBMP4 #2 or si CTL for 48 h, and then lysates were analyzed for p-p53 and total p53 by immunoblotting.

3.3.5 Suppression of BMP signaling inhibits the growth of EGFR-TKI-resistant NSCLC cells

Fotinos *et al* recently reported that the suppression of BMP signaling is a valid therapeutic strategy in lung cancer (Fotinos et al., 2014) and that the dorsomorphin derivative LDN-193189, a BMP type I receptor inhibitor, had significant growth-inhibitory activity against NSCLC cells compared to non-transformed cells (Fotinos et al., 2014). Our findings in this study confirm that BMP4 is one of the principal paracrine factors that stimulate the growth of drug-resistant cancer cells. To further confirm whether knockdown of the BMP-BMPR pathway may suppress the growth of drug-resistant cancer cells, the efficacy of LDN-193189 was investigated in tumor growth. LDN-193189 effectively inhibits the growth of cancer cells (Figure 40A); this effect was in part associated with the suppression of Smad1/5 activation (p-Smad1/5) in the resistant cancer cells (Figure 40B). Interestingly, we observed that LDN-193189 might stimulate the expression of miR-139-5p in the drug-resistant NSCLC cells (Figure 41). These findings demonstrated to us a possible therapeutic approach using a combination of LDN-193189 and YD, an antitumor agent that may potentially induce miR-139-5p expression, in drug-resistant cancer treatment. As shown in Figure 42, the combination of LDN-193189 and YD enhanced growth inhibition in cancer cells compared to treatment with LDN-193189 alone.

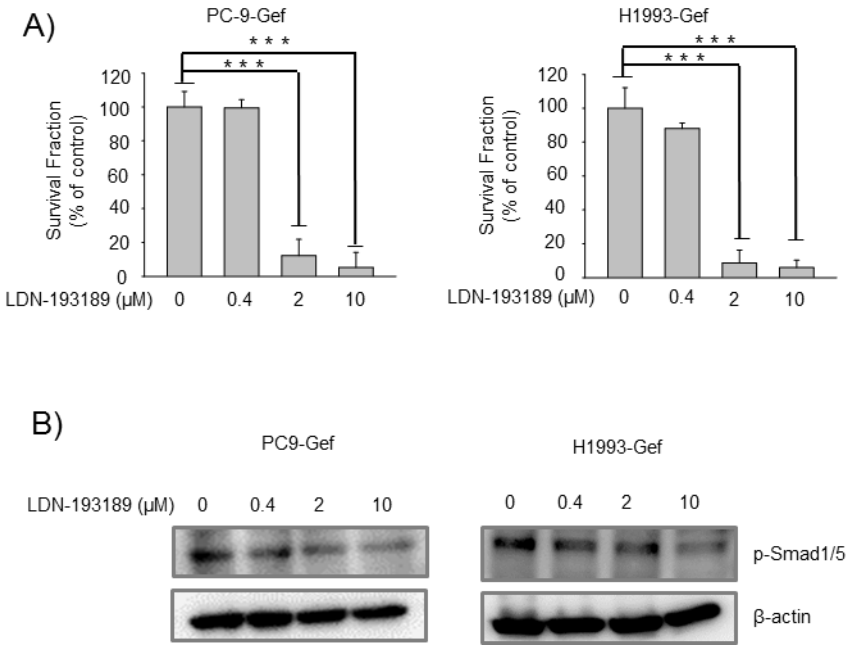

Figure 40: Effects of LDN-193189 on cell proliferation and BMP pathways in gef-resistant NSCLC cells. (A) The indicated cells were treated with LDN-193189 for 72 h and cell proliferation was determined by SRB assay. The IC_{50} values were calculated using the TableCurve 2D software and the data are presented as the mean ± SD. (B) PC9-Gef cells and H1993-Gef cells were treated with the indicated concentrations of LDN-193189 for 24 h, and the cell lysates were further analyzed by immunoblotting using β-actin as a loading control.

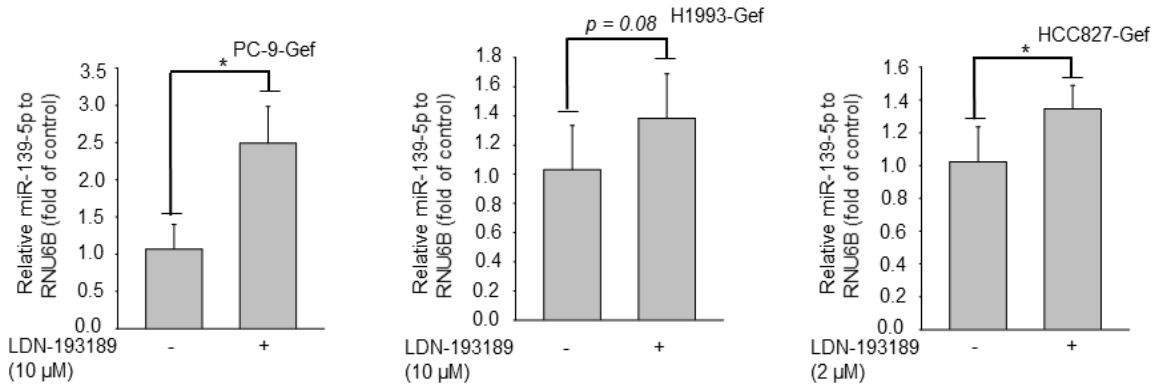

Figure 41: Effects of LDN-193189 on miR-139-5p in gef-resistant NSCLC cells. The indicated cells were treated with the indicated concentrations of LDN-193189 for 24 h, and then the cell lysates were analyzed by Taqman PCR using U6 snRNA as an internal control.

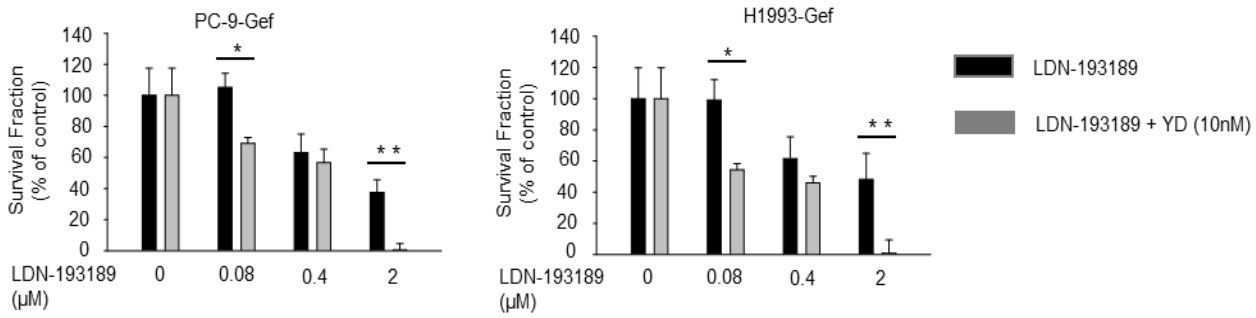

Figure 42: Effects of LDN-193189 in combination with YD in gef-resistant NSCLC cells. PC9-Gef cells and H1993-Gef cells were treated with the indicated concentrations of LDN-193189 either alone or in combination with 10 nM of YD for 48 h. Cell proliferation was determined by SRB assay.

Notably, LDN-193189 also effectively suppressed tumor growth in nude mice bearing gef-resistant NSCLC cells *in vivo* (Figure 43A & B) without any significant change in body weight (Figure 43C). The analysis of tumor tissues also revealed suppressed expression of the cell proliferation biomarker Ki-67 (Figure 44A) and the up-regulation of miR-139-5p levels (Figure 44B), as confirmed by consistent findings in *in vitro* cell culture systems. These data suggest that the suppression of endogenous BMP signaling may represent a possible strategy for the treatment of drug-resistant NSCLC cells.

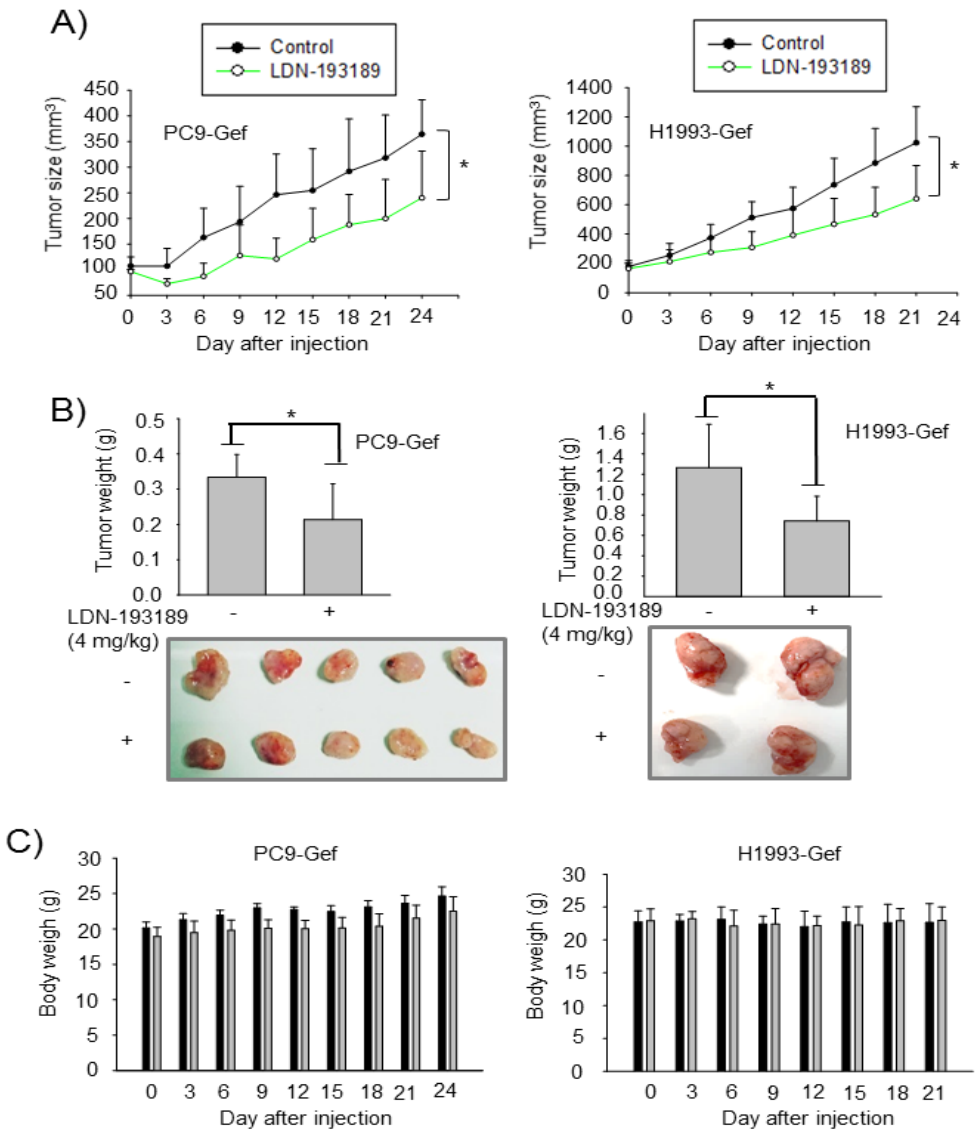

Figure 43: Effects of LDN-193189 on the gef-resistant NSCLC cells *in vivo* models. (A) PC9-Gef cells (6×10^6 cells/mouse) and H1993-Gef cells (5×10^6 cells/mouse) were implanted subcutaneously into the flanks of BALB/c-nude mice. Three weeks of dosing with LDN (4 mg/kg body weight for PC9-Gef cells or 5 mg/kg body weight for H1993-Gef cells) was initiated when the PC9-Gef tumor volumes reached approximately 100 mm^3 and H1993-Gef tumor sizes reached approximately 170 mm^3. The tumor volumes were measured every 3 days (n = 5 mice per group). The error bars represent the means ± SD. (B) Tumors were excised from animals on day 24 after treatment and tumor weights were measured. (C) Body weights of the mice were monitored during the experiments for toxicity.

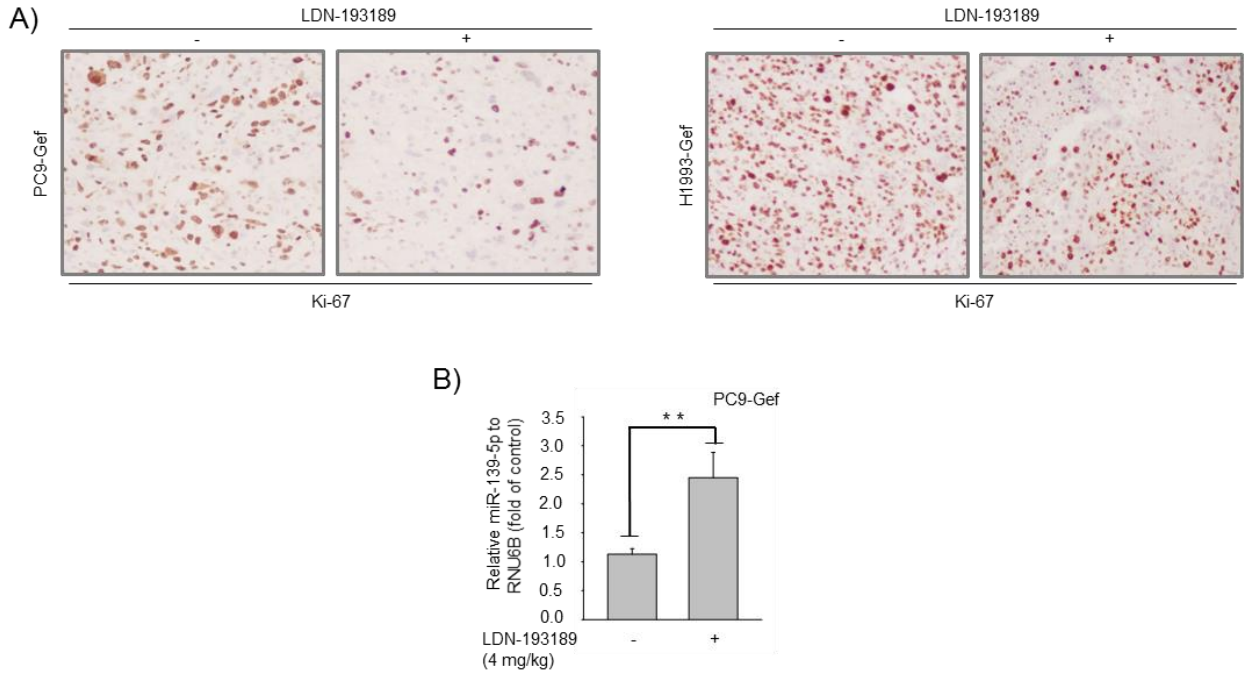

Figure 44: Effects of LDN-193189 on gef-resistant NSCLC cells *ex vivo*. (A) Immunohistochemical analysis of PC9-Gef and H1993-Gef xenograft tumors. Formalin fixed, paraffin-embedded tumor sections were blocked and probed with an antibody against Ki-67, which was detected using the LSAB^{TM} + System-HRP kit (Dako). (B) Taqman PCR analysis of PC9-Gef xenograft tumors. The expression levels of miR-139-5p were determined by Taqman PCR analysis as described in Materials and Methods.

3.4 Discussion

Recent studies revealed that miRNAs might be applicable as potential biomarkers to predict responses to chemotherapy and survival of patients with malignant tumors (Bach et al., 2017a). Indeed, down-regulation of miR-139-5p was observed in colorectal cancer (Zhang et al., 2014b), hepatocellular carcinoma (HCC) (Wong et al., 2011) and NSCLC (Sun et al., 2015a). BMP4 genetic variants and protein expression are also highly associated with platinum-based chemotherapy response and prognosis in NSCLC (Xian et al., 2014). NSCLC patients with high BMP4 expression were more likely to be resistant to chemotherapy than those with low BMP4 expression (Xian et al., 2014). Recent studies using integrated epigenomics also identified BMP4 as a modulator of cisplatin sensitivity in gastric cancer (GC) and indicated that its expression status may elicit promising biomarkers for cisplatin-resistant GC (Ivanova et al., 2013; Wood, 2012). In colorectal cancer, however, BMP4 can stimulate terminal differentiation and increase the response to chemotherapy in chemo-resistant colorectal cancer stem cells (CRC-SCs) (Lombardo et al., 2011).

In the present study, we found that the expression of miR-139-5p is significantly down-regulated in gef-resistant NSCLC cells compared to parental cells, suggesting that dysregulation of miR-139-5p is involved in the development of drug-resistant lung cancer. The function of miR-139-5p in the resistant cancer cells was confirmed by employing the antitumor agent yuanhuadine (YD) to effectively up-regulate the expression of miR-139-5p in gef-resistant NSCLC cells. Further studies were designed to identify the putative role of miR-139-5p in gef-resistant cancer cells. The combination of cDNA profile arrays and miRNA arrays, with YD-induced restoration of miR-139-5p, led to the novel identification of BMP4 as one of the most overexpressed genes in gef-resistant NSCLC cells. These findings suggest that there is an inverse correlation between the expression of miR-139-5p and BMP4 levels in EGFR-TKI-resistant NSCLC cells. Therefore, the modulation of either miR-139-5p or BMP4 might be a novel strategy to overcome EGFR-TKI-resistance in EGFR-mutant NSCLC cells. Indeed, we demonstrated the pro-tumorigenic role of BMP4 through knockdown of BMP4 in gef-resistant NSCLC cells. We also revealed that BMP4 regulates ACSL4 to affect lipid metabolism. The up-regulation of BMP4 and ACSL4 leads to higher energy metabolism in resistant cancer cells, enabling cancer cells to enhance cell growth and acquire drug resistance. Additionally, the relationship between BMP4 and energy metabolism was also confirmed by the enhanced expression of p53 in BMP4-depleted EGFR mutant gef-resistant

NSCLC cells (PC9-Gef). Recent findings suggest that activation of the BMP-BMPR pathway may confer resistance to EGFR-TKIs in lung cancer patients with EGFR mutations (Wang et al., 2015). Subsequently, targeting the BMP pathway with various BMP inhibitors could provide a potential therapy for cancer treatment. In this vein, the dorsomorphin derivative LDN-193189 was reported to significantly suppress the proliferation of NSCLC cells but not non-transformed cells (Fotinos et al., 2014). LDN-193189 was also effective against chemotherapy-resistant epithelial ovarian cancer cells (Ali et al., 2015) and enhanced the chemo-sensitivity of Smad4-silenced colorectal cancer cells (Voorneveld et al., 2015). Based on these studies, we attempted to determine whether LDN-193189 is able to suppress gef-resistant NSCLC tumor growth *in vivo*. LDN-193189 effectively suppressed tumor growth in nude mice bearing gef-resistant NSCLC cells. Moreover, LDN-193189 also induced the expression of miR-139-5p; these effects were found to be synergistic with the effects of YD, suggesting that a therapeutic strategy utilizing both the inhibition of BMP4 and induction of miR-139-5p could potentially be of use in the treatment of gef-resistant NSCLC.

In conclusion, BMP4 overexpression is partially associated with gef-resistance in NSCLC cells, and BMP4 can be suppressed by miR-139-5p and YD. BMP4 also interacts with ACSL4 and the p53 signaling pathway, both of which are highly connected to lipid energy metabolism in cancer cells (Figure 45). These findings suggest that BMP4 may be considered a potential prognostic biomarker or therapeutic target for patients with gef-resistant NSCLC.

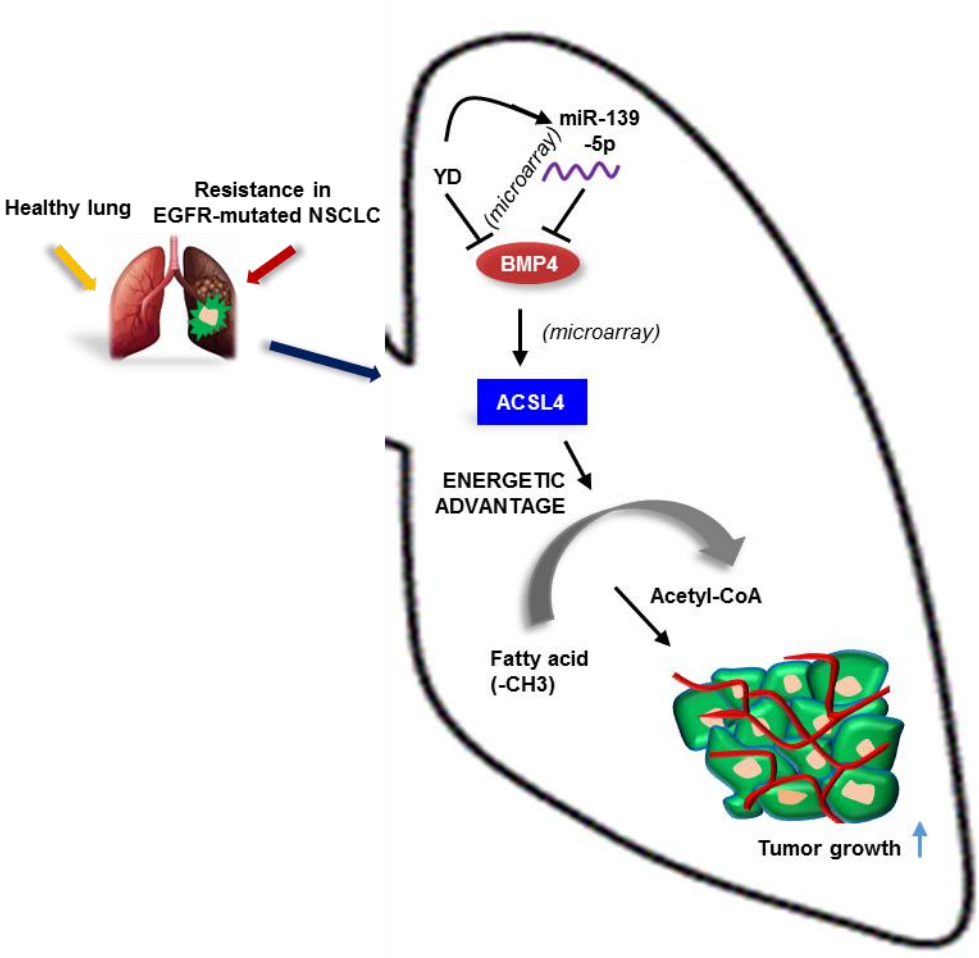

Figure 45: Scheme mechanism action of miR-139-5p and BMP4 in gef-resistant NSCLC cells.

4. Conclusions

The present study aimed to investigate the novel mechanisms of epidermal growth factor receptor-tyrosine kinase inhibitor (EGFR-TKI) resistance and finally indicated several possible mechanisms that can be used as novel therapeutic targets to overcome acquired gefitinib resistance in non-small cell lung cancer (NSCLC) cells. The findings from each study are summarized as follows.

In Chapter 2, Nicotinamide N-methyltransferase (NNMT), a cancer-associated metabolic enzyme, is commonly over-expressed in various human tumors. Emerging evidence also suggests a crucial loss of function of microRNAs (miRNAs) in modulating tumor progression in response to standard therapies. However, their precise roles in regulating the development of drug-resistant tumorigenesis are still poorly understood. Herein, we established EGFR-TKI-resistant non-small cell lung cancer (NSCLC) models and observed a negative correlation between the expression levels of NNMT and miR-449a in tumor cells. Additionally, knockdown of NNMT suppressed p-Akt and tumorigenesis, while re-expression of miR-449a induced phosphatase and tensin homolog (PTEN) and inhibited tumor growth. Furthermore, yuanhuadine (YD), an antitumor agent, significantly up-regulated miR-449a levels while critically suppressing NNMT expression. These findings suggest a novel therapeutic approach for overcoming EGFR-TKI resistance to NSCLC treatment.

In Chapter 3, in particular, NSCLC cells harboring EGFR mutations are associated with resistance development of EGFR tyrosine kinase inhibitors (EGFR-TKIs) treatment. Recent findings suggest that bone morphogenetic proteins (BMPs) and miRNAs might act as oncogenes or tumor suppressors in the tumor microenvironment. In this study, for the first time, we identified the potential roles of BMPs and miRNAs involved in EGFR-TKI resistance by analyzing datasets from a pair of parental cells and NSCLC cells with acquired EGFR TKI-resistance. BMP4 was observed to be significantly over-expressed in the EGFR-TKI resistant cells, and its mechanism of action was strongly associated with the induction of cancer cell energy metabolism through the modulation of Acyl-CoA synthetase long-chain family member 4. In addition, miR-139-5p was observed to be significantly down-regulated in the resistant NSCLC cells. The combination of miR-139-5p and YD, a naturally-derived antitumor agent, synergistically suppressed BMP4 expression in the resistant cells. We further confirmed that LDN-193189, a small molecule BMP receptor 1 inhibitor, effectively inhibited tumor growth in a xenograft nude mouse model

implanted with the EFGR-TKI resistant cells. These findings suggest a novel role of BMP4-mediated tumorigenesis in the progression of acquired drug resistance in EGFR-mutant NSCLC cells.

The present studies are significant based on the identified novel mechanisms of acquired gefitinib resistance, and these mechanisms were proven to be potential therapeutic targets to overcome gefitinib resistance by the application of the natural product yuanhuadine in NSCLC cells.

References:

Ahmed, M.I., Mardaryev, A.N., Lewis, C.J., Sharov, A.A., Botchkareva, N.V., 2011. MicroRNA-21 is an important downstream component of BMP signalling in epidermal keratinocytes. Journal of Cell Science 124, 3399-3404.

Ahmed, S., Metpally, R.P., Sangadala, S., Reddy, B.V., 2010. Virtual screening and selection of drug-like compounds to block noggin interaction with bone morphogenetic proteins. Journal of Molecular Graphics & Modelling 28, 670-682.

Ali, J.L., Lagasse, B.J., Minuk, A.J., Love, A.J., Moraya, A.I., Lam, L., Arthur, G., Gibson, S.B., Morrison, L.C., Werbowetski-Ogilvie, T.E., Fu, Y., Nachtigal, M.W., 2015. Differential cellular responses induced by dorsomorphin and LDN-193189 in chemotherapy-sensitive and chemotherapy-resistant human epithelial ovarian cancer cells. International Journal of Cancer 136, E455-469.

Ambros, V., 2003. MicroRNA pathways in flies and worms: growth, death, fat, stress, and timing. Cell 113, 673-676.

An, Y.J., Xu, W.J., Jin, X., Wen, H., Kim, H., Lee, J., Park, S., 2012. Metabotyping of the C. elegans sir-2.1 mutant using in vivo labeling and 13C-heteronuclear multidimensional NMR metabolomics. ACS Chemical Biology 7, 2012-2018.

Bach, D.-H., Hong, J.-Y., Park, H.J., Lee, S.K., 2017a. The role of exosomes and miRNAs in drug-resistance of cancer cells. International Journal of Cancer 141, 220-230.

Bach, D.-H., Kim, D., Bae, S.Y., Kim, W.K., Hong, J.-Y., Lee, H.-J., Rajasekaran, N., Kwon, S., Fan, Y., Luu, T.-T.-T., Shin, Y.K., Lee, J., Lee, S.K., 2018a. Targeting nicotinamide N-methyltransferase and miR-449a in EGFR-TKI-resistant non-small-cell lung cancer cells. Molecular Therapy - Nucleic Acids 11, 455-467.

Bach, D.-H., Lee, S.K., 2018. Long noncoding RNAs in cancer cells. Cancer Letters 419, 152-166.

Bach, D.-H., Liu, J.-Y., Kim, W.K., Hong, J.-Y., Park, S.H., Kim, D., Qin, S.-N., Luu, T.-T.-T., Park, H.J., Xu, Y.-N., Lee, S.K., 2017b. Synthesis and biological activity of new phthalimides as potential anti-inflammatory agents. Bioorganic & Medicinal Chemistry 25, 3396-3405.

Bach, D.-H., Park, H.J., Lee, S.K., 2018b. The dual role of bone morphogenetic proteins in cancer. Molecular Therapy - Oncolytics 8, 1-13.

Bach, D.H., Kim, S.H., Hong, J.Y., Park, H.J., Oh, D.C., Lee, S.K., 2015. Salternamide A suppresses hypoxia-induced accumulation of HIF-1alpha and induces apoptosis in human colorectal cancer cells. Marine Drugs 13, 6962-6976.

Bachegowda, L., Morrone, K., Winski, S.L., Mantzaris, I., Bartenstein, M., Ramachandra, N., Giricz, O., Sukrithan, V., Nwankwo, G., Shahnaz, S., Bhagat, T., Bhattacharyya, S., Assal, A., Shastri, A., Gordon-Mitchell, S., Pellagatti, A., Boultwood, J., Schinke, C., Yu, Y., Guha, C., Rizzi, J., Garrus, J., Brown, S., Wollenberg, L., Hogeland, G., Wright, D., Munson, M., Rodriguez, M., Gross, S., Chantry, D., Zou, Y., Platanias, L., Burgess, L.E., Pradhan, K., Steidl, U., Verma, A., 2016. Pexmetinib: a novel dual inhibitor of Tie2 and p38 MAPK with efficacy in preclinical models of myelodysplastic syndromes and acute myeloid leukemia. Cancer Research 76, 4841-4849.

Bae, S.Y., Hong, J.Y., Lee, H.J., Park, H.J., Lee, S.K., 2015. Targeting the degradation of AXL receptor tyrosine kinase to overcome resistance in gefitinib-resistant non-small cell lung cancer. Oncotarget 6, 10146-10160.

Bae, S.Y., Park, H.J., Hong, J.Y., Lee, H.J., Lee, S.K., 2016. Down-regulation of SerpinB2 is associated with gefitinib resistance in non-small cell lung cancer and enhances invadopodia-like structure protrusions. Scientific Reports 6, 32258.

Bartel, D.P., 2004. MicroRNAs: genomics, biogenesis, mechanism, and function. Cell 116, 281-297.

Bartel, D.P., 2009. MicroRNAs: target recognition and regulatory functions. Cell 136, 215-233.

Bourguignon, L.Y., Wong, G., Earle, C., Chen, L., 2012. Hyaluronan-CD44v3 interaction with Oct4-Sox2-Nanog promotes miR-302 expression leading to self-renewal, clonal formation, and cisplatin resistance in cancer stem cells from head and neck squamous cell carcinoma. The Journal of Biological Chemistry 287, 32800-32824.

Braig, S., Mueller, D.W., Rothhammer, T., Bosserhoff, A.K., 2010. MicroRNA miR-196a is a central regulator of HOX-B7 and BMP4 expression in malignant melanoma. Cellular and Molecular Life Sciences 67, 3535-3548.

Brunen, D., Willems, S.M., Kellner, U., Midgley, R., Simon, I., Bernards, R., 2013. TGF-beta: an emerging player in drug resistance. Cell Cycle 12, 2960-2968.

Chan, B.A., Hughes, B.G.M., 2015. Targeted therapy for non-small cell lung cancer: current standards and the promise of the future. Translational Lung Cancer Research 4, 36-54.

Chen, L., Yi, X., Goswami, S., Ahn, Y.H., Roybal, J.D., Yang, Y., Diao, L., Peng, D., Peng, D., Fradette, J.J., Wang, J., Byers, L.A., Kurie, J.M., Ullrich, S.E., Qin, F.X., Gibbons, D.L., 2016. Growth and metastasis of lung adenocarcinoma is potentiated by BMP4-mediated immunosuppression. Oncoimmunology 5, e1234570.

Chen, P.-Y., Sun, J.-S., Tsuang, Y.-H., Chen, M.-H., Weng, P.-W., Lin, F.-H., 2010. Simvastatin promotes osteoblast viability and differentiation via Ras/Smad/Erk/BMP-2 signaling pathway. Nutrition Research 30, 191-199.

Chiarini, F., Del Sole, M., Mongiorgi, S., Gaboardi, G.C., Cappellini, A., Mantovani, I., Follo, M.Y., McCubrey, J.A., Martelli, A.M., 2008. The novel Akt inhibitor, perifosine, induces caspase-dependent apoptosis and downregulates P-glycoprotein expression in multidrug-resistant human T-acute leukemia cells by a JNK-dependent mechanism. Leukemia 22, 1106-1116.

Cho, Y.E., Kim, S.H., Lee, B.H., Baek, M.C., 2017. Circulating plasma and exosomal microRNAs as indicators of drug-induced organ injury in rodent models. Biomolecules & Therapeutics 25, 367-373.

Choi, Y.J., Ingram, P.N., Yang, K., Coffman, L., Iyengar, M., Bai, S., Thomas, D.G., Yoon, E., Buckanovich, R.J., 2015. Identifying an ovarian cancer cell hierarchy regulated by bone morphogenetic protein 2. Proceedings of the National Academy of Sciences of the United States of America 112, E6882-6888.

Chou, T.C., 2006. Theoretical basis, experimental design, and computerized simulation of synergism and antagonism in drug combination studies. Pharmacological Reviews 58, 621-681.

Coffman, L.G., Choi, Y.J., McLean, K., Allen, B.L., di Magliano, M.P., Buckanovich, R.J., 2016. Human carcinoma-associated mesenchymal stem cells promote ovarian cancer chemotherapy resistance via a BMP4/HH signaling loop. Oncotarget 7, 6916-6932.

Corcoran, C., Rani, S., O'Brien, K., O'Neill, A., Prencipe, M., Sheikh, R., Webb, G., McDermott, R., Watson, W., Crown, J., O'Driscoll, L., 2012. Docetaxel-resistance in prostate cancer: evaluating associated phenotypic changes and potential for resistance transfer via exosomes. PLoS One 7, e50999.

Craft, C.S., Xu, L., Romero, D., Vary, C.P.H., Bergan, R.C., 2008. Genistein induces phenotypic reversion of endoglin deficiency in human prostate cancer cells. Molecular Pharmacology 73, 235-242.

Diaz Jr, L.A., Williams, R.T., Wu, J., Kinde, I., Hecht, J.R., Berlin, J., Allen, B., Bozic, I., Reiter, J.G., Nowak, M.A., Kinzler, K.W., Oliner, K.S., Vogelstein, B., 2012. The molecular evolution of acquired resistance to targeted EGFR blockade in colorectal cancers. Nature 486, 537-540.

Du, M., Su, X.M., Zhang, T., Xing, Y.J., 2014. Aberrant promoter DNA methylation inhibits bone morphogenetic protein 2 expression and contributes to drug resistance in breast cancer. Molecular Medicine Reports 10, 1051-1055.

Easwaran, H., Tsai, H.-C., Baylin, S.B., 2014. Cancer epigenetics: tumor heterogeneity, plasticity of stem-like states, and drug resistance. Molecular Cell 54, 716-727.

Engelman, J.A., Settleman, J., 2008. Acquired resistance to tyrosine kinase inhibitors during cancer therapy. Current Opinion in Genetics & Development 18, 73-79.

Eramo, A., Ricci-Vitiani, L., Zeuner, A., Pallini, R., Lotti, F., Sette, G., Pilozzi, E., Larocca, L.M., Peschle, C., De Maria, R., 2006. Chemotherapy resistance of glioblastoma stem cells. Cell Death & Differentiation 13, 1238-1241.

Fotinos, A., Nagarajan, N., Martins, A.S., Fritz, D.T., Garsetti, D., Lee, A.T., Hong, C.C., Rogers, M.B., 2014. Bone morphogenetic protein-focused strategies to induce cytotoxicity in lung cancer cells. Anticancer Research 34, 2095-2104.

Fry, M.J., 2001. Phosphoinositide 3-kinase signalling in breast cancer: how big a role might it play? Breast Cancer Research 3, 304-312.

Gazdar, A.F., 2009. Activating and resistance mutations of EGFR in non-small-cell lung cancer: role in clinical response to EGFR tyrosine kinase inhibitors. Oncogene 28, S24-S31.

Guo, X., Wang, X.F., 2009. Signaling cross-talk between TGF-beta/BMP and other pathways. Cell Research 19, 71-88.

Hallahan, A.R., Pritchard, J.I., Chandraratna, R.A., Ellenbogen, R.G., Geyer, J.R., Overland, R.P., Strand, A.D., Tapscott, S.J., Olson, J.M., 2003. BMP-2 mediates retinoid-induced apoptosis in medulloblastoma cells through a paracrine effect. Nature Medicine 9, 1033-1038.

Hao, J., Lee, R., Chang, A., Fan, J., Labib, C., Parsa, C., Orlando, R., Andresen, B., Huang, Y., 2014. DMH1, a small molecule inhibitor of BMP type I receptors, suppresses growth and invasion of lung cancer. PLoS One 9, e90748.

Hardwick, J.C., Kodach, L.L., Offerhaus, G.J., van den Brink, G.R., 2008. Bone morphogenetic protein signalling in colorectal cancer. Nature Review Cancer 8, 806-812.

Hino, R., Uozaki, H., Murakami, N., Ushiku, T., Shinozaki, A., Ishikawa, S., Morikawa, T., Nakaya, T., Sakatani, T., Takada, K., Fukayama, M., 2009. Activation of DNA methyltransferase 1 by EBV latent membrane protein 2A leads to promoter hypermethylation of PTEN gene in gastric carcinoma. Cancer Research 69, 2766-2774.

Holohan, C., Van Schaeybroeck, S., Longley, D.B., Johnston, P.G., 2013. Cancer drug resistance: an evolving paradigm. Nature Review Cancer 13, 714-726.

Hong, J.Y., Chung, H.J., Lee, H.J., Park, H.J., Lee, S.K., 2011. Growth inhibition of human lung cancer cells via down-regulation of epidermal growth factor receptor signaling by yuanhuadine, a daphnane diterpene from *Daphne genkwa*. Journal of Natural Products 74, 2102-2108.

Hu, G., Drescher, K.M., Chen, X.M., 2012. Exosomal miRNAs: biological properties and therapeutic potential. Frontiers in Genetics 3, 56.

Ivanova, T., Zouridis, H., Wu, Y., Cheng, L.L., Tan, I.B., Gopalakrishnan, V., Ooi, C.H., Lee, J., Qin, L., Wu, J., Lee, M., Rha, S.Y., Huang, D., Liem, N., Yeoh, K.G., Yong, W.P., Teh, B.T., Tan, P., 2013. Integrated epigenomics identifies BMP4 as a modulator of cisplatin sensitivity in gastric cancer. Gut 62, 22-33.

Jones, V.S., Huang, R.-Y., Chen, L.-P., Chen, Z.-S., Fu, L., Huang, R.-P., 2016. Cytokines in cancer drug resistance: Cues to new therapeutic strategies. Biochimica et Biophysica Acta (BBA) - Reviews on Cancer 1865, 255-265.

Kannt, A., Rajagopal, S., Kadnur, S.V., Suresh, J., Bhamidipati, R.K., Swaminathan, S., Hallur, M.S., Kristam, R., Elvert, R., Czech, J., Pfenninger, A., Rudolph, C., Schreuder, H., Chandrasekar, D.V., Mane, V.S., Birudukota, S., Shaik, S., Zope, B.R., Burri, R.R., Anand, N.N., Thakur, M.K., Singh, M., Parveen, R., Kandan, S., Mullangi, R., Yura, T., Gosu, R., Ruf, S., Dhakshinamoorthy, S., 2018. A small molecule inhibitor of Nicotinamide N-methyltransferase for the treatment of metabolic disorders. Scientific Reports 8, 3660.

Kim, J.S., Kurie, J.M., Ahn, Y.H., 2015. BMP4 depletion by miR-200 inhibits tumorigenesis and metastasis of lung adenocarcinoma cells. Molecular Cancer 14, 173.

Kim, W.K., Bach, D.-H., Ryu, H.W., Oh, J., Park, H.J., Hong, J.-Y., Song, H.-H., Eum, S., Bach, T.T., Lee, S.K., 2017. Cytotoxic activities of Telectadium dongnaiense and its constituents by inhibition of the Wnt/β-catenin signaling pathway. Phytomedicine 34, 136-142.

Kitano, H., 2003. Cancer robustness: tumour tactics. Nature 426, 125.

Kitano, H., 2004. Cancer as a robust system: implications for anticancer therapy. Natire Review Cancer 4, 227-235.

Kodach, L.L., Bleuming, S.A., Peppelenbosch, M.P., Hommes, D.W., van den Brink, G.R., Hardwick, J.C.H., 2007. The effect of statins in colorectal cancer is mediated through the bone morphogenetic protein pathway. Gastroenterology 133, 1272-1281.

Kokubo, Y., Gemma, A., Noro, R., Seike, M., Kataoka, K., Matsuda, K., Okano, T., Minegishi, Y., Yoshimura, A., Shibuya, M., Kudoh, S., 2005. Reduction of PTEN protein and loss of epidermal growth factor receptor gene mutation in lung cancer with natural resistance to gefitinib (IRESSA). British Journal of Cancer 92, 1711-1719.

Lagos-Quintana, M., Rauhut, R., Lendeckel, W., Tuschl, T., 2001. Identification of novel genes coding for small expressed RNAs. Science 294, 853-858.

Langenfeld, E., Deen, M., Zachariah, E., Langenfeld, J., 2013. Small molecule antagonist of the bone morphogenetic protein type I receptors suppresses growth and expression of Id1 and Id3 in lung cancer cells expressing Oct4 or nestin. Molecular Cancer 12, 129.

Lee, G.T., Jung, Y.S., Ha, Y.S., Kim, J.H., Kim, W.J., Kim, I.Y., 2013. Bone morphogenetic protein-6 induces castration resistance in prostate cancer cells through tumor infiltrating macrophages. Cancer Science 104, 1027-1032.

Li, L., Liu, Y., Guo, Y., Liu, B., Zhao, Y., Li, P., Song, F., Zheng, H., Yu, J., Song, T., Niu, R., Li, Q., Wang, X.W., Zhang, W., Chen, K., 2015. Regulatory MiR-148a-ACVR1/BMP circuit defines a cancer stem cell-like aggressive subtype of hepatocellular carcinoma. Hepatology 61, 574-584.

Li, Q., Liang, X., Wang, Y., Meng, X., Xu, Y., Cai, S., Wang, Z., Liu, J., Cai, G., 2016. miR-139-5p inhibits the epithelial-mesenchymal transition and enhances the chemotherapeutic sensitivity of colorectal cancer cells by downregulating BCL2. Scientific Reports 6, 27157.

Li, Z., Hassan, M.Q., Volinia, S., van Wijnen, A.J., Stein, J.L., Croce, C.M., Lian, J.B., Stein, G.S., 2008. A microRNA signature for a BMP2-induced osteoblast lineage commitment program. Proceedings of the National Academy of Sciences of the United States of America 105, 13906-13911.

Lian, W.J., Liu, G., Liu, Y.J., Zhao, Z.W., Yi, T., Zhou, H.Y., 2013. Downregulation of BMP6 enhances cell proliferation and chemoresistance via activation of the ERK signaling pathway in breast cancer. Oncology Reports 30, 193-200.

Liang, L., Zeng, M., Pan, H., Liu, H., He, Y., 2018. Nicotinamide N-methyltransferase promotes epithelial-mesenchymal transition in gastric cancer cells by activating transforming growth factor-beta1 expression. Oncology Letters 15, 4592-4598.

Liang, Y., Liu, J., Feng, Z., 2013. The regulation of cellular metabolism by tumor suppressor p53. Cell & Bioscience 3, 9.

Liu, G., Liu, Y.J., Lian, W.J., Zhao, Z.W., Yi, T., Zhou, H.Y., 2014. Reduced BMP6 expression by DNA methylation contributes to EMT and drug resistance in breast cancer cells. Oncology Reports 32, 581-588.

Liu, J., Valencia-Sanchez, M.A., Hannon, G.J., Parker, R., 2005. MicroRNA-dependent localization of targeted mRNAs to mammalian P-bodies. Nature Cell Biology 7, 719-723.

Liu, J., Zhang, C., Hu, W., Feng, Z., 2015. Tumor suppressor p53 and its mutants in cancer metabolism. Cancer Letters 356, 197-203.

Lombardo, Y., Scopelliti, A., Cammareri, P., Todaro, M., Iovino, F., Ricci-Vitiani, L., Gulotta, G., Dieli, F., de Maria, R., Stassi, G., 2011. Bone morphogenetic protein 4 induces differentiation of colorectal cancer stem cells and increases their response to chemotherapy in mice. Gastroenterology 140, 297-309.

Lu, J., Getz, G., Miska, E.A., Alvarez-Saavedra, E., Lamb, J., Peck, D., Sweet-Cordero, A., Ebert, B.L., Mak, R.H., Ferrando, A.A., Downing, J.R., Jacks, T., Horvitz, H.R., Golub, T.R., 2005. MicroRNA expression profiles classify human cancers. Nature 435, 834-838.

Luo, W., Huang, B., Li, Z., Li, H., Sun, L., Zhang, Q., Qiu, X., Wang, E., 2013. MicroRNA-449a is downregulated in non-small cell lung cancer and inhibits migration and invasion by targeting c-Met. PLoS One 8, e64759.

Ma, L., Teruya-Feldstein, J., Weinberg, R.A., 2007. Tumour invasion and metastasis initiated by microRNA-10b in breast cancer. Nature 449, 682-688.

Maeda, M., Murakami, Y., Watari, K., Kuwano, M., Izumi, H., Ono, M., 2015. CpG hypermethylation contributes to decreased expression of PTEN during acquired resistance to gefitinib in human lung cancer cell lines. Lung Cancer 87, 265-271.

Maemondo, M., Inoue, A., Kobayashi, K., Sugawara, S., Oizumi, S., Isobe, H., Gemma, A., Harada, M., Yoshizawa, H., Kinoshita, I., Fujita, Y., Okinaga, S., Hirano, H., Yoshimori, K., Harada, T., Ogura, T., Ando, M., Miyazawa, H., Tanaka, T., Saijo, Y., Hagiwara, K., Morita, S., Nukiwa, T., 2010. Gefitinib or chemotherapy for non-small-cell lung cancer with mutated EGFR. New England Journal of Medicine 362, 2380-2388.

Maloberti, P.M., Duarte, A.B., Orlando, U.D., Pasqualini, M.E., Solano, A.R., Lopez-Otin, C., Podesta, E.J., 2010. Functional interaction between acyl-CoA synthetase 4, lipooxygenases and cyclooxygenase-2 in the aggressive phenotype of breast cancer cells. PLoS One 5, e15540.

Mao, M., Tian, F., Mariadason, J.M., Tsao, C.C., Lemos, R., Jr., Dayyani, F., Gopal, Y.N., Jiang, Z.Q., Wistuba, II, Tang, X.M., Bornman, W.G., Bollag, G., Mills, G.B., Powis, G., Desai, J., Gallick, G.E., Davies, M.A., Kopetz, S., 2013. Resistance to BRAF inhibition in BRAF-mutant colon cancer can be overcome with PI3K inhibition or demethylating agents. Clinical Cancer Research 19, 657-667.

McCubrey, J.A., Steelman, L.S., Kempf, C.R., Chappell, W.H., Abrams, S.L., Stivala, F., Malaponte, G., Nicoletti, F., Libra, M., Basecke, J., Maksimovic-Ivanic, D., Mijatovic, S., Montalto, G., Cervello, M., Cocco, L., Martelli, A.M., 2011. Therapeutic resistance resulting from mutations in Raf/MEK/ERK and PI3K/PTEN/Akt/mTOR signaling pathways. Journal of Cellular Physiology 226, 2762-2781.

Migliore, C., Giordano, S., 2013. Resistance to targeted therapies: a role for microRNAs? Trends in Molecular Medicine 19, 633-642.

Miyares, Rosa L., Stein, C., Renisch, B., Anderson, Jennifer L., Hammerschmidt, M., Farber, Steven A., 2013. Long-chain Acyl-CoA synthetase 4A regulates smad activity and dorsoventral patterning in the zebrafish embryo. Developmental Cell 27, 635-647.

Modica, S., Wolfrum, C., 2017. The dual role of BMP4 in adipogenesis and metabolism. Adipocyte 6, 141-146.

Mok , T.S., Wu , Y.-L., Thongprasert , S., Yang , C.-H., Chu , D.-T., Saijo , N., Sunpaweravong , P., Han , B., Margono , B., Ichinose , Y., Nishiwaki , Y., Ohe , Y., Yang , J.-J., Chewaskulyong , B., Jiang , H., Duffield , E.L., Watkins , C.L., Armour , A.A., Fukuoka , M., 2009. Gefitinib or carboplatin–paclitaxel in pulmonary adenocarcinoma. New England Journal of Medicine 361, 947-957.

Molina, J.R., Yang, P., Cassivi, S.D., Schild, S.E., Adjei, A.A., 2008. Non–small cell lung cancer: epidemiology, risk factors, treatment, and survivorship. Mayo Clinic Proceedings 83, 584-594.

Nakata, A., Gotoh, N., 2012. Recent understanding of the molecular mechanisms for the efficacy and resistance of EGF receptor-specific tyrosine kinase inhibitors in non-small cell lung cancer. Expert Opinion on Therapeutic Targets 16, 771-781.

O'Brien, K., Rani, S., Corcoran, C., Wallace, R., Hughes, L., Friel, A.M., McDonnell, S., Crown, J., Radomski, M.W., O'Driscoll, L., 2013. Exosomes from triple-negative breast cancer cells can transfer phenotypic traits representing their cells of origin to secondary cells. European Journal of Cancer 49, 1845-1859.

Ogawa, Y., Kanai-Azuma, M., Akimoto, Y., Kawakami, H., Yanoshita, R., 2008. Exosome-like vesicles with dipeptidyl peptidase IV in human saliva. Biological & Pharmaceutical Bulletin 31, 1059-1062.

Padanad, M.S., Konstantinidou, G., Venkateswaran, N., Melegari, M., Rindhe, S., Mitsche, M., Yang, C., Batten, K., Huffman, K.E., Liu, J., Tang, X., Rodriguez-Canales, J., Kalhor, N., Shay,

J.W., Minna, J.D., McDonald, J., Wistuba, I.I., DeBerardinis, R.J., Scaglioni, P.P., 2016. Fatty acid oxidation mediated by Acyl-CoA synthetase long chain 3 is required for mutant KRAS lung tumorigenesis. Cell Reports 16, 1614-1628.

Palanichamy, K., Kanji, S., Gordon, N., Thirumoorthy, K., Jacob, J.R., Litzenberg, K.T., Patel, D., Chakravarti, A., 2017. NNMT silencing activates tumor suppressor PP2A, inactivates oncogenic STKs, and inhibits tumor forming ability. Clinical Cancer Ressearch 23, 2325-2334.

Pao, W., Miller, V.A., Politi, K.A., Riely, G.J., Somwar, R., Zakowski, M.F., Kris, M.G., Varmus, H., 2005. Acquired resistance of lung adenocarcinomas to gefitinib or erlotinib is associated with a second mutation in the EGFR kinase domain. PLoS Medicine 2, e73.

Peng, Y., Sartini, D., Pozzi, V., Wilk, D., Emanuelli, M., Yee, V.C., 2011. Structural basis of substrate recognition in human nicotinamide N-methyltransferase. Biochemistry 50, 7800-7808.

Persano, L., Pistollato, F., Rampazzo, E., Della Puppa, A., Abbadi, S., Frasson, C., Volpin, F., Indraccolo, S., Scienza, R., Basso, G., 2012. BMP2 sensitizes glioblastoma stem-like cells to Temozolomide by affecting HIF-1alpha stability and MGMT expression. Cell Death & Disease 3, e412.

Phan, A.N.H., Vo, V.T.A., Hua, T.N.M., Kim, M.K., Jo, S.Y., Choi, J.W., Kim, H.W., Son, J., Suh, Y.A., Jeong, Y., 2017. PPARgamma sumoylation-mediated lipid accumulation in lung cancer. Oncotarget 8, 82491-82505.

Qian, S.W., Tang, Y., Li, X., Liu, Y., Zhang, Y.Y., Huang, H.Y., Xue, R.D., Yu, H.Y., Guo, L., Gao, H.D., Liu, Y., Sun, X., Li, Y.M., Jia, W.P., Tang, Q.Q., 2013. BMP4-mediated brown fat-like changes in white adipose tissue alter glucose and energy homeostasis. Proceedings of the National Academy of Sciences of the United States of America 110, E798-807.

Qin, W., Zhao, B., Shi, Y., Yao, C., Jin, L., Jin, Y., 2009. BMPRII is a direct target of miR-21. Acta Biochimica et Biophysica Sinica 41, 618-623.

Qu, L., Ding, J., Chen, C., Wu, Z.J., Liu, B., Gao, Y., Chen, W., Liu, F., Sun, W., Li, X.F., Wang, X., Wang, Y., Xu, Z.Y., Gao, L., Yang, Q., Xu, B., Li, Y.M., Fang, Z.Y., Xu, Z.P., Bao, Y., Wu, D.S., Miao, X., Sun, H.Y., Sun, Y.H., Wang, H.Y., Wang, L.H., 2016. Exosome-transmitted lncARSR promotes sunitinib resistance in renal cancer by acting as a competing endogenous RNA. Cancer Cell 29, 653-668.

Rai, D., Kim, S.W., McKeller, M.R., Dahia, P.L., Aguiar, R.C., 2010. Targeting of SMAD5 links microRNA-155 to the TGF-beta pathway and lymphomagenesis. Proceedings of the National Academy of Sciences of the United States of America 107, 3111-3116.

Roessler, M., Rollinger, W., Palme, S., Hagmann, M.L., Berndt, P., Engel, A.M., Schneidinger, B., Pfeffer, M., Andres, H., Karl, J., Bodenmuller, H., Ruschoff, J., Henkel, T., Rohr, G., Rossol, S., Rosch, W., Langen, H., Zolg, W., Tacke, M., 2005. Identification of nicotinamide N-methyltransferase as a novel serum tumor marker for colorectal cancer. Clinical Cancer Research 11, 6550-6557.

Safaei, R., Larson, B.J., Cheng, T.C., Gibson, M.A., Otani, S., Naerdemann, W., Howell, S.B., 2005. Abnormal lysosomal trafficking and enhanced exosomal export of cisplatin in drug-resistant human ovarian carcinoma cells. Molecular Cancer Therapeutics 4, 1595-1604.

Sanchez-Martinez, R., Cruz-Gil, S., Gomez de Cedron, M., Alvarez-Fernandez, M., Vargas, T., Molina, S., Garcia, B., Herranz, J., Moreno-Rubio, J., Reglero, G., Perez-Moreno, M., Feliu, J., Malumbres, M., Ramirez de Molina, A., 2015. A link between lipid metabolism and epithelial-mesenchymal transition provides a target for colon cancer therapy. Oncotarget 6, 38719-38736.

Santarelli, L., Strafella, E., Staffolani, S., Amati, M., Emanuelli, M., Sartini, D., Pozzi, V., Carbonari, D., Bracci, M., Pignotti, E., Mazzanti, P., Sabbatini, A., Ranaldi, R., Gasparini, S., Neuzil, J., Tomasetti, M., 2011. Association of MiR-126 with soluble mesothelin-related peptides, a marker for malignant mesothelioma. PLoS One 6, e18232.

Saxena, S., Jonsson, Z.O., Dutta, A., 2003. Small RNAs with imperfect match to endogenous mRNA repress translation. Implications for off-target activity of small inhibitory RNA in mammalian cells. The Journal of Biological Chemistry 278, 44312-44319.

Shanker, M., Willcutts, D., Roth, J.A., Ramesh, R., 2010. Drug resistance in lung cancer. Lung Cancer: Targets and Therapy 1, 23-36.

Sharma, S.V., Bell, D.W., Settleman, J., Haber, D.A., 2007. Epidermal growth factor receptor mutations in lung cancer. Nature Review Cancer 7, 169-181.

Simons, M., Raposo, G., 2009. Exosomes--vesicular carriers for intercellular communication. Current Opinion in Cell Biology 21, 575-581.

Sos, M.L., Koker, M., Weir, B.A., Heynck, S., Rabinovsky, R., Zander, T., Seeger, J.M., Weiss, J., Fischer, F., Frommolt, P., Michel, K., Peifer, M., Mermel, C., Girard, L., Peyton, M., Gazdar, A.F., Minna, J.D., Garraway, L.A., Kashkar, H., Pao, W., Meyerson, M., Thomas, R.K., 2009. PTEN loss contributes to erlotinib resistance in EGFR-mutant lung cancer by activation of Akt and EGFR. Cancer Research 69, 3256-3261.

Stambolic, V., Suzuki, A., de la Pompa, J.L., Brothers, G.M., Mirtsos, C., Sasaki, T., Ruland, J., Penninger, J.M., Siderovski, D.P., Mak, T.W., 1998. Negative regulation of PKB/Akt-dependent cell survival by the tumor suppressor PTEN. Cell 95, 29-39.

Sun, C., Li, N., Yang, Z., Zhou, B., He, Y., Weng, D., Fang, Y., Wu, P., Chen, P., Yang, X., Ma, D., Zhou, J., Chen, G., 2013. miR-9 regulation of BRCA1 and ovarian cancer sensitivity to cisplatin and PARP inhibition. Journal of the National Cancer Institute 105, 1750-1758.

Sun, C., Sang, M., Li, S., Sun, X., Yang, C., Xi, Y., Wang, L., Zhang, F., Bi, Y., Fu, Y., Li, D., 2015a. Hsa-miR-139-5p inhibits proliferation and causes apoptosis associated with down-regulation of c-Met. Oncotarget 6, 39756-39792.

Sun, C., Sang, M., Li, S., Sun, X., Yang, C., Xi, Y., Wang, L., Zhang, F., Bi, Y., Fu, Y., Li, D., 2015b. Hsa-miR-139-5p inhibits proliferation and causes apoptosis associated with down-regulation of c-Met. Oncotarget 6, 39756-39792.

Tang, S.W., Yang, T.C., Lin, W.C., Chang, W.H., Wang, C.C., Lai, M.K., Lin, J.Y., 2011. Nicotinamide N-methyltransferase induces cellular invasion through activating matrix metalloproteinase-2 expression in clear cell renal cell carcinoma cells. Carcinogenesis 32, 138-145.

Tang, Y., Qian, S.-W., Wu, M.-Y., Wang, J., Lu, P., Li, X., Huang, H.-Y., Guo, L., Sun, X., Xu, C.-J., Tang, Q.-Q., 2016. BMP4 mediates the interplay between adipogenesis and angiogenesis during expansion of subcutaneous white adipose tissue. Journal of Molecular Cell Biology 8, 302-312.

Tate, C.M., Pallini, R., Ricci-Vitiani, L., Dowless, M., Shiyanova, T., D'Alessandris, G.Q., Morgante, L., Giannetti, S., Larocca, L.M., di Martino, S., Rowlinson, S.W., De Maria, R., Stancato, L., 2012. A BMP7 variant inhibits the tumorigenic potential of glioblastoma stem-like cells. Cell Death & Differentiation 19, 1644-1654.

Taylor, D.D., Gercel-Taylor, C., 2008. MicroRNA signatures of tumor-derived exosomes as diagnostic biomarkers of ovarian cancer. Gynecologic Oncology 110, 13-21.

Tazzari, P.L., Cappellini, A., Ricci, F., Evangelisti, C., Papa, V., Grafone, T., Martinelli, G., Conte, R., Cocco, L., McCubrey, J.A., Martelli, A.M., 2007. Multidrug resistance-associated protein 1 expression is under the control of the phosphoinositide 3 kinase/Akt signal transduction network in human acute myelogenous leukemia blasts. Leukemia 21, 427-438.

Tazzari, P.L., Tabellini, G., Ricci, F., Papa, V., Bortul, R., Chiarini, F., Evangelisti, C., Martinelli, G., Bontadini, A., Cocco, L., McCubrey, J.A., Martelli, A.M., 2008. Synergistic proapoptotic activity of recombinant TRAIL plus the Akt inhibitor Perifosine in acute myelogenous leukemia cells. Cancer Research 68, 9394-9403.

Tomida, M., Ohtake, H., Yokota, T., Kobayashi, Y., Kurosumi, M., 2008. Stat3 up-regulates expression of nicotinamide N-methyltransferase in human cancer cells. Journal of Cancer Research and Clinical Oncology 134, 551-559.

Ulanovskaya, O.A., Zuhl, A.M., Cravatt, B.F., 2013. NNMT promotes epigenetic remodeling in cancer by creating a metabolic methylation sink. Nature Chemical Biology 9, 300-306.

Um, S., Bach, D.-H., Shin, B., Ahn, C.-H., Kim, S.-H., Bang, H.-S., Oh, K.-B., Lee, S.K., Shin, J., Oh, D.-C., 2016. Naphthoquinone–oxindole alkaloids, coprisidins A and B, from a gut-associated bacterium in the dung beetle, copris tripartitus. Organic Letters 18, 5792-5795.

Urist, M.R., 1965. Bone: formation by autoinduction. Science 150, 893-899.

Voorneveld, P.W., Kodach, L.L., Jacobs, R.J., van Noesel, C.J.M., Peppelenbosch, M.P., Korkmaz, K.S., Molendijk, I., Dekker, E., Morreau, H., van Pelt, G.W., Tollenaar, R.A.E.M., Mesker, W., Hawinkels, L.J.A.C., Paauwe, M., Verspaget, H.W., Geraets, D.T., Hommes, D.W., Offerhaus, G.J.A., van den Brink, G.R., ten Dijke, P., Hardwick, J.C.H., 2015. The BMP pathway either enhances or inhibits the Wnt pathway depending on the SMAD4 and p53 status in CRC. British Journal of Cancer 112, 122-130.

Wang, D., Zhu, H., Zhu, Y., Liu, Y., Shen, H., Yin, R., Zhang, Z., Su, Z., 2013. CD133(+)/CD44(+)/Oct4(+)/Nestin(+) stem-like cells isolated from Panc-1 cell line may contribute to multi-resistance and metastasis of pancreatic cancer. Acta Histochemica 115, 349-356.

Wang, R.N., Green, J., Wang, Z., Deng, Y., Qiao, M., Peabody, M., Zhang, Q., Ye, J., Yan, Z., Denduluri, S., Idowu, O., Li, M., Shen, C., Hu, A., Haydon, R.C., Kang, R., Mok, J., Lee, M.J., Luu, H.L., Shi, L.L., 2014. Bone Morphogenetic Protein (BMP) signaling in development and human diseases. Genes & Diseases 1, 87-105.

Wang, Z., Shen, Z., Li, Z., Duan, J., Fu, S., Liu, Z., Bai, H., Zhang, Z., Zhao, J., Wang, X., Wang, J., 2015. Activation of the BMP-BMPR pathway conferred resistance to EGFR-TKIs in lung squamous cell carcinoma patients with EGFR mutations. Proceedings of the National Academy of Sciences of the United States of America 112, 9990-9995.

Weir, H.M., Bradbury, R.H., Lawson, M., Rabow, A.A., Buttar, D., Callis, R.J., Curwen, J.O., de Almeida, C., Ballard, P., Hulse, M., Donald, C.S., Feron, L.J., Karoutchi, G., MacFaul, P., Moss, T., Norman, R.A., Pearson, S.E., Tonge, M., Davies, G., Walker, G.E., Wilson, Z., Rowlinson, R., Powell, S., Sadler, C., Richmond, G., Ladd, B., Pazolli, E., Mazzola, A.M., D'Cruz, C., De Savi, C., 2016. AZD9496: an oral estrogen receptor inhibitor that blocks the growth of ER-positive and ESR1-mutant breast tumors in preclinical models. Cancer Research 76, 3307-3318.

Wen, K., Fu, Z., Wu, X., Feng, J., Chen, W., Qian, J., 2013. Oct-4 is required for an antiapoptotic behavior of chemoresistant colorectal cancer cells enriched for cancer stem cells: effects associated with STAT3/Survivin. Cancer Letters 333, 56-65.

Williams, A.C., Ramsden, D.B., 2005. Nicotinamide homeostasis: a xenobiotic pathway that is key to development and degenerative diseases. Medical Hypotheses 65, 353-362.

Wong, C.C., Wong, C.M., Tung, E.K., Au, S.L., Lee, J.M., Poon, R.T., Man, K., Ng, I.O., 2011. The microRNA miR-139 suppresses metastasis and progression of hepatocellular carcinoma by down-regulating Rho-kinase 2. Gastroenterology 140, 322-331.

Wood, N.J., 2012. Cancer: Integrated epigenomic analysis sheds light on role of BMP4 in regulating cisplatin sensitivity in gastric cancer. Nature Review Gastroenterology Hepatology 9, 301-301.

Wu, T., Zhou, H., Hong, Y., Li, J., Jiang, X., Huang, H., 2012. miR-30 family members negatively regulate osteoblast differentiation. Journal of Biological Chemistry.

Xian, S., Jilu, L., Zhennan, T., Yang, Z., Yang, H., Jingshu, G., Songbin, F., 2014. BMP-4 genetic variants and protein expression are associated with platinum-based chemotherapy response and prognosis in NSCLC. BioMed Research International 2014, 8.

Xie, X., Liu, H., Wang, Y., Zhou, Y., Yu, H., Li, G., Ruan, Z., Li, F., Wang, X., Zhang, J., 2016. Nicotinamide N-methyltransferase enhances resistance to 5-fluorouracil in colorectal cancer cells through inhibition of the ASK1-p38 MAPK pathway. Oncotarget 7, 45837-45848.

Xu, W., Hang, M., Yuan, C.Y., Wu, F.L., Chen, S.B., Xue, K., 2015. MicroRNA-139-5p inhibits cell proliferation and invasion by targeting insulin-like growth factor 1 receptor in human non-small cell lung cancer. International Journal of Clinical and Experimental Pathology 8, 3864-3870.

Yamamoto, C., Basaki, Y., Kawahara, A., Nakashima, K., Kage, M., Izumi, H., Kohno, K., Uramoto, H., Yasumoto, K., Kuwano, M., Ono, M., 2010. Loss of PTEN expression by blocking nuclear translocation of EGR1 in gefitinib-resistant lung cancer cells harboring epidermal growth factor receptor–activating mutations. Cancer Research 70, 8715-8725.

Yamasaki, F., Johansen, M.J., Zhang, D., Krishnamurthy, S., Felix, E., Bartholomeusz, C., Aguilar, R.J., Kurisu, K., Mills, G.B., Hortobagyi, G.N., Ueno, N.T., 2007. Acquired resistance to erlotinib in A-431 epidermoid cancer cells requires down-regulation of MMAC1/PTEN and up-regulation of phosphorylated Akt. Cancer Research 67, 5779-5788.

Yu, T., Wang, Y.T., Chen, P., Li, Y.H., Chen, Y.X., Zeng, H., Yu, A.M., Huang, M., Bi, H.C., 2015. Effects of nicotinamide N-methyltransferase on PANC-1 cells proliferation, metastatic potential and survival under metabolic stress. Cellular Physiology and Biochemistry 35, 710-721.

Yu, Z.Y., Xiao, H., Wang, L.M., Shen, X., Jing, Y., Wang, L., Sun, W.F., Zhang, Y.F., Cui, Y., Shan, Y.J., Zhou, W.B., Xing, S., Xiong, G.L., Liu, X.L., Dong, B., Feng, J.N., Wang, L.S., Luo, Q.L., Zhao, Q.S., Cong, Y.W., 2016. Natural product vibsanin A induces differentiation of myeloid leukemia cells through PKC activation. Cancer Research 76, 2698-2709.

Zhang, J., Wang, Y., Li, G., Yu, H., Xie, X., 2014a. Down-regulation of nicotinamide N-methyltransferase induces apoptosis in human breast cancer cells via the mitochondria-mediated pathway. PLoS One 9, e89202.

Zhang, L., Dong, Y., Zhu, N., Tsoi, H., Zhao, Z., Wu, C.W., Wang, K., Zheng, S., Ng, S.S., Chan, F.K., Sung, J.J., Yu, J., 2014b. microRNA-139-5p exerts tumor suppressor function by targeting Notch1 in colorectal cancer. Molecular Cancer 13, 124.

Zhang, S., Zhang, F., Li, X., Dong, W., Wen, L., Wang, S., 2007. Evaluation of *Daphne genkwa* diterpenes: fingerprint and quantitative analysis by high performance liquid chromatography. Phytochemical Analysis 18, 91-97.

Zhang, Y.W., Staal, B., Essenburg, C., Su, Y., Kang, L., West, R., Kaufman, D., Dekoning, T., Eagleson, B., Buchanan, S.G., Vande Woude, G.F., 2010. MET kinase inhibitor SGX523 synergizes with epidermal growth factor receptor inhibitor erlotinib in a hepatocyte growth factor-dependent fashion to suppress carcinoma growth. Cancer Research 70, 6880-6890.

Zhou, X., Yuan, P., Liu, Q., Liu, Z., 2017. LncRNA MEG3 regulates imatinib resistance in chronic myeloid leukemia via suppressing microRNA-21. Biomolecules & Therapeutics 25, 490-496.